NAVAL POSTGRADUATE SCHOOL
Monterey, California

THESIS

FLAPPING-WING PROPULSION AS A MEANS OF DRAG REDUCTION FOR LIGHT SAILPLANES

by

Brian H. Randall

September 2002

Thesis Advisor:	K. D. Jones
Second Reader:	M. F. Platzer

Approved for public release; distribution is unlimited

THIS PAGE INTENTIONALLY LEFT BLANK

REPORT DOCUMENTATION PAGE			Form Approved OMB No. 0704-0188
Public reporting burden for this collection of information is estimated to average 1 hour per response, including the time for reviewing instruction, searching existing data sources, gathering and maintaining the data needed, and completing and reviewing the collection of information. Send comments regarding this burden estimate or any other aspect of this collection of information, including suggestions for reducing this burden, to Washington headquarters Services, Directorate for Information Operations and Reports, 1215 Jefferson Davis Highway, Suite 1204, Arlington, VA 22202-4302, and to the Office of Management and Budget, Paperwork Reduction Project (0704-0188) Washington DC 20503.			
1. AGENCY USE ONLY ***(Leave blank)***	**2. REPORT DATE** September 2002	**3. REPORT TYPE AND DATES COVERED** Master's Thesis	
4. TITLE AND SUBTITLE: Flapping-wing Propulsion as a Means of Drag Reduction for Light Sailplanes			**5. FUNDING NUMBERS**
6. AUTHOR(S) Randall, Brian H.			
7. PERFORMING ORGANIZATION NAME(S) AND ADDRESS(ES) Naval Postgraduate School Monterey, CA 93943-5000			**8. PERFORMING ORGANIZATION REPORT NUMBER**
9. SPONSORING /MONITORING AGENCY NAME(S) AND ADDRESS(ES) N/A			**10. SPONSORING/MONITORING AGENCY REPORT NUMBER**
11. SUPPLEMENTARY NOTES The views expressed in this thesis are those of the author and do not reflect the official policy or position of the Department of Defense or the U.S. Government.			
12a. DISTRIBUTION / AVAILABILITY STATEMENT Approved for public release; distribution is unlimited			**12b. DISTRIBUTION CODE** A

13. ABSTRACT ***(maximum 200 words)***

In this paper, flapping-wing propulsion as a means of drag reduction for light sailplanes is investigated numerically. The feasibility of markedly improving minimum sink and L/D_{max} performance parameters in light sailplanes by flapping their flexible, high aspect ratio wings at their natural frequencies is considered. Two propulsive systems are explored: a human-powered system that is used to partially offset airframe drag, and a sustainer system that uses an electric motor with sufficient power for limited climb rates. A numerical analysis is conducted using a strip-theory approach with UPOT (Unsteady Potential code) data. Thrust and power coefficients are computed for 2-D sections. 3-D spanwise load factors are applied to calculate total wing thrust production and power consumption. The results show that theoretical drag reduction in excess of 20%, and improvements of minimum sink by 24% are possible with a human-powered flapping system.

14. SUBJECT TERMS Flapping-Wing Propulsion, Drag-Reduction, Light Sailplanes			**15. NUMBER OF PAGES** 112
			16. PRICE CODE
17. SECURITY CLASSIFICATION OF REPORT Unclassified	**18. SECURITY CLASSIFICATION OF THIS PAGE** Unclassified	**19. SECURITY CLASSIFICATION OF ABSTRACT** Unclassified	**20. LIMITATION OF ABSTRACT** UL

NSN 7540-01-280-5500 Standard Form 298 (Rev. 2-89)
Prescribed by ANSI Std. 239-18

THIS PAGE INTENTIONALLY LEFT BLANK

Approved for public release; distribution is unlimited

FLAPPING-WING PROPULSION AS A MEANS OF DRAG REDUCTION FOR LIGHT SAILPLANES

Brian H. Randall
Lieutenant, United States Navy
B.S., United States Naval Academy, 1994

Submitted in partial fulfillment of the
requirements for the degree of

MASTER OF SCIENCE IN AERONAUTICAL ENGINEERING

from the

NAVAL POSTGRADUATE SCHOOL
September 2002

Author: Brian H. Randall

Approved by: Kevin D. Jones
Thesis Advisor

Max F. Platzer
Second Reader/Co-Advisor

Max F. Platzer
Chairman, Department of Aeronautics and Astronautics

THIS PAGE INTENTIONALLY LEFT BLANK

ABSTRACT

In this paper, flapping-wing propulsion as a means of drag reduction for light sailplanes is investigated numerically. The feasibility of markedly improving minimum sink and L/D_{max} performance parameters in light sailplanes by flapping their flexible, high aspect ratio wings at their natural frequencies is considered. Two propulsive systems are explored: a human-powered system that is used to partially offset airframe drag, and a sustainer system that uses an electric motor with sufficient power for limited climb rates. A numerical analysis is conducted using a strip-theory approach with UPOT (Unsteady Potential code) data. Thrust and power coefficients are computed for 2-D sections. 3-D spanwise load factors are applied to calculate total wing thrust production and power consumption. The results show that theoretical drag reduction in excess of 20% and improvements of minimum sink by 24% are possible with a human-powered flapping system.

THIS PAGE INTENTIONALLY LEFT BLANK

TABLE OF CONTENTS

LIST OF SYMBOLS

AR	aspect ratio, b^2/S
b	effective wing span
b/2	half span
bhp	brake horsepower
c	chord length
Cd	drag coefficient
Cl	lift coefficient
Cr	root chord
Ct	tip chord
f	oscillation frequency in Hz
h	plunge amplitude in terms of *c*
k	reduced frequency, $2\pi fc/U$
L/D	lift to drag ratio, *Cl/Cd*
M	mass
S	wing area, *bc*
t	time
U	velocity in m/s
w	weight in kg
W	Watts power
y(t)	vertical displacement in terms of *c*
Dy	plunge displacement in terms of *c*
α	angle of attack in degrees
β	angle of bank in degrees
ϕ	flapping angle in degrees
η	propulsive efficiency
λ	taper ratio

THIS PAGE INTENTIONALLY LEFT BLANK

LIST OF FIGURES

ACKNOWLEDGMENTS

I would like to thank Professors Kevin D. Jones and Max F. Platzer for their guidance, countless instruction sessions, time, and patience in the completion of this study. I wish to thank Steve Pollard for providing CMARC solutions necessary for the validation of the numerical method employed in this study. I also wish to thank the numerous sailplane manufacturers for providing information on their aircraft; in particular, Greg Cole, of Windward Performance for data on the *SparrowHawk* ultralight sailplane, as well as Danny Howell for data on the *Light Hawk* ultralight sailplane.

Last, but not least, I would like to thank my wife, Amy, for her tireless support.

THIS PAGE INTENTIONALLY LEFT BLANK

I. INTRODUCTION

A. OVERVIEW

In this paper, flapping-wing propulsion as a means of drag reduction is investigated numerically. The feasibility of markedly improving minimum sink and L/D_{max} performance parameters in light sailplanes by flapping their flexible, high aspect ratio wings at their natural frequencies is considered. Two propulsive systems are explored: a human-powered system that partially offsets airframe drag, and a sustainer system that uses an electric motor with sufficient power for limited climb rates. In either case, the aircraft is not intended to be self-launching (i.e. it will be unable to takeoff under its own power), requiring a winch launch, an auto-tow, or aero-tow as do conventional gliders. By restricting the flapping of the aircraft's wings to the in-flight regime, the issue of wingtip/ground clearance is avoided. The objective of this research is to apply flapping-wing aerodynamics to increase the performance parameters of existing sailplanes.

A numerical analysis is conducted using a strip-theory approach with UPOT (Unsteady Potential code) data. UPOT, a panel-code developed at NPS by Teng [Ref 1], models harmonically flapping airfoil sections in inviscid flow. Thrust and power coefficients are computed for 2-Dimensional sections. Spanwise load factors are applied to calculate total wing section thrust production and power consumption.

B. FLAPPING-WING PROPULSION

Nature gives us numerous examples of flying creatures using their wings for creating both lift and thrust. This rather graceful and efficient mode of propulsion has eluded mankind's best efforts. The understanding of the complex aerodynamic principles at work in the flight of birds, insects, and mammals is still limited.

Some of the limiting factors that man has yet to overcome include mechanical and structural scaling issues. The dynamic forces encountered by man-carrying flapping-wing airframes result in either structures that are significantly heavier than conventional

airframes, or structures unable to withstand the dynamic forces of this method of propulsion.

Purely plunging airfoils have been the subjects of some of the earliest scientific theories concerning flapping-wing flight. In 1909 Knoller[2] and in 1912 Betz[3] independently published papers providing the first theoretical explanations of plunging airfoil thrust generation. Both recognized that flapping an airfoil in a flow produces an induced angle of attack. The normal force vector is, by definition, always perpendicular to the effective flow. With this induced angle of attack, the normal force vector, which contains elements of lift (cross-stream direction) and thrust (stream wise direction) is canted forward, as shown in Figure 1. The key parameter for determining whether an airfoil creates thrust is the effective angle of attack. [Ref. 4] The relationship can be derived from the airfoil's position, which is a function of the reduced frequency, *k*, and the non-dimensional flapping amplitude, *h*. Where:

$$k = \frac{2p\ fc}{U} \tag{1}$$

$$h = \frac{\Delta y}{c} \tag{2}$$

The position of the airfoil as a function of time is:

$$y(t) = h\cos(kt) \tag{3}$$

The maximum induced velocity is given by differentiating equation (3) with respect to time:

$$y'(t) = -hk\sin(kt) \tag{4}$$

And the maximum value is given by:

$$y'_{\max} = hk \tag{5}$$

Such that the maximum induced angle, $\alpha_{i,}$ is:

$$a_i = \arctan(hk) \tag{6}$$

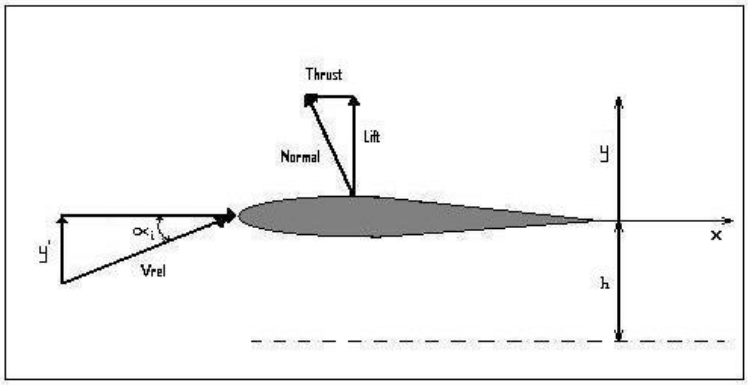

Figure 1. Thrust Production of Purely Plunging Airfoil

In nature, flapping wings generally follow complex patterns that include both pitching and plunging at offset phases. This is done to not only preserve energy, but as a result of the organisms' muscular-skeletal structure. However, motions such as these do not lend themselves easily to an analysis due to the large parameter space involved. This preliminary study would be limited to a simplified look at combinations of wing geometries, flapping frequencies, and different flight speeds. In the interest of time, the flapping was confined to purely plunging motion vice pitching and plunging to simplify the data acquisition.

C. HIGH PERFORMANCE SAILPLANES

High aspect ratio sailplanes with their flexible composite structures exhibit large wing deflections in flight as demonstrated in Figure 2. If the inherent flexibility of these wings could be harnessed to "flap" at their natural frequency, perhaps it would be possible to offset some of the airframe's drag through a purely plunging motion. [Ref. 5]

Figure 2. Natural High Performance Sailplane Wing Deflection

The wing flapping would be accomplished by exciting the aircraft at its 1st bending mode- as shown in Figure 3. This would minimize the power requirement of the mechanical flapping mechanism, as will be discussed in a later section.

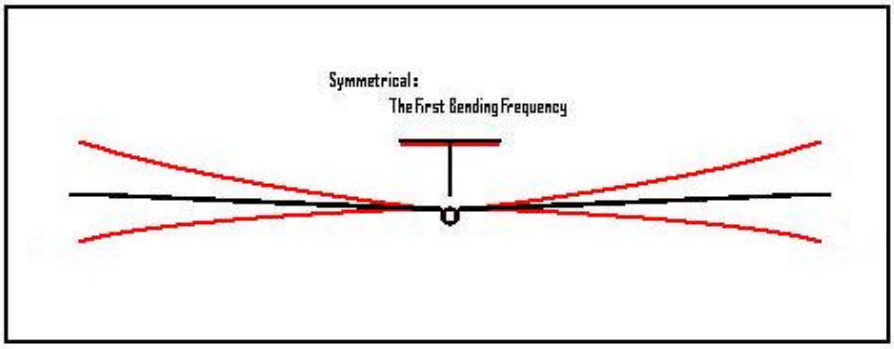

Figure 3. 1st Bending Mode Flapping

1. Improving Existing Aircraft

Research into human-powered vehicles revealed that the continuous power output for an average human is in the 200W range with possible momentary spikes up to 500W- that typically lead to oxygen debt. Trained athletes are able to surpass 300W of continuous power. [Ref. 6] For the purposes of this study, it was assumed that 210W would be available; and assuming 5% mechanical losses, only 200W could be expected to power a flapping propulsion system. In the interest of quantifying the drag reduction that could be accomplished by human-powered means, several European sailplane manufacturers were contacted for specifications and performance information on the aircraft that presently dominate the sport of soaring: Schempp-Hirth, Schliecher, LAK, just to name a few. A database was produced that included forty different sailplanes and several of their variants. The categories of aircraft included: Two seat, Federation Aeronautique Internationale (FAI) 15m class, World Class (wingspan < 15m), Open Class (wingspan > 15m), and Ultralight as defined by FAR Part 103. In addition, several companies that produce motorglider/sustainer gliders were contacted to provide specifications for the database. The databases are presented in Appendix A in spreadsheet format.

The drag force acting on each sailplane and the horsepower required for flight at their respective L/D_{max}, and min sink velocities were calculated using power required in Watts from Reference 7 defined by:

$$W = \frac{wU\cos b}{.0614h(L/D)} \qquad (7)$$

For a given L/D, as the weight and/or the velocity of the aircraft is decreased, the power requirement is reduced.

2. Reducing the Power Requirement

As the data was examined, it became clear that human power alone would not make a significant impact on drag. These sailplanes, at an average 300kg weight, were simply too heavy, and their power requirements too high. 200W human power limit could theoretically provide a modest 5% increase in L/D_{max} or minimum sink. This was the equivalent of going from an L/D of 36 to 37.8, or decreasing min sink from 0.63m/s to 0.60m/s. Clearly, this wouldn't go very far towards helping a desperate pilot clear the next ridge or to stay aloft long enough to find better lift conditions. For this study to be worthwhile, it was important to make a more significant impact on both parameters, which are important in their own ways. The velocity at which L/D_{max} occurs may be flown between lift zones for cross-country flights, while the velocity at which minimum sink occurs buys a pilot time in weak lift conditions until stronger conditions can be found to avert an off-field landing and make it home.

The second factor in decreasing power requirement was velocity. In order to get the most out of the 200W human power limit, the aircraft would have to be flown at slower airspeeds than current gliders were optimized for since the power required increases as the cube of the velocity. The optimal flight regime appeared to favor hang glider-like velocities of 11m/s to 23m/s, rather than high performance sailplanes with flight velocities of 28m/s to 40m/s.

Looking at the power equations for propeller-driven aircraft, minimum power required velocity occurs when $Cl^{1.5}/Cd$ is at a maximum. This corresponds to max endurance airspeed, or, in sailplane lingo, minimum sink airspeed, as shown in Figure 4.

Since L/D_{max} occurs at a higher airspeed corresponding to maximum range, and minimum sink occurs at a lower airspeed corresponding to maximum endurance, 200W would have a more significant impact on improving minimum sink than it would L/D_{max}.

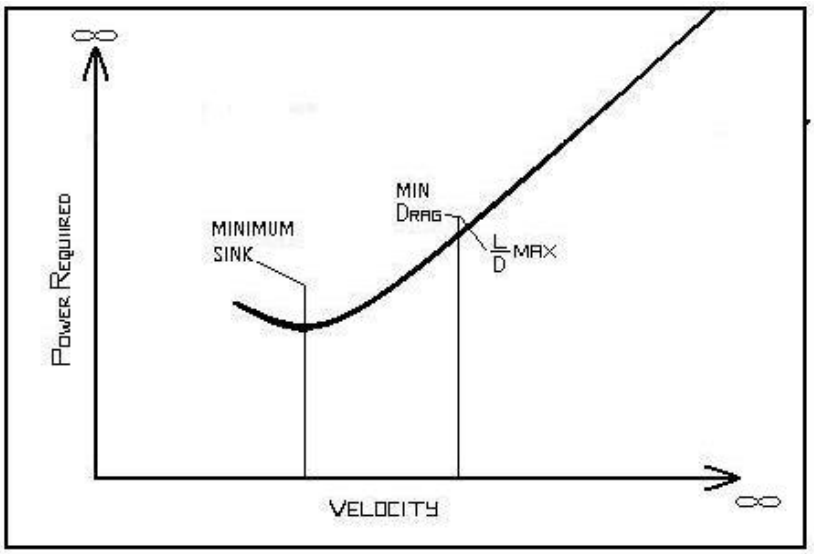

Figure 4. Power Required vs. Velocity

Only when lighter, slower flying aircraft could be found would a human-powered drag reduction system become more viable.

3. Existing Sustainer Sailplanes

Unlike motorglider propulsive systems, sustainer systems are designed as an added measure of safety to prevent off-field landings, for example, while being as unobtrusive (i.e. not taxing the airframe with unnecessary weight, drag) as possible. Aircraft equipped with this safety device are capable of modest climb rates of 0.89m/s or less. To minimize weight and drag, most sustainers use compact, lightweight propulsive systems, and small diameter propeller disks with multiple blades that are stowed within the fuselage. As a result, sustainer systems compromise propulsive efficiency. In addition, the cut outs made for the internal storage bay of the system reduces the structural rigidity of the fuselage and increases weight.

Figure 5. Sustainer-Equipped Duo Discus Sailplane

Schemp-Hirth Flugzeugbau employs sustainers for their Discus and Duo Discus sailplanes as shown in Figures 5 and 6. The mechanism is stowed inside the gliders with its propeller blades folded forward. When the pilots of their sustainer gliders wish to use the propulsive system to avert an off field landing, the mechanism must be extended into the freestream. The pilot then puts the aircraft in a slight dive to increase the free stream velocity. This extends the folded propeller blades and they begin to windmill. The propeller acts as a starter and brings the engine to life. There is no other starter mechanism or throttle; the motor is either full on or off. See Appendix B for more information concerning Schemp-Hirth Flugzeugbau sustainer data.

Figure 6. 2 Views of Deployed Sustainer Systems

The design is simple, but not without hazards. If an unsuccessful motor start is experienced there would be a significant increase in the aircraft's rate of descent due to the high drag of the extended mechanism. With insufficient altitude- this would make a bad situation even worse. Also, the high thrust line of the system would cause an abrupt nose-up pitching moment if the motor were to cease operating. During a slow speed climbout- this could lead to stall/spin entry.

A flapping-wing sustainer system would not require extending any high-drag system out of the fuselage. Neither would the fuselage require cut-outs for an internal

bay. Finally, this study will show that a sustainer system need not be a compromise in propulsive efficiency.

4. Ultralight Sailplanes

Data from existing sailplanes began to show that human-powered drag reduction would not be practical due to the limited effect 200W afforded to current relatively heavy sailplanes. However, several sailplane manufacturers showcased new aircraft at the Soaring Society of America's Air Expo in Los Angeles in February of 2002. Most notable were Windward Performance's *SparrowHawk*, and Pure-Flight's *Light Hawk* aircraft. Both of these aircraft fall into the ultralight aircraft category as defined by FAR Part 103. As per regulations, ultralight aircraft must weigh less than 70.3kg if unpowered, and 115.2kg if powered. See Appendix B for more information concerning FAR Part 103 regulations.

The *SparrowHawk,* shown in Figure 7, is designed and sold by Windward Performance of Bend, Oregon. Although the *SparrowHawk* is a legal ultralight, it is designed to fly in many of the same conditions as existing sailplanes. Due to its relatively high wing loading and high aspect ratio for an ultralight, Windward Performance claims, "it will cruise between thermals at speeds much greater than existing light sailplanes with more altitude retention. It will climb exceptionally well with its low sink-rate and tight turning radius afforded by its low stall speed and small size. Perhaps most significantly, the small all-carbon airframe gives quick and nimble handling." [Ref. 8]

Figure 7. *SparrowHawk* Ultralight Sailplane

SparrowHawk Specifications:

Wingspan 11m	Empty Weight 70.3 kg
Aspect Ratio 18.6	MTOW 188.2 kg
Wing Area 6.5m^2	Min sink 0.66m/s @ 19.5m/s
Wing Loading 25.6 kg/m^2	Best L/D 36:1 @ 27.9m/s

The *Light Hawk,* shown in Figure 8, is another FAR Part 103 ultralight sailplane developed by Pure Flight, Inc. of Bellingham, Washington. Because this aircraft was optimized for low speed flight; with a 15m span and light wing loading, it proved to be even more promising than the *SparrowHawk*. Pure Flight Inc. claims that, "The low wing loading and excellent maneuverability will allow pilots to climb in weaker lift than ever before. *Light Hawk* pilots can expect to outclimb any other gliding aircraft in the sky, and to get extended flights on even very weak days." [Ref. 9]

Because of its exceptionally low flight speed and light weight, human power has the potential to go much further towards drag reduction than on any other aircraft considered.

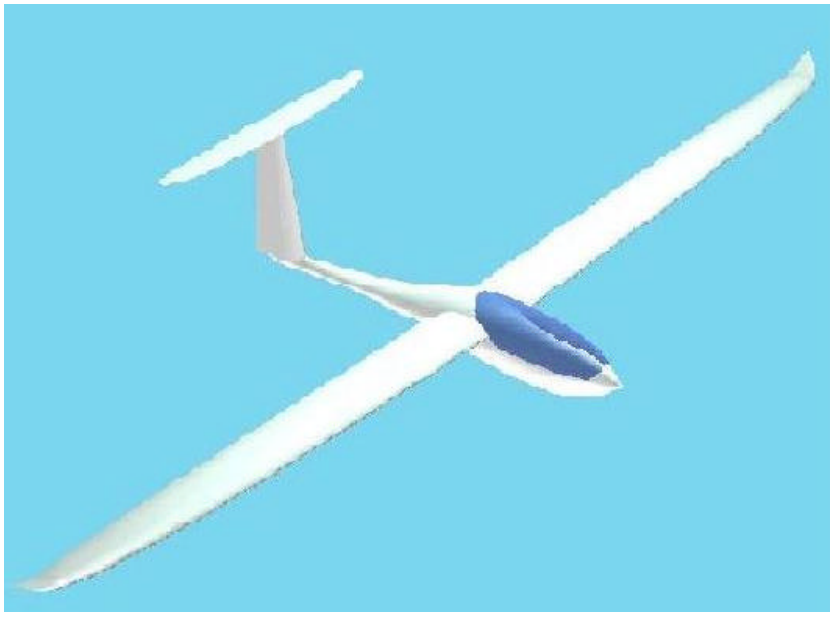

Figure 8. *Light Hawk* Ultralight Sailplane

Light Hawk Specifications:

Wingspan 15 m	Empty Weight 70.3 kg
Aspect Ratio 19.22	MTOW 161 kg
Wing Area 11.71 m^2	Min sink 0.42 m/s @ 12.5 m/s
Wing Loading 13.49 kg/m^2	Best L/D est. 35:1 @ 16.94 m/s

These two aircraft in the ultralight category essentially have expanded the envelope of soaring flight. Their light weight allows them to operate in much weaker conditions than existing sailplanes. The *Light Hawk's* design further pushes the flight regime to the left in the velocity scale as shown in Figure 9. Improving the performance of the *Sparrow Hawk* and *Light Hawk* aircraft became the focus of the study.

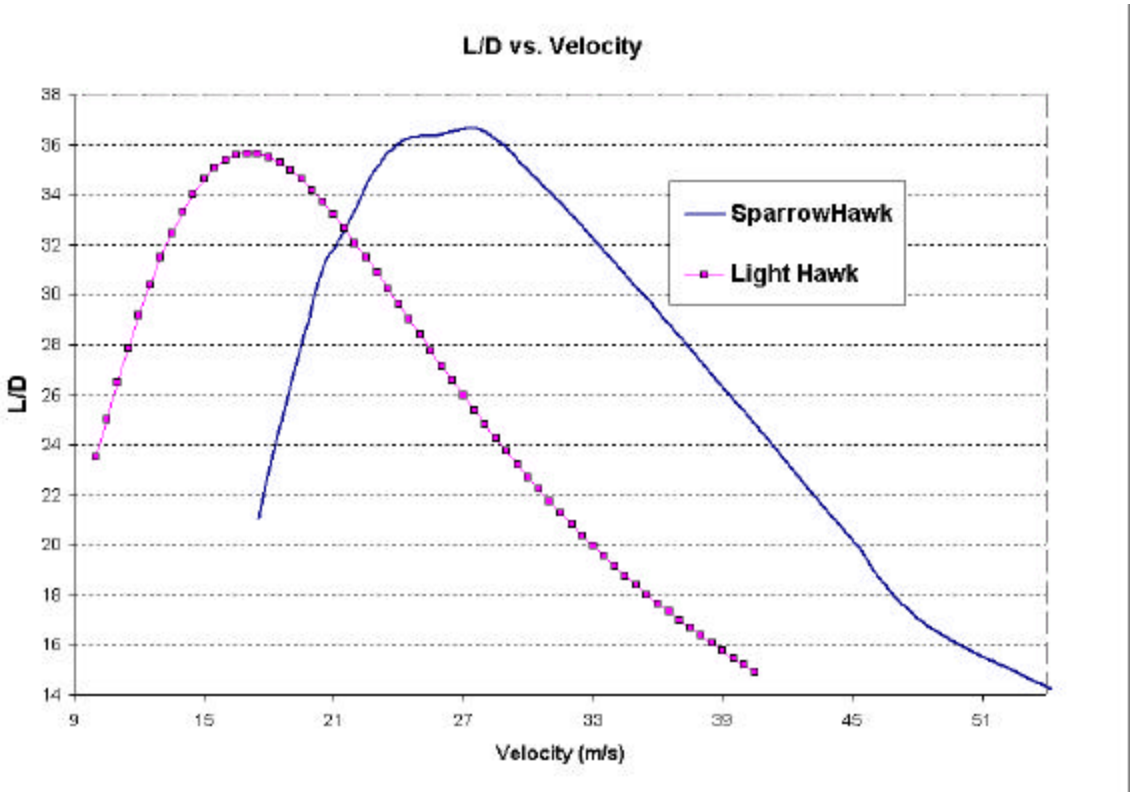

Figure 9. L/D vs. Velocity for *Sparrowhawk* and *Light Hawk*

5. Flapping Mechanism

It is beyond the scope of this study to design and analyze the details of the flapping mechanism. However, preliminary proposals for how a human-powered flapping system and an electric-powered sustainer are included. The general idea behind the two for producing low power flapping-wing propulsion lies in exciting a spring-mass system at its natural frequency, thereby minimizing the mechanical power requirements.

The lowest power requirement would exist if the wing flapping exactly matched the wing's natural frequency. With a mechanical system exciting high aspect ratio wings at their 1st bending mode, the inherent flexibility of the wing structure would help produce large flap amplitudes. From correspondence with sailplane manufacturers, their aircraft wing 1st bending mode frequencies ranged from 1.2 to 2.8Hz. As expected, the greater the wingspan of the sailplane, the lower the natural frequency of its wings. Flapping a wing structure to 1.2Hz and above would be challenging from a human-powered perspective because reduced frequency, k, would be high, and the resultant

propulsive efficiency, h, would be low. However, there are ways to lower the natural frequency of a wing structure: decreasing its stiffness, or adding mass, for example. Decreasing the stiffness of the structure was deemed unacceptable as it would require extensive modifications to existing wings, and it would decrease the dive speed of the aircraft. Adding weight to an aircraft is not desirable either. However, the penalty is minimized by adding weight at the wing tips. To "tune" the 1st bending mode to a more achievable range, it was hoped that this method would be the least intrusive from a performance perspective.

If we treat the wing structure like a constant section, constant chord cantilever beam and add a point mass near the tip, as shown in Figure 10, the natural frequency changes as:

$$f = \frac{1}{2p}\left[\frac{3EI}{L^3\left(M_{TIP} + 0.2357 M_{BEAM}\right)}\right]^{\frac{1}{2}} \qquad (8)$$

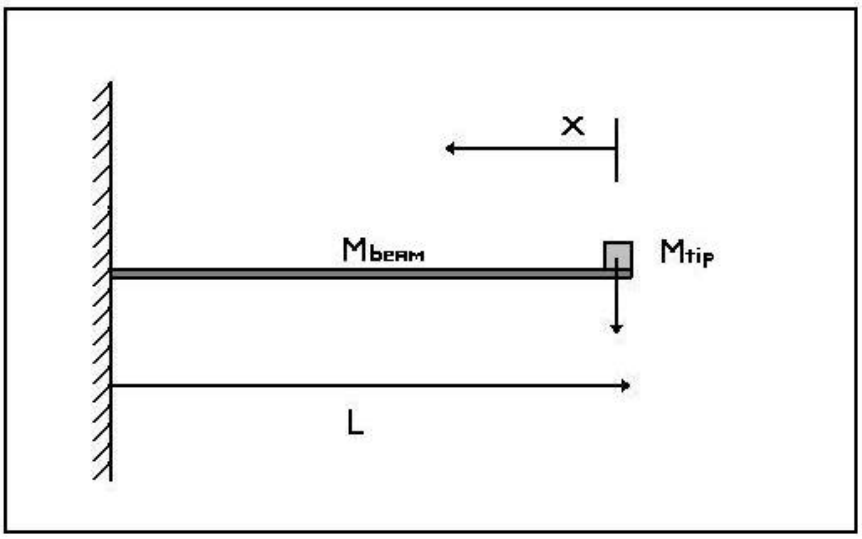

Figure 10. Cantilever with Point Mass

It was found that reducing the natural frequency of an existing wing structure by half required an addition of 70% of the wing's original mass at the tip. While this may seem excessive, in the case of the *SparrowHawk* and *Light Hawk* aircraft with individual wing panel weights of just 16.8kg, "tuning" the natural frequency to half of its original

value could be achieved by adding 11.8kg of water ballast at the wing tips, the equivalent of 4.4gallons for each wing. Because wing sections are tapered, and have more of their mass near the root, the true ballast requirement would probably be lower. Since many of today's competition gliders incorporate water ballast tanks much larger than this inside their wings- adding tanks near the wing tips would not be an unreasonable modification. However, to lower the natural frequency even more, the required additional mass would become excessive. In addition, with wing tip ballast in place, consideration must be given to a reduction in flight speeds to avoid the possibility of flutter. Therefore, in order to not limit either aircraft's performance, the addition of mass would be used as a secondary means to fine-tune the aircraft's natural frequency to the range that offers the best thrust and efficiency. The primary means to ensure lower natural frequencies are achievable would be to allow the spar anchoring point to move freely, on demand, within a race with internal springs that would be tuned to be a sub-harmonic of the wing's 1st bending frequency, as shown in Figure 11. The pilot would be able to lock the anchoring pin to limit movement when flapping was not desired, and thus, limit the potential for flutter.

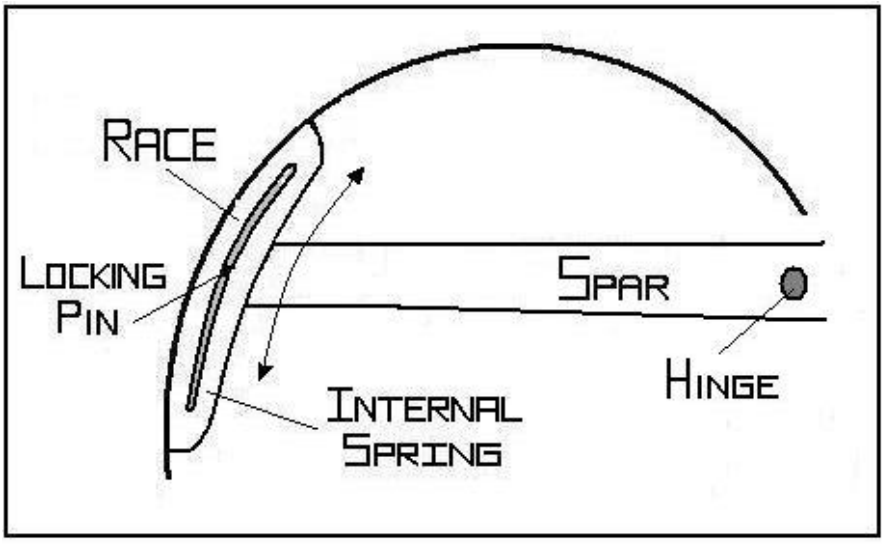

Figure 11. Spar Anchoring Point Movement

a. Human-Powered System

Employing a bicycle-type pedal system with a front sprocket, rear sprocket, and a chain to transfer power to the movement of the wings, the mechanical losses could be expected to be low. A simple bicycle chain is one of the most mechanically efficient drive systems available; with efficiencies up to 98.6%. This means that less than 2 percent of the power used to turn a bike train is lost to friction-related heat. [Ref. 10] The chain would rotate a flapping crankshaft, as shown in Figure 12.

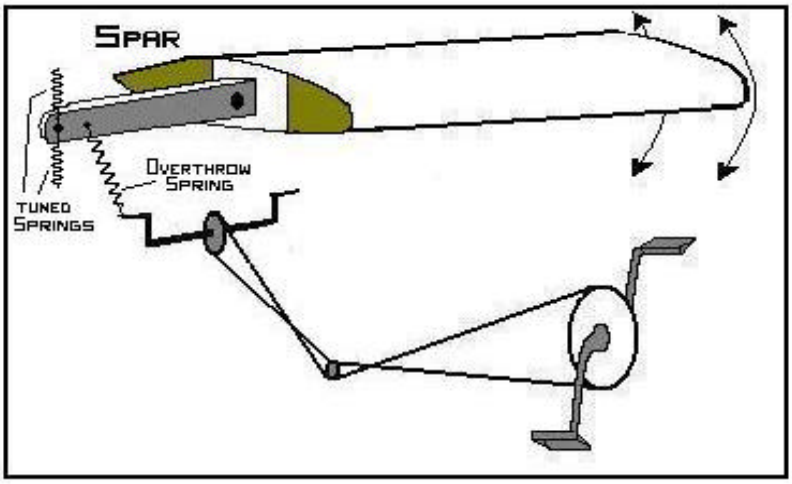

Figure 12. Chain-driven Pedal System

Considering the flapping movement, work is done at each wing stroke to overcome the aerodynamic forces resisting the flapping wings. Inertial work must be done to accelerate the wings at the start of every stroke. However, if the example set by the common fruit fly is followed, the kinetic energy of each wing stroke could be recovered through elastic storage, allowing much of the energy to be available for the next stroke. Hence, through the use of tuned springs, inertial mechanical losses can be assumed to be negligible. [Ref. 11] The main spar would have a hinge point near the root of the wing. The spar anchoring point would move freely in a race with internal springs that are tuned to a sub-harmonic of the wing's bending frequency. The spar itself would be attached to the flapping crankshaft by means of an overthrow spring to allow for variable flap amplitude. This system would exploit the spar and the wing's inherent

flexibility. Thus, for every rotation of the flapping crankshaft, the spar would move twice- flexing the wing rhythmically, as shown in Figure 13.

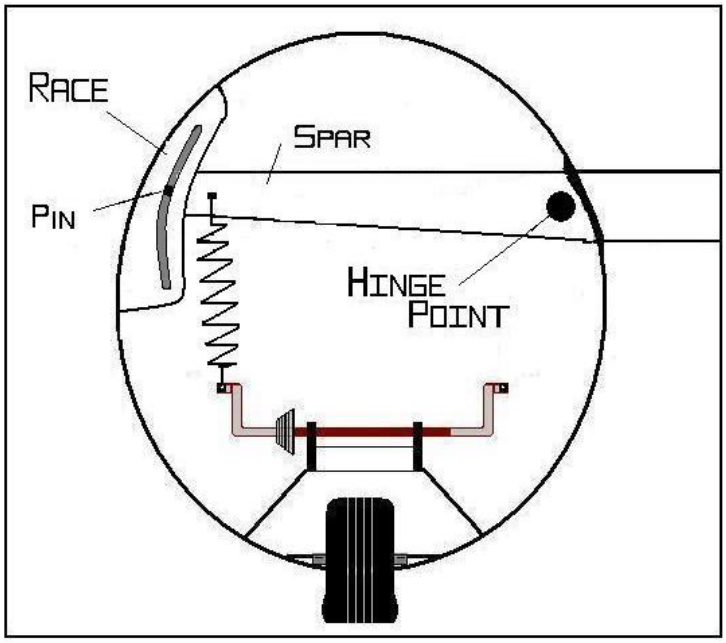

Figure 13. Fuselage Cross Section

b. Sustainer System

A sustainer system would have to be more robust than a human-powered system. The requirement for this system is to arrest rate of descent and provide for a 0.85m/s rate of climb. Assuming an increase in maximum takeoff weight to 200kg to account for strengthening the airframe, batteries, electric motor, and peripherals, the power requirements for *SparrowHawk* or *Light Hawk* based sustainers would be 2713W and 2475W respectively. Assuming 11% electrical system losses, and 5% mechanical losses, the requirement equates to 3147W (4.2bhp) and 2871W (3.9bhp), both of which could be satisfied with small electric motors using lightweight lithium ion batteries. Because the power requirement is low, and the system would be used periodically- only when needed; the potential exists to use solar arrays to charge the batteries during normal flight conditions.

II. NUMERICAL ANALYSIS

A. STRIP-THEORY APPROACH

While 3-Dimensional tools may provide results with a higher level of detail, the 2-Dimensional strip-theory approach employed in this study provides an inexpensive means to study a large parameter space. This is especially useful in studying flapping-wing propulsion with its virtually infinite number of parameters. Once trends are made visible through the strip-theory approach, more accurate methods can be used to provide a closer look.

Critical to the method was the ability to treat drag and thrust independently. This meant that as long as boundary layer separation was minimal, the profile drag of the aircraft encountered during normal flight (steady case) would not change in flapping-wing flight (unsteady case). Then, the thrust produced through flapping would be subtracted from the existing drag. From Reference 12: "Effectively, Ct only accounts for the forces due to unsteady pressure distribution around the wing, since skin friction is nearly constant in time and thus equal in steady and unsteady case."

A strip-theory approach was used to calculate the thrust and power for a given flapping-wing. Assumptions made in utilizing this approach included: negligible mechanical inertial losses with no structural damping, 2-D flow parallel to the fuselage axis at every section, and flapping was geometrically linear as shown in Figure 14.

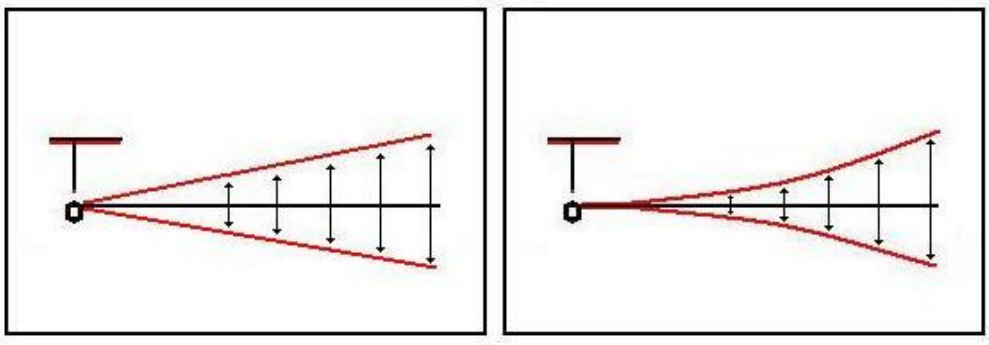

Figure 14. Modeled Semi Span Flapping (left) vs. Actual Flapping (right)

It was initially assumed that thrust and power followed elliptical span-wise distributions- effectively scaling as lift, as shown in Figure 15, but it was soon realized that this was inadequate, and eventually it was assumed that sectional weighting factors from 3-D flow solutions were used to modify 2-D data to approximate 3-D effects, such as tip losses, for power and thrust calculations.

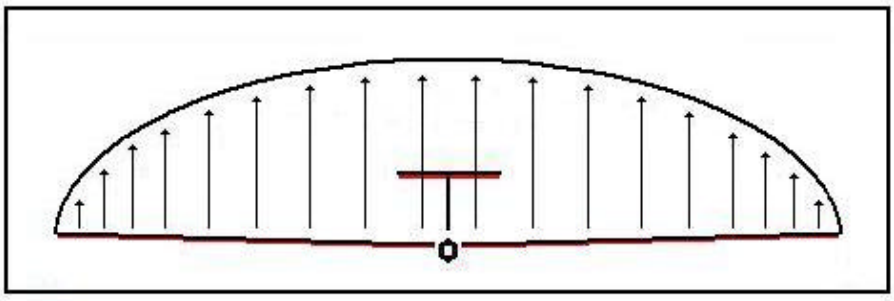

Figure 15. Elliptical Lift Distribution

The analysis began by defining the geometry of a sailplane's half-span wing section. The geometry and dimensions of the wing were: half span, *b/2*, root chord, *Cr*, tip chord, *Ct*, taper ratio, λ (defined as *Ct/Cr*), half span area, *S*, and flapping angle, θ, as shown in Figure 16. Because the wing undergoes bird-like flapping, flap amplitude, *h*, varies in the spanwise direction. Since the wing is tapered (i.e. the chord length changes) the reduced frequency, *k*, also varies as a function of span position. The coefficients of thrust and power are calculated for each individual station as it flaps at the corresponding reduced-frequency and non-dimensional amplitude for its location.

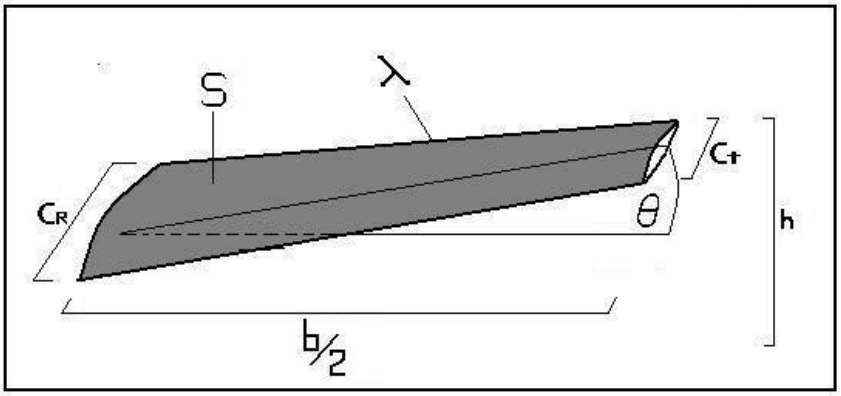

Figure 16. Half Span Dimensions of Interest

Using the strip-theory approach, the half wing is approximated by a finite number of sections with set areas, reduced frequencies, and flapping amplitudes as shown in Figure 17. Pre-computed 2-D solutions were applied individually to determine the thrust, and power coefficients for each segment. The 2-D segment data was corrected with 3-D spanwise loading factors at each station. The results were summed up to provide half-span thrust and power. Using symmetry, the total wing thrust production and power requirement were solved. Finally, aircraft-specific drag-polar and sink-rate data were introduced to provide net-drag and net-sink rates.

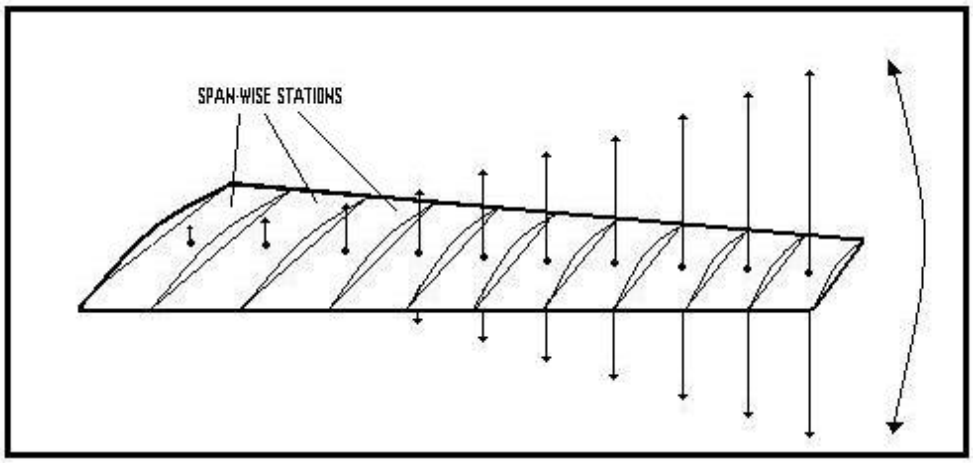

Figure 17. Strip-theory Segmentation for Flapping-wing

B. 2-D SOLUTION METHOD

Numerical analysis was conducted using a strip-theory approach with UPOT data computed for each segment. UPOT is a locally developed code originally developed by Teng [Ref. 1] and is based on Hess and Smith's [Ref. 13] method to analyze steady, inviscid flow over an airfoil. The unsteady portion employs the vorticity shedding procedure of Basu and Hancock. [Ref. 14] With additional features and graphic user interface (GUI) developed by Jones and Center [Ref. 15].

The panel-code is subject to several limitations. The Laplace equation on which it is based is a simplified version of the Navier-Stokes equation. The viscous effects are neglected, and subsequently the effects of separation/stall are not predicted. The panel-code is valid only for low speed, incompressible flow ($M < 0.3$). As a 2-D code, it does

not analyze 3-D effects such as wing-tip vortices, however, it does predict unsteady streamwise pressure contributions with results that agree well with theory, extensive experimental work, and other numerical methods. [Ref. 16]

Maximum plunge speed occurs as the product of h and k. Recall from equation 6:

$$\arctan(hk) = \alpha_i \qquad (6)$$

When the product of h and k approaches 0.8, the airfoil experiences high-induced angles of attack. Because airfoil stall is a progressive, not instantaneous development, a plunging airfoil typically experiences the onset of dynamic stall at much higher values of angle of attack. The peak value occurs when the airfoil passes through the midpoint of its flapping sequence; where its vertical velocity is highest. As will be shown in a later section, the peak value occurs about the 85% span location. The time-averaged thrust coefficient vs. reduced-frequency from Reference 12, is shown in Figure 18, illustrating that the panel-code predicts thrust accurately to an astonishing 39 degrees. This is valid for values where $k > 1.5$. However, for lower k values, this may not be the case. In the low reduced-frequency regime, mimicking birds' aeroelastic pitch variations in the flapping cycle would be necessary to reduce the induced angle of attack out at the tips where α_i is large.

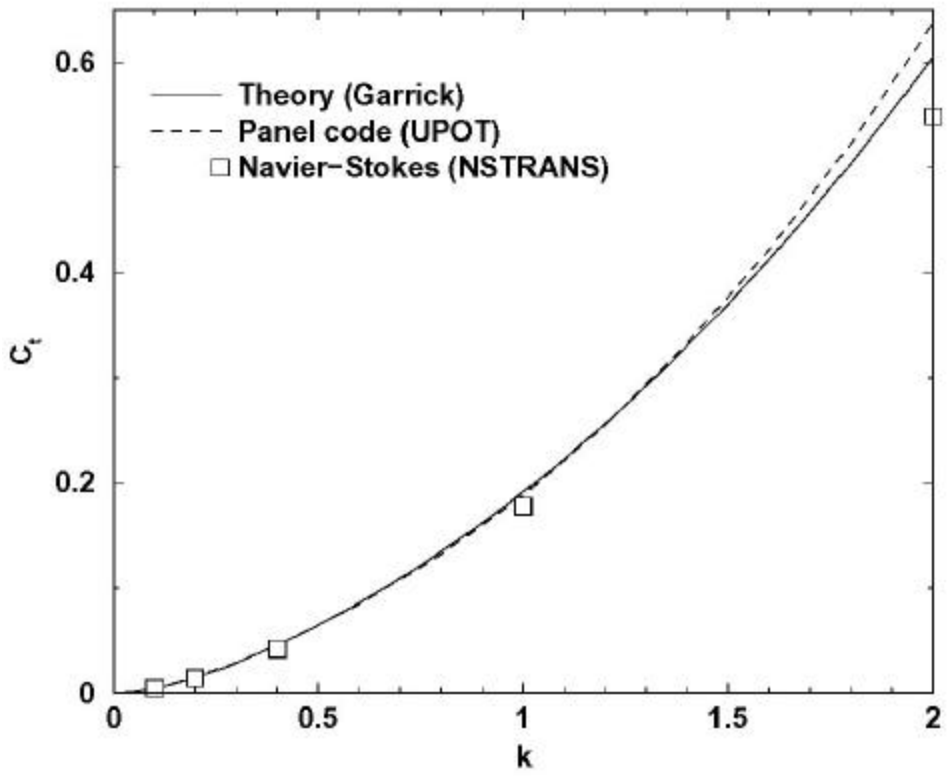

Figure 18. Time Averaged Thrust Coefficient vs. Reduced Frequency

Further details concerning the panel-code, UPOT, its validation, and its limitations are available in references 1, 16, 18, 19.

Modern sailplane wings possess numerous variables at different span locations, such as: optimized laminar and turbulent airfoils, transition areas for these different airfoil sections, and complex multiple wing tapering; it was necessary to determine how sensitive flapping-wing thrust production was to airfoil shape and angle of attack. If these factors proved not to be critical, then a simplified 2-D panel method using a single airfoil section would sufficiently approximate the flow around different sailplane wing sections. Basically, the simple strip-theory approach will only work if thrust production is independent of angle of attack and airfoil shape.

In Reference 12 it was shown that thrust production was independent to changes in mean angle of attack. In Reference 18**,** the effect of airfoil thickness and camber on thrust and power production for purely plunging airfoils was also shown to be negligible.

UPOT was used to verify data from these references. Several NACA airfoils of increasing thickness were put through purely plunging motion in the UPOT code. The range of flapping amplitude, *h*, was 0.25 to 2.0, while the range of reduced frequency, *k*, was 0.055 to 0.443.

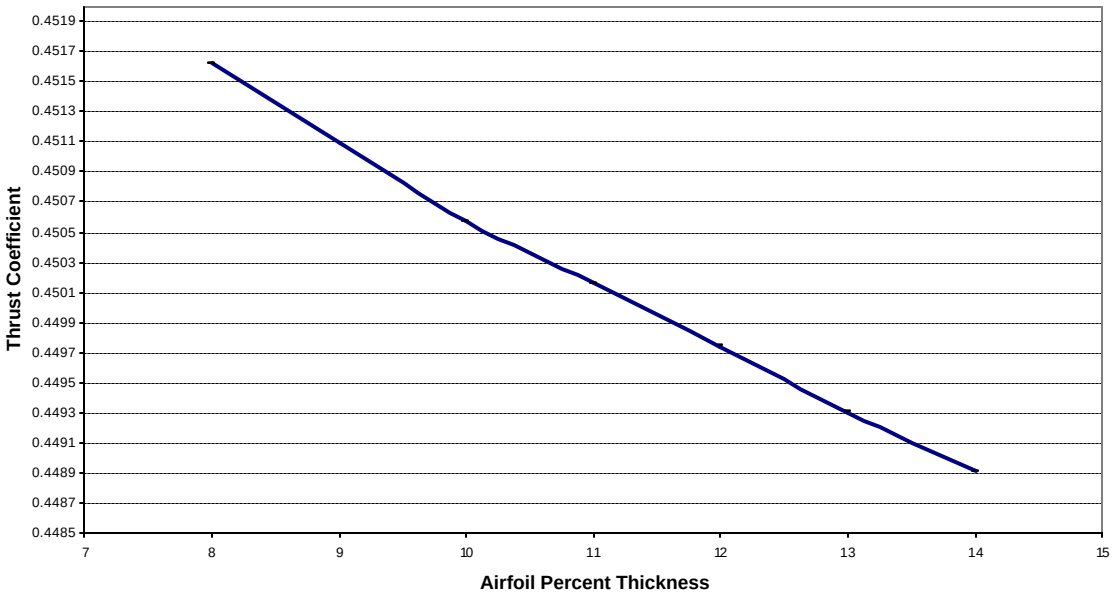

Figure 19. Airfoil Thickness vs. Thrust Coefficient

It was found that the effect of thickness on a purely plunging airfoil's thrust production is negligible. The plot in Figure 19 is misleading as it appears to show a decrease in thrust as thickness increases. However, the vertical scale represents a very small percentage change in thrust coefficient; well below the numerical accuracy of the method.

Determining if thrust was sensitive to changes in airfoil camber was accomplished by putting several NACA airfoils of increasing camber through purely plunging motion in UPOT.

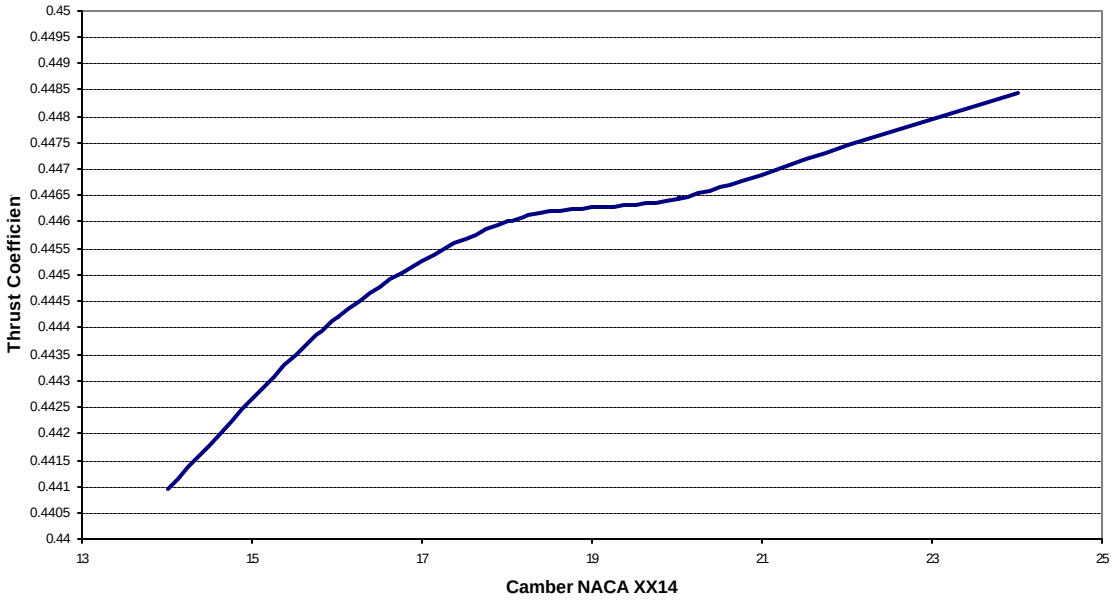

Figure 20. Airfoil Camber vs. Thrust Coefficient

The effect of camber on a purely plunging airfoil's thrust production is also negligible. Again, the apparent increase in Figure 20 is deceptive because the vertical scale shows a small percentage change that is below the numerical accuracy of the method.

Therefore, these runs verified that thrust production is independent of mean angle of attack and airfoil shape. This effectively allowed one airfoil at a given angle of attack to approximate the numerous different combinations of sailplane wings at different flight velocities for thrust production. The screen image of a typical UPOT run is shown in Figure 21. The runs also showed how individual UPOT runs were very time-consuming. The data used to produce the above plots required a few hours of user-intensive computing time. To apply a strip-theory approach, it would be necessary to sweep through numerous cases of reduced-frequency and amplitude. Because user time was limited, a matrix-generating version of UPOT was created to produce the required volumes of data in a more efficient manner.

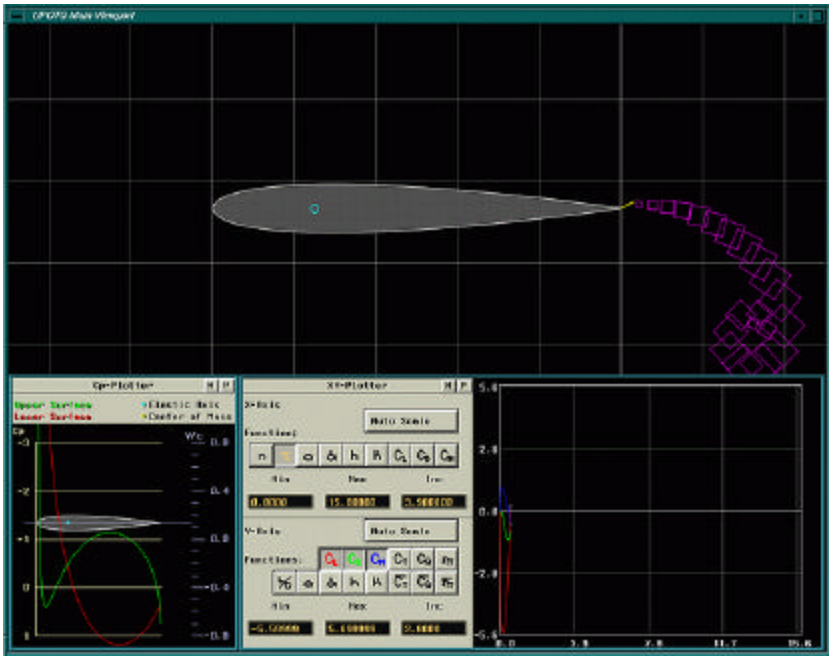

Figure 21. Purely Plunging Airfoil UPOT Screen Image

Once the results of the matrix-generating version of UPOT became available, the data was loaded into MATLAB codes that used the strip-theory approach to calculate power requirements and thrust production of flapping-wing sections.

C. 3-D CORRECTIONS

CMARC is a low order, 3-D flow-solving module from the Digital Wind Tunnel (DWT) software suite from AeroLogic. [Ref. 12] CMARC, is a PC-based version of PMARC (Panel Method Ames Research Center), that performs 3-D potential flow simulations. CMARC has been used to study similar cases of flapping-wing propulsion [Ref. 12] and compares favorably with FLOWer, a finite volume, Euler, Navier/Stokes code developed at the DLR Braunschweig (Deutsches Zentrum fur Luft- und Raumfahrt), Germany [20, 21, 22].

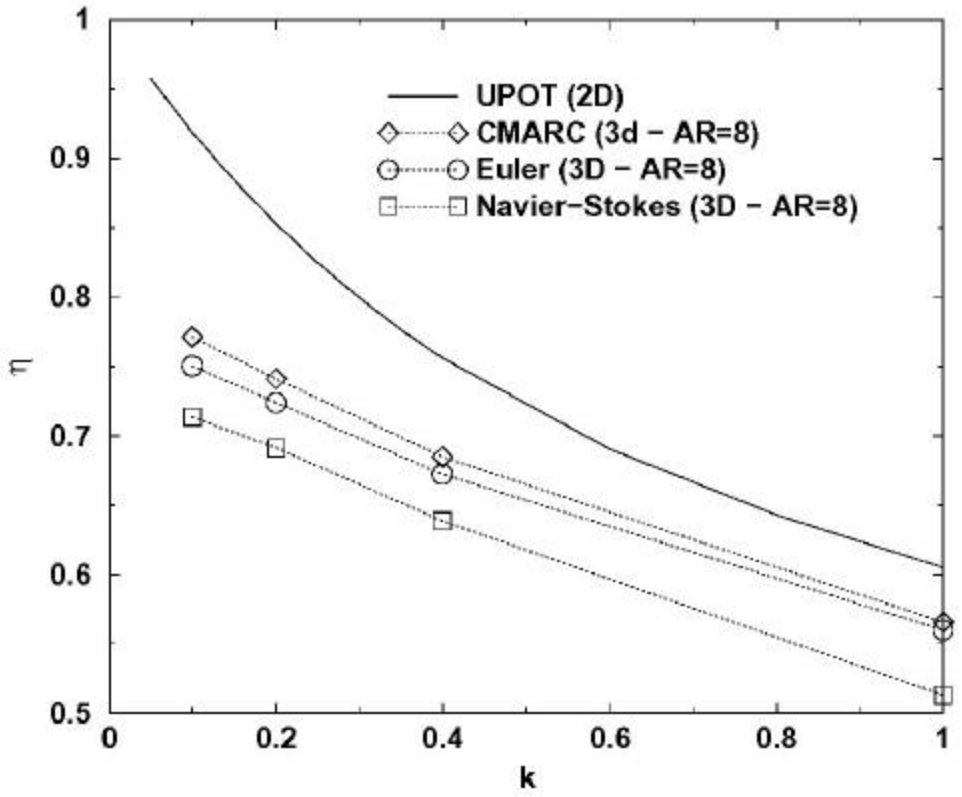

Figure 22. Propulsive Efficiency vs. Reduced Frequency

CMARC predicts higher values than the Navier-Stokes solver, but very closely approximates the Euler results, as can be seen, in Figure 22.

Earlier versions of the strip-theory code revealed that using elliptic correction factors for both thrust and power calculation was flawed. This earlier code did not include wing aspect ratio as a component, nor were thrust and power coefficients scaled appropriately.

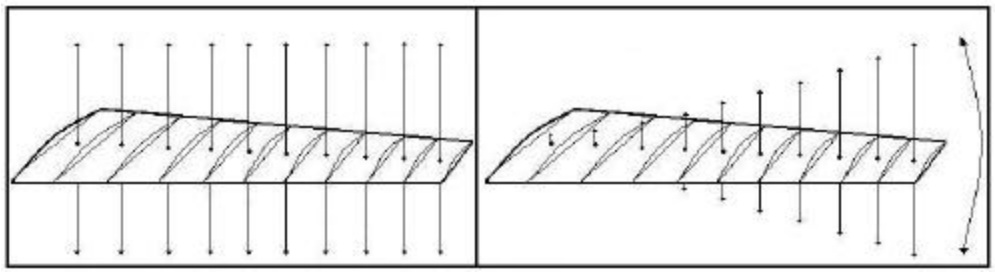

Figure 23. Straight Plunge vs. Bird-flapping Motions

Using CMARC data for a straight plunge wing section, spanwise load factors were produced. CMARC solutions were generously provided by S. Pollard. [Ref. 23] The straight plunge motion was used instead of bird-flapping motion, as shown in Figure 23, because it provided a more direct comparison with UPOT, and it offered the best approximation for spanwise load factors. Interpolating this data provided corrections for purely plunging wing sections of differing aspect ratios, as shown in Figures 24 and 25. The interpolating segment of code was added to the existing MATLAB programs to create spanwise load factors for the strip-theory approach in calculating thrust and power.

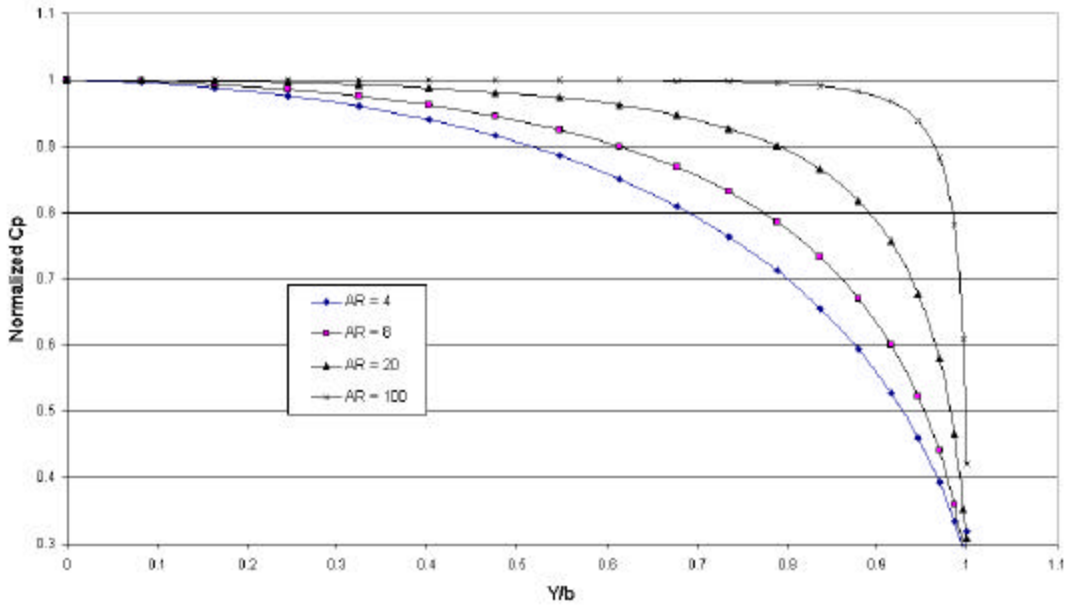

Figure 24. Normalized Power Coefficient Semi-span Distribution

It is clearly shown in Figures 24 and 25 that thrust and power coefficients do not follow elliptical distributions, and are different from one another as well. The span-wise distribution of normalized power coefficient is shown in Figure 24; while the span-wise distribution of normalized thrust coefficient is shown in Figure 25.

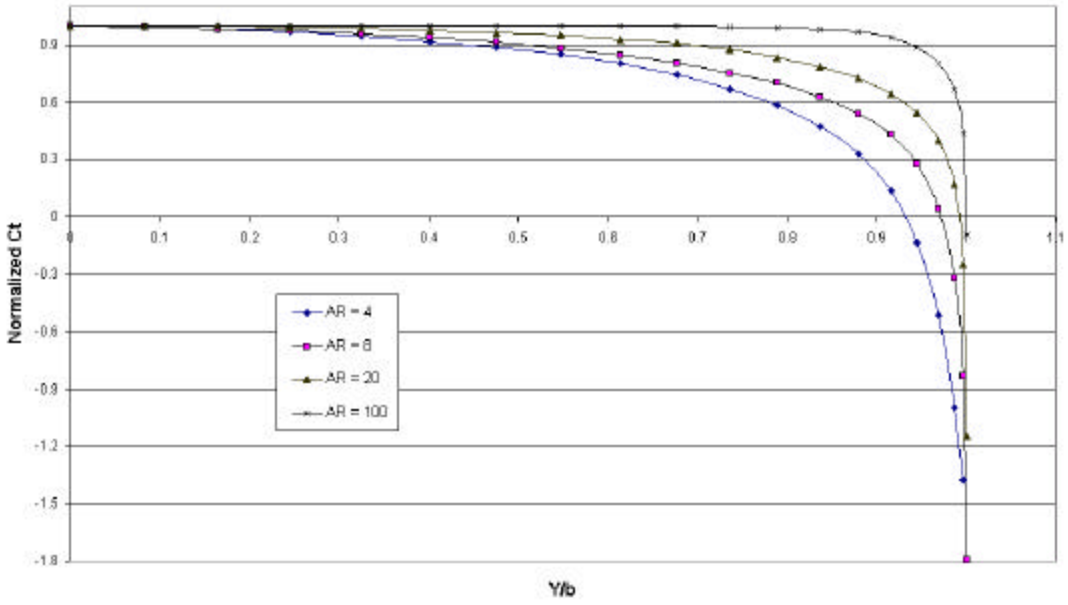

Figure 25. Normalized Thrust Coefficient Semi-span Distribution

It can also be seen that as aspect ratio increases, the 3-D results rapidly approach the 2-D results as the losses are confined to a small region near the tip. There is a clear difference between aspect ratio 4, which exhibits degradation of thrust starting from 35% span and aspect ratio 100 that shows little losses up to 90% span. Aspect ratio 20, which has good thrust performance up to 70% span, closely approximates the *Sparrow Hawk* and *Light Hawk* ultralight sailplanes with aspect ratios of 18.6 and 19.2 respectively.

Because of 3-D effects, the wingtip is immersed in the wingtip vortex. Therefore the limiting induced angle of attack occurs inboard along the span. The plot of CMARC data for span-wise thrust coefficient distribution in Figure 26 illustrates this phenomenon.

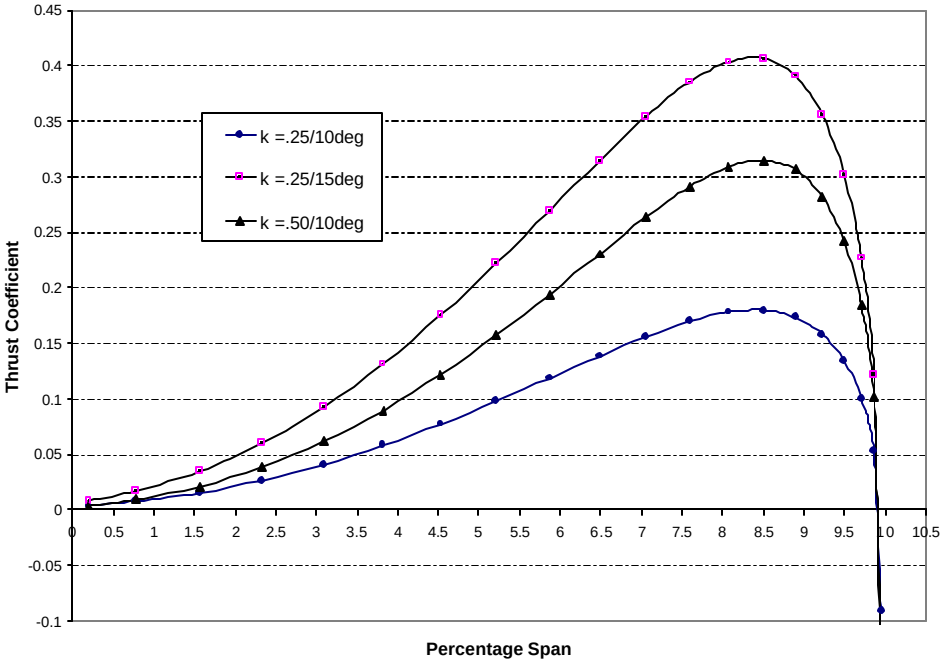

Figure 26. Thrust Coefficient vs. Semi-span Position

Thrust peaks at the 85% semi-span location, as the figure also shows. This position is where the 39 degree induced angle of attack limit should be applied.

D. VALIDATION

It was necessary to determine if the assumptions that were made for the numerical method were valid. CMARC solutions for bird-like flapping wings were produced by S. Pollard. [Ref. 23] A new application of the strip-theory MATLAB code was created in hopes of reproducing the CMARC solutions.

The output from this version of the code was compared with CMARC solutions for a finite-span flapping-wing. Several runs were made with varying values of reduced frequency, k, and flapping angles, F, to match the flapping-wing data provided with CMARC. The three runs were for an aspect ratio 20 wing, with no taper, with a flapping angle of 10 degrees: $k = 0.2$, $k = 0.4$, $k = 0.6$.

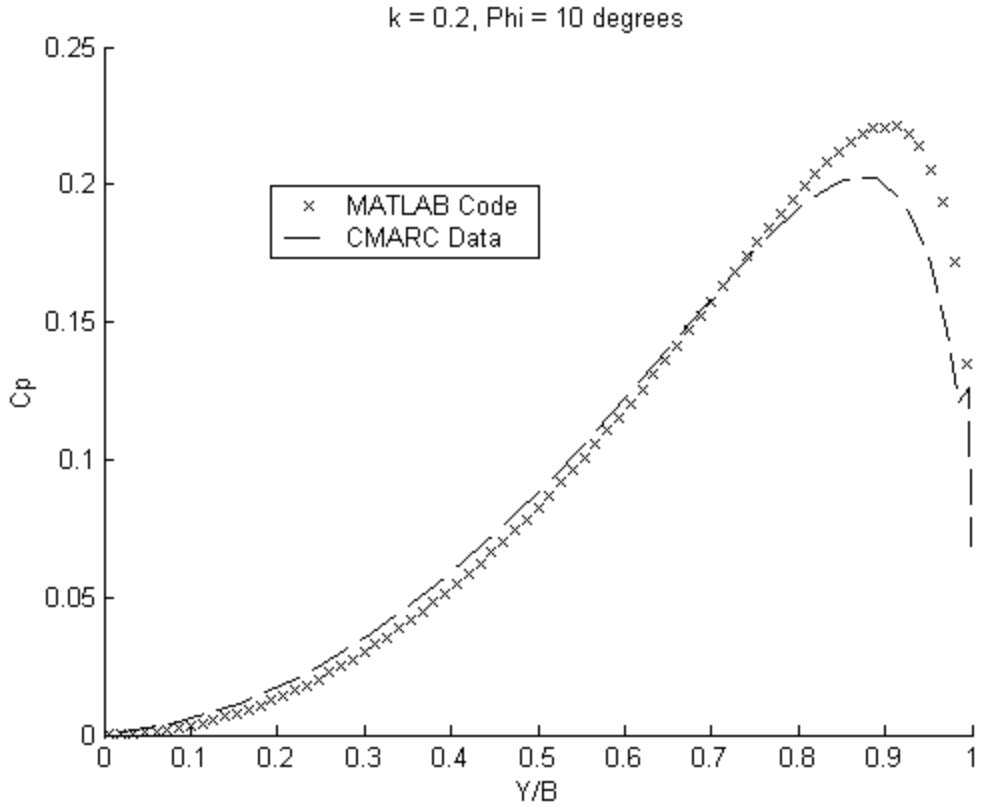

Figure 27. Validation code vs. CMARC Data for Cp

The strip-theory approach utilized in this study closely approximates the CMARC data for span-wise variation of power-coefficient, as shown in Figure 27. The close correlation provided validation for the numerical method employed in solving flapping-wing thrust production and power consumption.

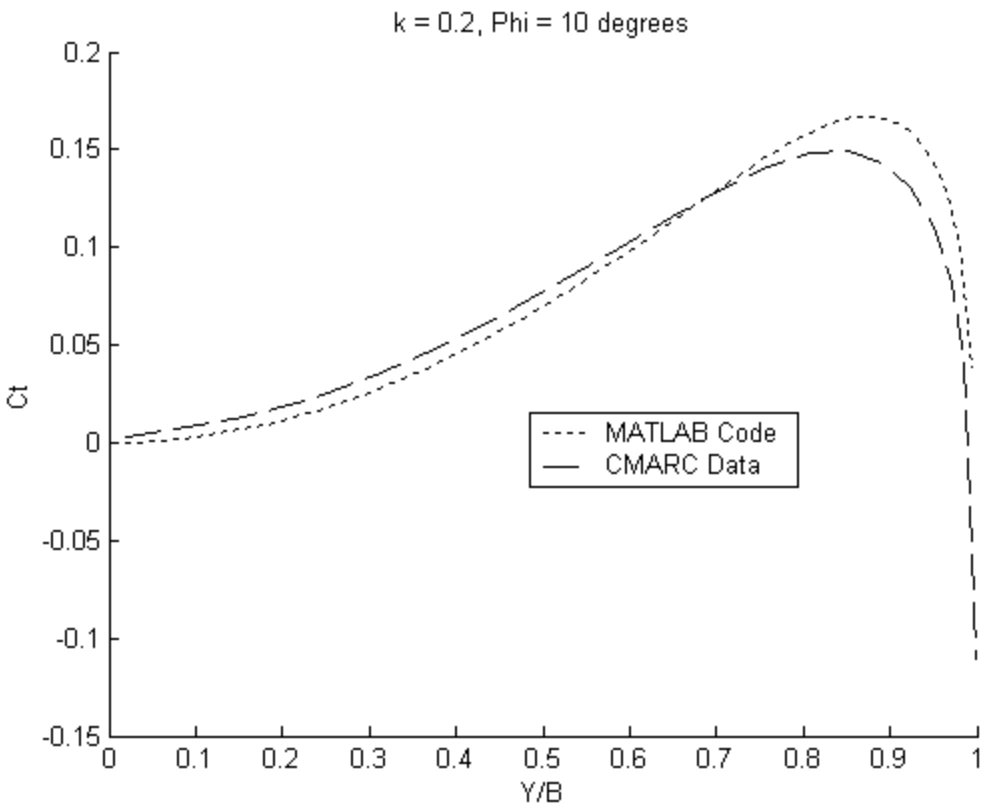

Figure 28. Validation code vs. CMARC Data for Ct

Similarly, the strip-theory approach closely approximates the results obtained from the CMARC data for span wise variation of thrust-coefficient, as illustrated in Figure 28. CMARC predicts more power and thrust from the wing root to about the mid-wing position, while less power and thrust occur near the wing tip. This is most likely due to the stronger tip vortex in the CMARC solution. Recall that the spanwise load correction factors used in the strip-theory approach were produced with a purely plunging motion, vice a bird-flapping motion. The bird-flapping model would experience a stronger tip vortex than the MATLAB code would experience. The strip-theory approach seems to provide a worst-case scenario for the wing load factor. Knowing this is beneficial as it would help the designer know how to build the wing sections as most flapping-induced load factors should remain below this predicted level.

The close correlation between the results from the numerical method and the results obtained from CMARC demonstrate that the strip-theory approach is valid.

III. RESULTS

A. IDENTIFYING TRENDS

The first three applications of the code utilized the strip-theory approach to calculate thrust output and power requirement of a flapping wing. The first application swept through flapping angles from 0 to 15 degrees and the velocity range of the aircraft with a user defined input for flapping frequency. The second application varied flapping angle and flapping frequency from 0.01 to 1.5Hz with a user defined input for flight velocity. The third application swept through the velocity and frequency range with a user defined input of flapping angle.

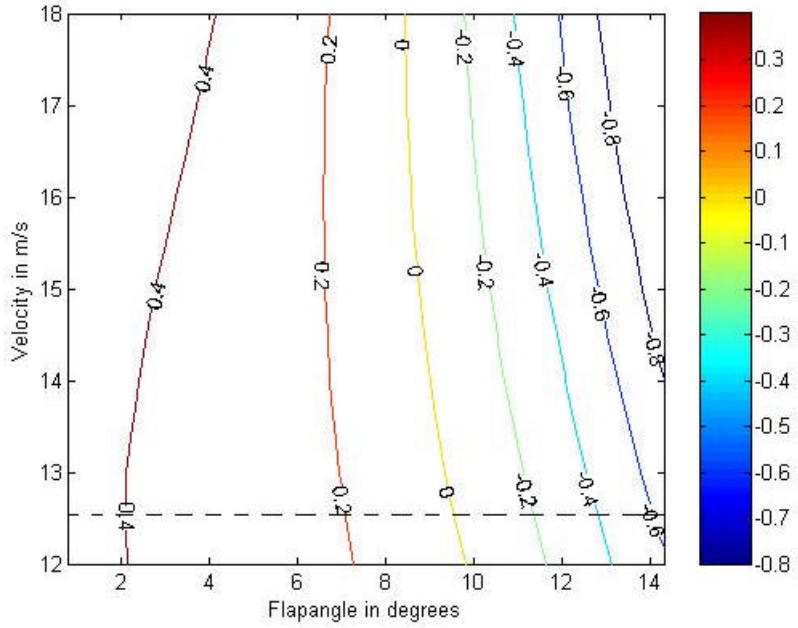

Figure 29. Sink-rate Contour for Varying Velocity and Flapping Angle

Loading the *Light Hawk* sailplane's drag data into the first application produced Figure 29, a contour of sink-rate for a flapping frequency of 0.75Hz, with velocity and flapping angle being varied. The negative contours, where flapping angle is high, apply to negative net sink, or actual climb rates. The minimum sink-rate of 0.42m/s for the

base *Light Hawk* aircraft occurs at a velocity of 12.5m/s, and is designated by the dashed horizontal line in the plot. As the flapping angle nears zero, thrust approaches zero, and the minimum sink velocity approaches the original minimum sink velocity of 12.5m/s. As the flapping angle increases the flapping amplitude, *h*, increases. The contour lines become closely spaced at the higher flapping angles, meaning that increased thrust is offsetting the sink-rate more effectively. This agrees well with 2-D theory where thrust increases as the flapping amplitude squared. The larger the flapping angle, the more beneficial it is to fly at higher velocities. Be aware this trend pays no heed to what the power requirement is.

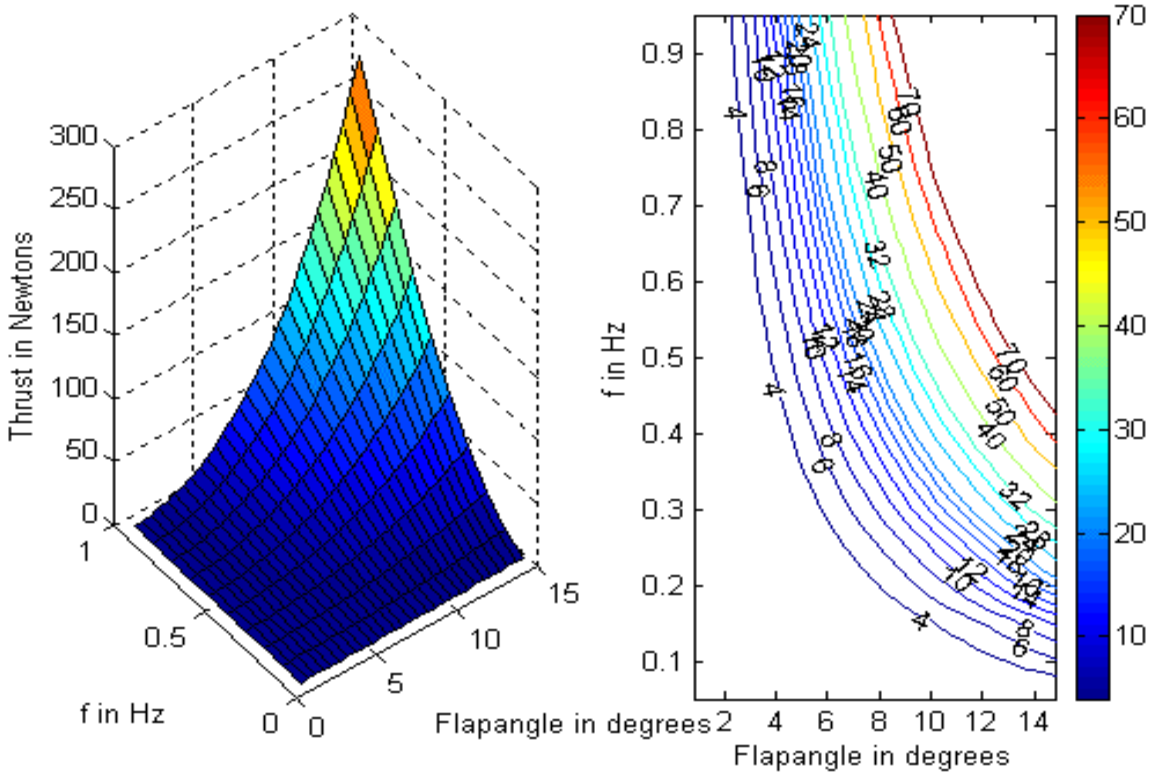

Figure 30. Thrust Plots for Varying Flapping Angles and Frequencies

The second application yields the behavior of thrust with varying flapping angles and flapping frequencies for the flight velocity of 15m/s. It is clear that the lower flapping angles produce very little benefit, in Figure 30. The thrust is accessible at low to medium frequencies where flapping angles are high.

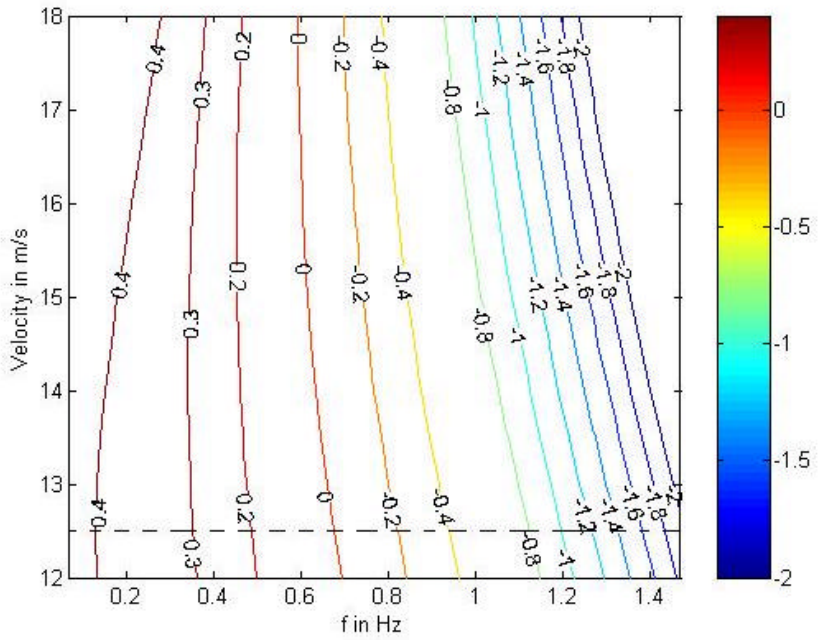

Figure 31. Sink-rate Contour for Varying Velocity and Frequency

The third application's sink-rate contour for a flapping angle of 10 degrees, with velocity and frequency being varied is shown in Figure 31. Again, the minimum sink-rate for the stock aircraft is 0.42m/s at a velocity of 12.5m/s designated by the horizontal dashed line. The close spacing of the contours as frequency increases points to the trend that thrust increases as the square of the flapping frequency. This suggests that it is more beneficial to fly at higher velocities if frequency is increased; essentially at a lower reduced frequency, *k*. However, like Figure 29 before, the power requirement is ignored. It is interesting to point out that if a line is drawn through each of the lowest sink-rate points (the vertical section of each contour line), the resulting curve asymptotically approaches the 12.5m/s minimum sink-rate of the stock aircraft. As an example, it can be seen that a 50% reduction in minimum sink would require a flapping angle of 7 degrees at a frequency of 0.45Hz.

The first three applications of the code were useful in viewing the relationships between the different parameters and helped point the way toward future optimizations. They showed that propulsive efficiency was least affected by changes in flapping angle- a trend that would be further exploited in later applications. The first applications of the

code suggest that propulsive efficiency increases at higher velocities. Recalling equation (1), efficiency increases as reduced frequency, k, decreases.

$$k = \frac{2p\ fc}{U} \qquad (1)$$

To make k as small as possible, it is necessary to increase velocity, decrease flapping frequency, and decrease chord length. This agrees with theory, where efficiency asymptotically approaches 100% as k goes to 0. [Ref. 17]

B. CONSTRAINTS

An improved application of the code was produced that included an iterative method for finding the maximum thrust available given a user-specified power constraint. Since the aircraft are limited by human power output (200W), what parameters could be optimized to maximize thrust? As mentioned earlier, propulsive efficiency was least affected by changes in flapping angle. In addition, flapping angle is not tied to the structure of the airframe. The constraining code used the secant method to determine the flapping angle that would satisfy the specified power restriction as velocity and flapping frequency were varied. As velocity increased, the allowable flap angle for a given frequency decreased, likewise, at lower velocities large flap angles were allowed with higher frequencies. An illustration of how this works is shown in Figure 32, where the power plateaus at the specified power restriction of 1250W.

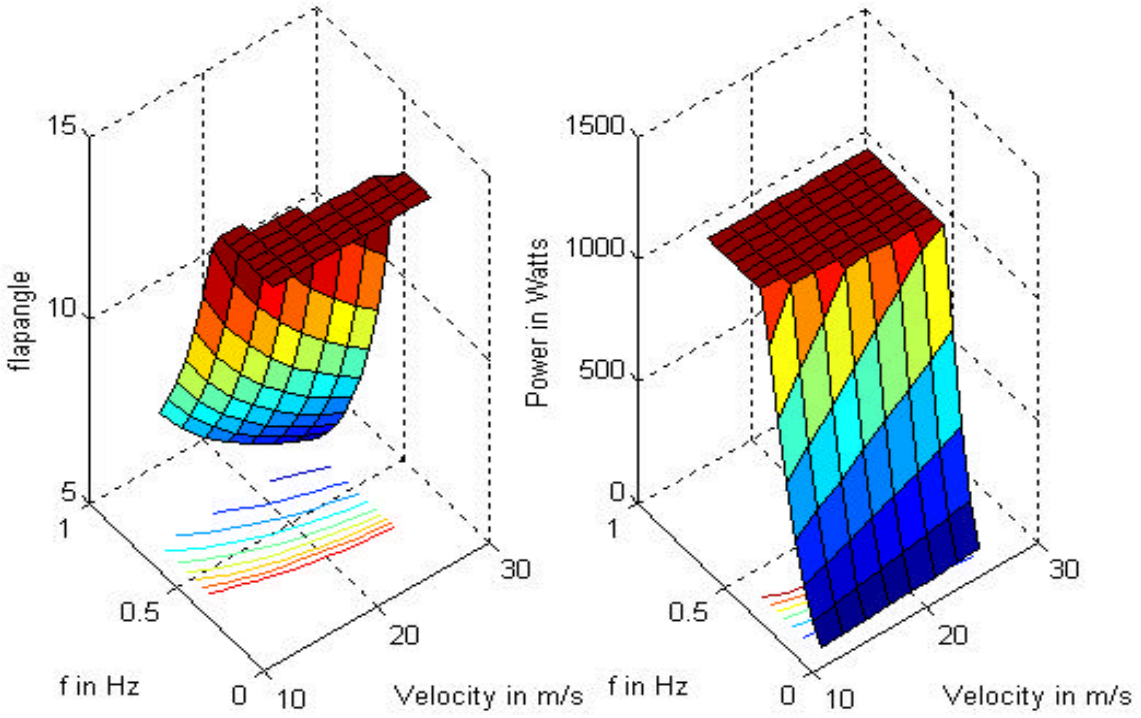

Figure 32. Specified Power Restriction of 1250W

The wing is free to move at the maximum flapping angle of 15 degrees until the power requirement reaches 1250W as shown by the plateau on the left. On the right, this corresponds to the rise of the power requirement as the flapping frequency increases for the given flapping angle of 15 degrees. When the power constraint is met, the flapping angle is curtailed to keep the power requirement at the limit. The power plateau on the right corresponds to the decrease in flapping angle to the left.

The constraining code was subsequently tailored to the three aircraft configurations in this study: the human-powered *SparrowHawk* and *Light Hawk* applications included aircraft-specific drag-polar data that was obtained from the respective manufacturers. In addition, the flight velocities, flapping frequencies, and flapping angles were tailored for the aircraft. The final aircraft was an electric-powered sustainer version of the *Light Hawk* sailplane. The guideline for the sustainer system is to arrest sink-rate and provide for a maximum 0.85m/s climb rate. As noted earlier, after losses were considered, the *Light Hawk* aircraft required 2875W to meet the criteria. The sustainer application found the most efficient means of thrust production using a 2875W imbedded power restriction.

1. Human-Powered *SparrowHawk* Results

The relatively short span of this configuration allows for larger maximum flap angles with a maximum flapping frequency of 1.0Hz. Limiting the 85% span location to a maximum of 39 degrees as shown in Reference 12 required holding the wing flapping angle below 16 degrees for the minimum sink velocity of 20.5m/s, and below 19 degrees for the L/D_{max} flight velocity of 27.9m/s. To ensure the solutions did not exceed the limits of UPOT, the flapping angle was limited to +/-15 degrees. The 200W imbedded power restriction allows for approximately 9N of thrust available at minimum sink velocity (20.5m/s), as shown in Figure 33. This requires 13 degrees of flapping angle with as low as a 0.25Hz flapping frequency. Under constraints the actual maximum induced angle of attack never exceeded 9.6 degrees.

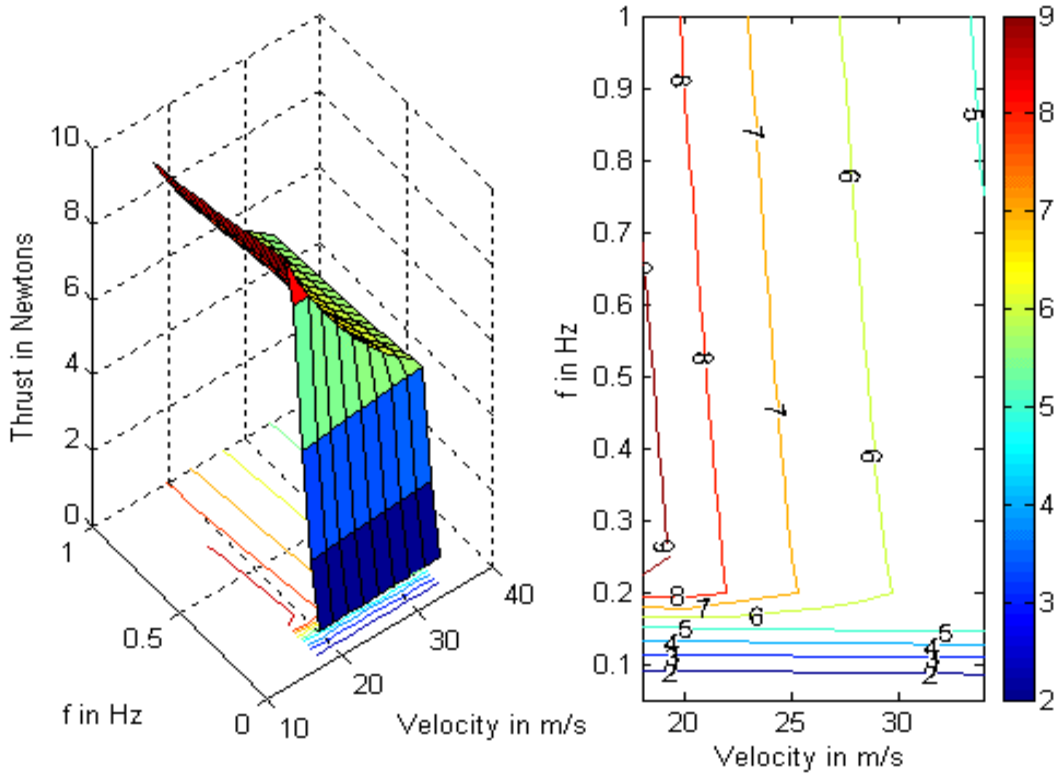

Figure 33. *SparrowHawk* Thrust Production

At the L/D_{max} velocity (27.9m/s) the thrust available is 6N, occurring at a flapping frequency of 0.2Hz and 13 to 14 degrees of flapping angle. This thrust partially offsets drag and reduces the *SparrowHawk's* sink-rate as shown in Figures 34, 35, and 36.

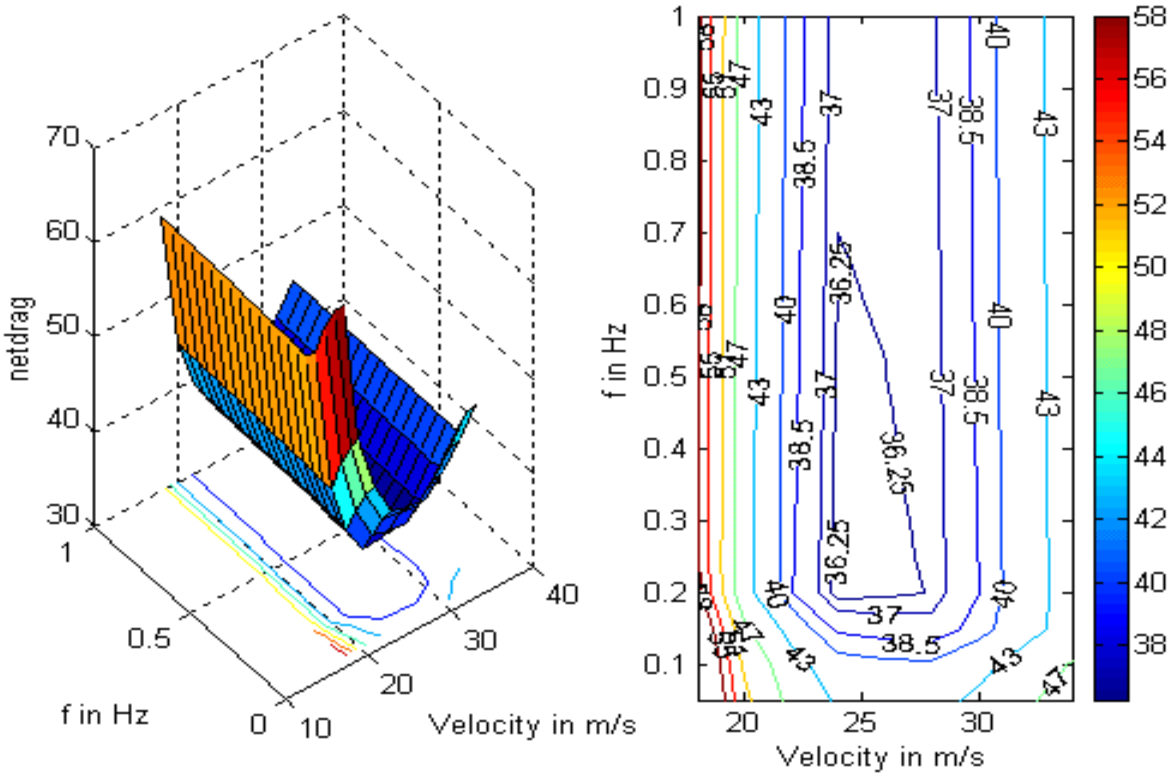

Figure 34. *SparrowHawk* Net Drag

The characteristic drag bucket is made more pronounced by thrust produced by the flapping-wing segments. The *SparrowHawk's* lowest drag count is normally 42.6N at L/D_{max} velocity. The value falls below 36.3N, a 15% reduction, as shown in Figure 34. The sailplane's new L/D_{max} increases from 36.5:1 to almost 43:1 on 200W of human power. It is interesting to note that the aircraft can now maintain the original L/D_{max} drag value of 42.6N, once available only at a singular flight speed, throughout the wide velocity range of 21m/s to 33m/s. Maintaining this low drag up to 33m/s equates to flying at L/D_{max} 20% faster than before.

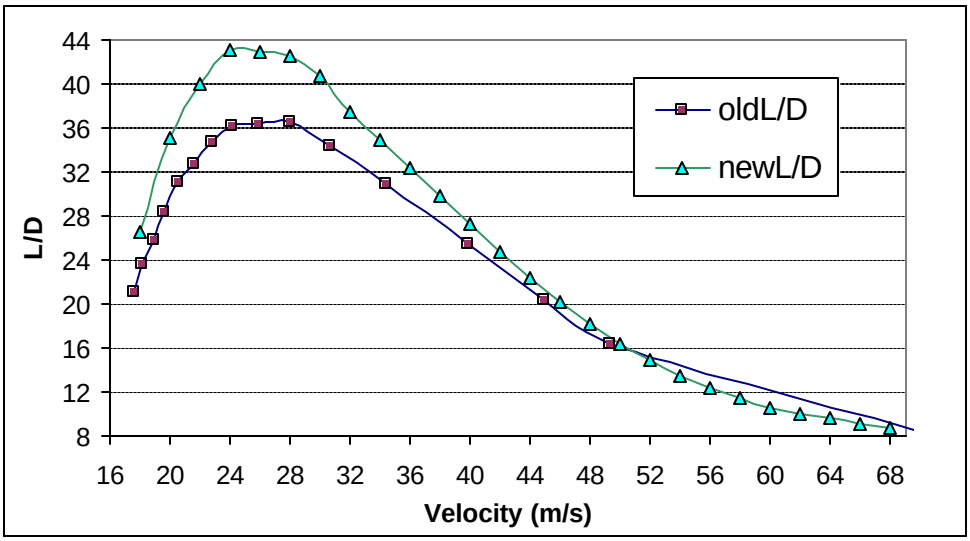

Figure 35. *SparrowHawk* expanded L/D vs. Velocity

To further illustrate the improvement in L/D, Figure 35 was created. Superimposed on the stock aircraft's curve is the flapping *SparrowHawk's* L/D data. The expanded flight envelope that makes for a more versatile cross-country sailplane can be clearly seen in the figure.

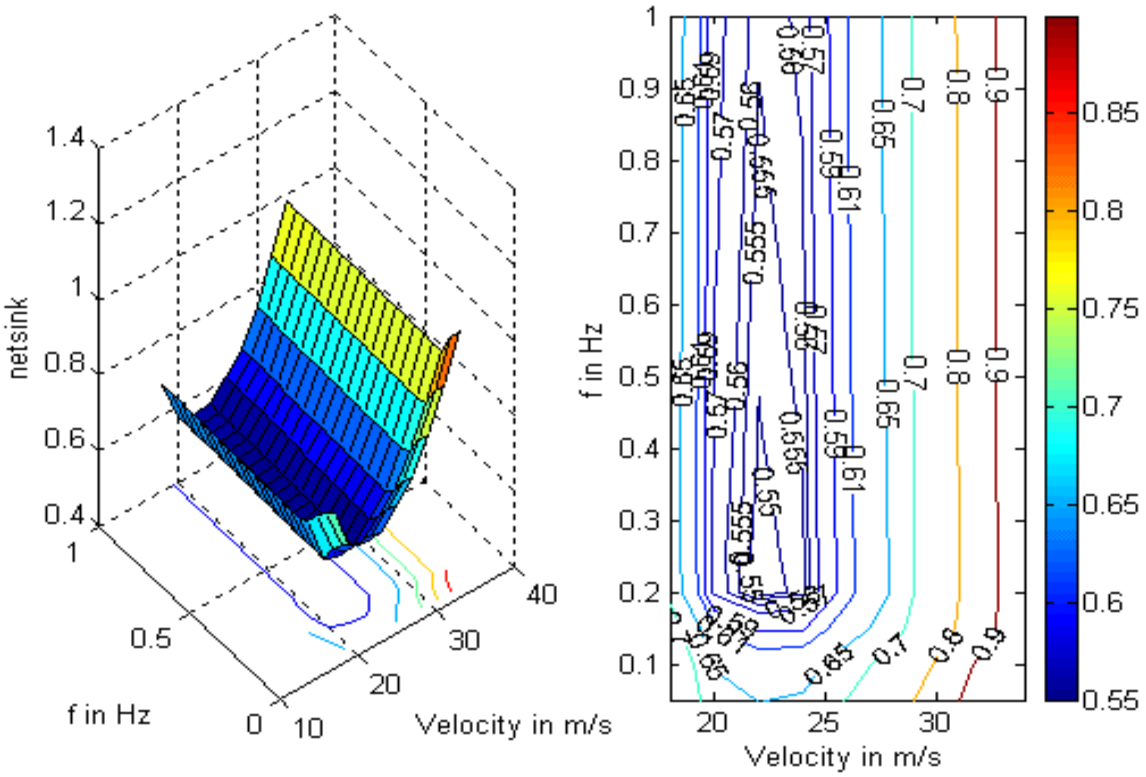

Figure 36. *SparrowHawk* Sink Rate

The benefits realized through flapping-wing propulsion in decreasing minimum sink are shown in Figure 36. The stock *SparrowHawk's* minimum sink-rate of 0.66m/s occurs at 20.5m/s. The net value of 0.55m/s is 16% lower and gives the *SparrowHawk* a lower minimum sink-rate than almost all FAI 15m class sailplanes. Moreover, a lower sink-rate than the original can be maintained throughout a range of flight speeds from just above stall speed to 26m/s. At the higher velocity, *SparrowHawk* would be flying 27% faster than its baseline minimum sink velocity with no increase in sink rate.

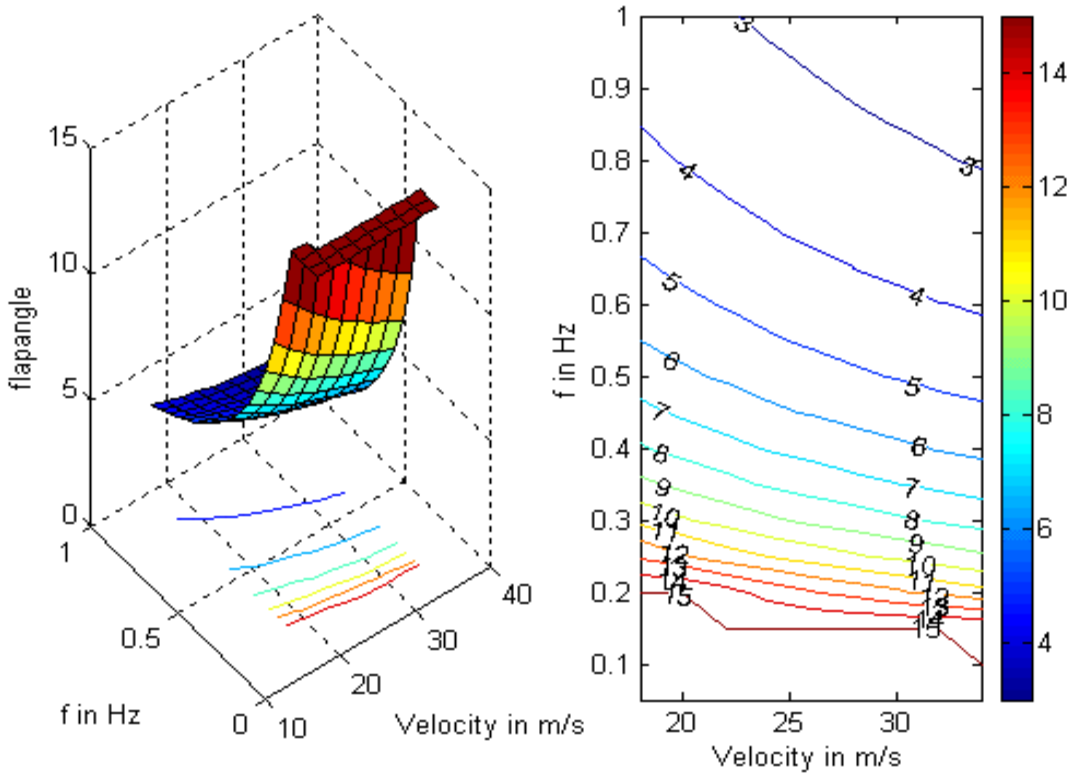

Figure 37. *SparrowHawk* Flapping Angle Variation

The way in which the code adjusts the flapping angle in response to the specified power restriction of 200W is shown in Figure 37. The wing is free to flap to the 15 degree maximum up to 0.2Hz near the stall speed, and 0.1Hz at the high end of the velocity range.

It is interesting to note from the figures that although specific levels of thrust, net-drag, and net-sink rates could also be achieved at high flapping frequencies with smaller flapping angles; the lowest frequency at which the desired parameter appeared was chosen, because propulsive efficiency favors low flapping frequencies and large flapping angles, as discussed earlier.

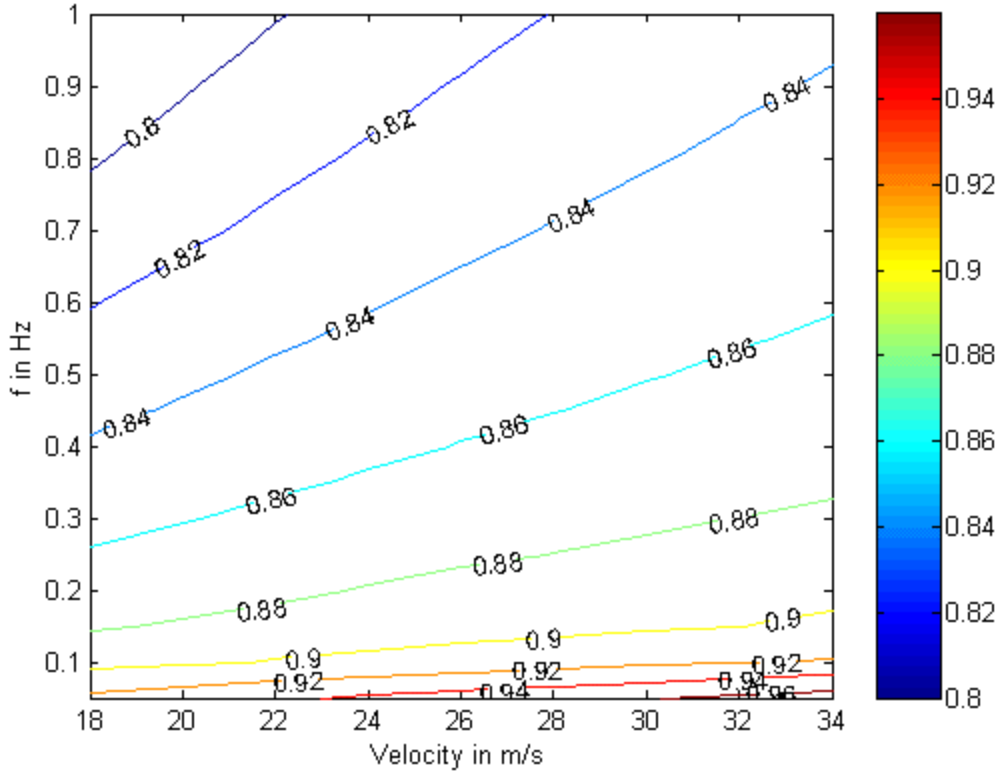

Figure 38. *SparrowHawk* Propulsive Efficiency Contour

The propulsive efficiency determined for *SparrowHawk* is approximately 87% for the minimum sink regime (20.5m/s), and 88% for the L/D_{max} regime (27.9m/s), as shown in Figure 38. The contours follow the trend stated earlier that propulsive efficiency favors higher airspeeds (i.e. L/D_{max}).

2. Human-Powered *Light Hawk* Results

With a more conventional 15m span and slower flight speeds, the flapping amplitude of the *Lighthawk* is limited by the induced angle of attack its wings would encounter as they flapped. Staying below 39 degrees angle of attack at the 85% span location requires holding the wing-flapping angle below +/-7 degrees for the minimum sink velocity of 12.5m/s, and 10 degrees for the L/D_{max} flight velocity of 16.9m/s. Clearly, the low flapping angles are not beneficial for thrust production. However, limiting the flapping frequency to 0.7Hz lowers the reduced frequency, k, to 0.18 at minimum sink velocity. This allows flapping angles of 15 degrees for L/D_{max} flight velocity, and 11 degrees for min sink velocity. To ensure no solution exceeded UPOT's

limits, the code was run with +/-10 degrees where maximum expected α_i at the 85% span location is 38 degrees. Under constraints the maximum induced angle of attack never exceeded 12.6 degrees.

The 200W specified power constraint allows for approximately 13N of thrust available at minimum sink velocity (12.5m/s), as shown in Figure 39. This requires 10 degrees of flapping angle with a low 0.25Hz flapping frequency.

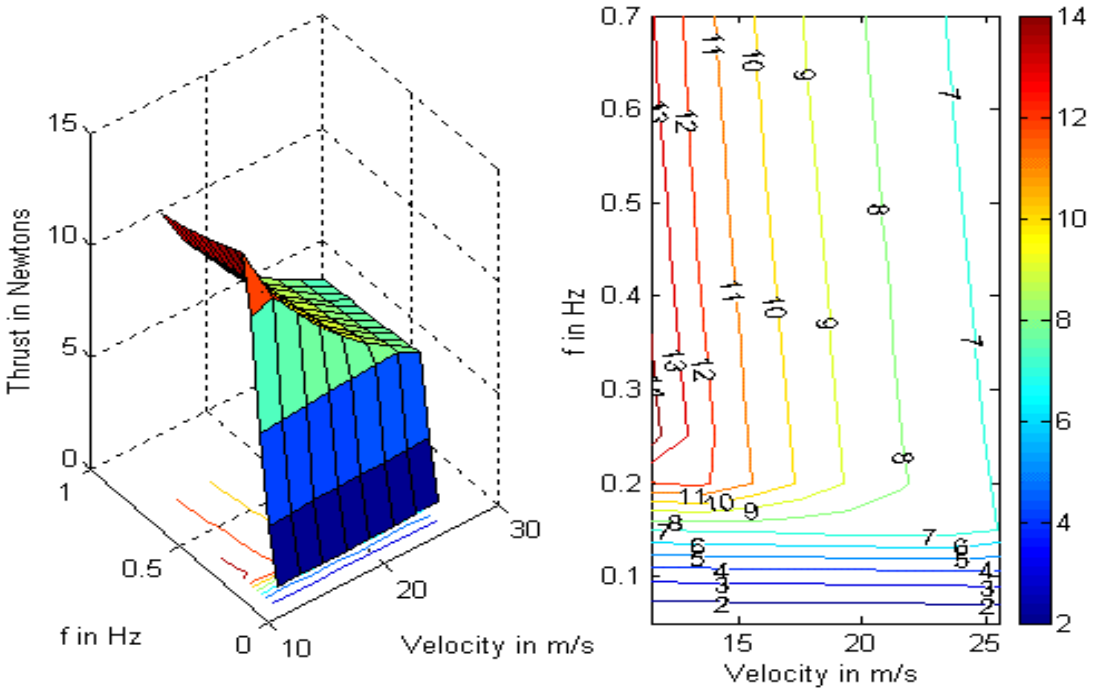

Figure 39. *Light Hawk* Thrust Production

At the L/D_{max} velocity (16.9m/s), 10N of thrust are available with the specified 200W power constraint. This level of thrust occurs at a flapping frequency of 0.2Hz and 9 to 10 degrees of flapping angle, and it partially offsets drag and reduces the *Light Hawk's* sink-rate as shown in Figures 40, 41, and 42.

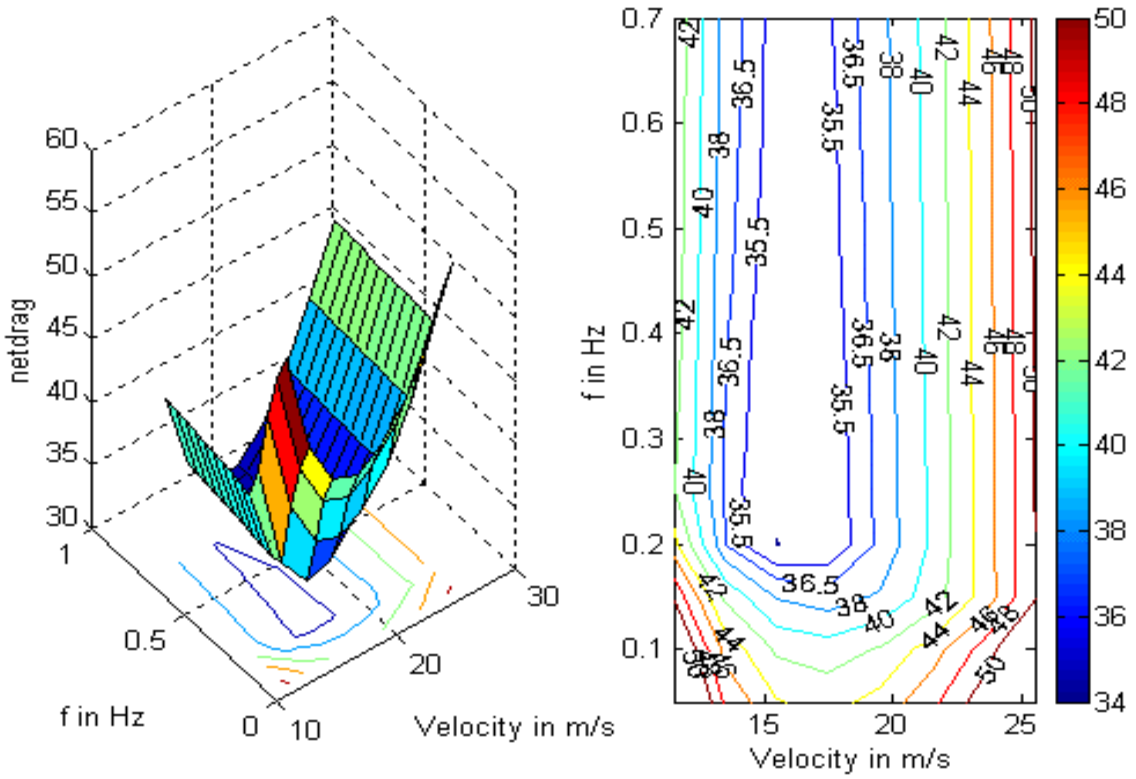

Figure 40. *Light Hawk* Drag Reduction

The *Light Hawk's* lowest drag force is normally 44.3N at L/D_{max} velocity (16.9m/s). Under human power, the value falls below 35.5N, a 20% reduction, as shown in Figure 40. The sailplane's new L/D_{max} increases from 35:1 to 41.8:1 on 200W of human power. The aircraft can now maintain its original L/D_{max} drag value of 44.3N, once available only at a singular flight speed, from just above stall speed to 23m/s. At 23m/s, the aircraft would be flying 36% faster than its original L/D_{max} velocity with the same low drag value.

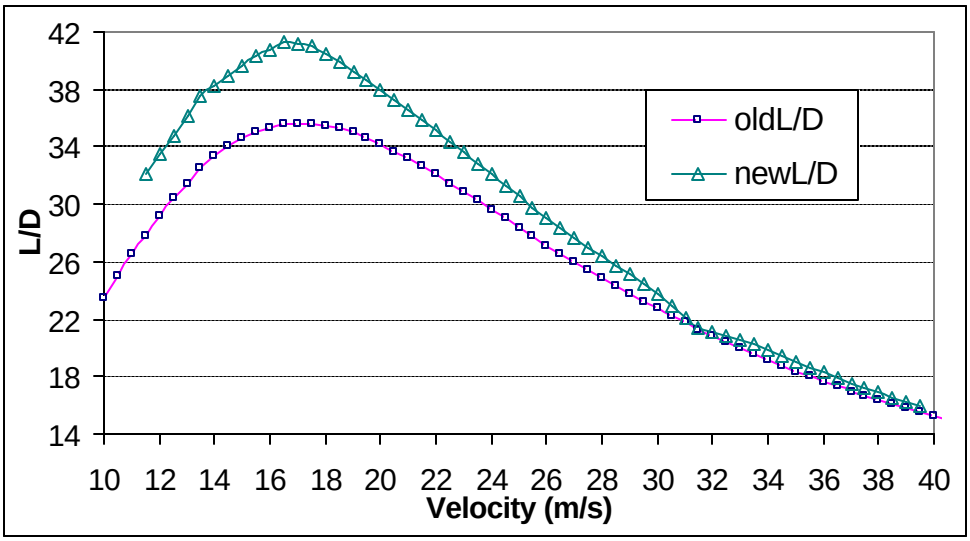

Figure 41. *Light Hawk* Expanded L/D vs. Velocity

The improvement in L/D is clearly shown in Figure 41. The new L/D data is superimposed on the stock aircraft's curve showing the flapping *Light Hawk's* expanded flight envelope. With the increase in L/D at the higher velocities, the aircraft would have improved cross-country potential.

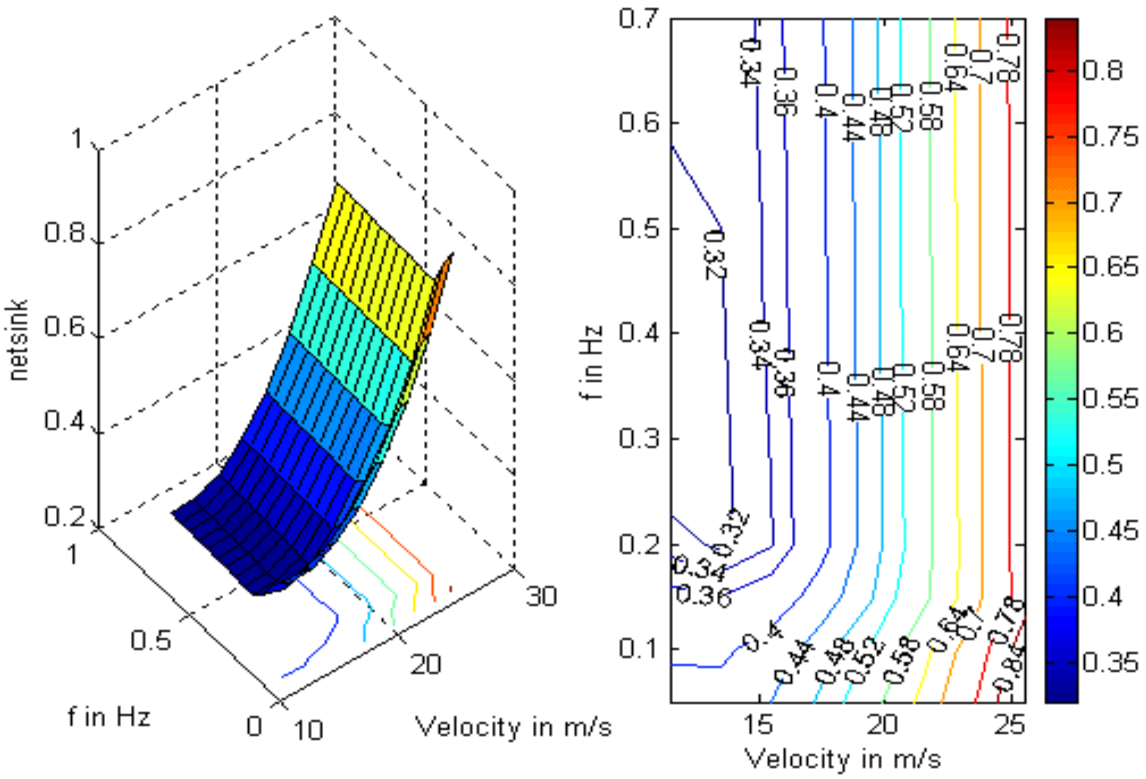

Figure 42. *Light Hawk* Sink Rate

The stock *Light Hawk's* benchmark minimum sink-rate of 0.42m/s at 12.5m/s is matched only by three open class sailplanes with wingspans greater than 24.5m. The net value of 0.32m/s, shown in Figure 42, lowers the sink-rate an additional 24%. No other sailplane, let alone bird or winged mammal, can match this sink rate. Moreover, sink rates lower than the stock aircraft can be maintained from just above stall speed to 17.5m/s. At the higher velocity, *Light Hawk* would be flying 40% faster than its baseline minimum sink velocity with no increase in sink rate.

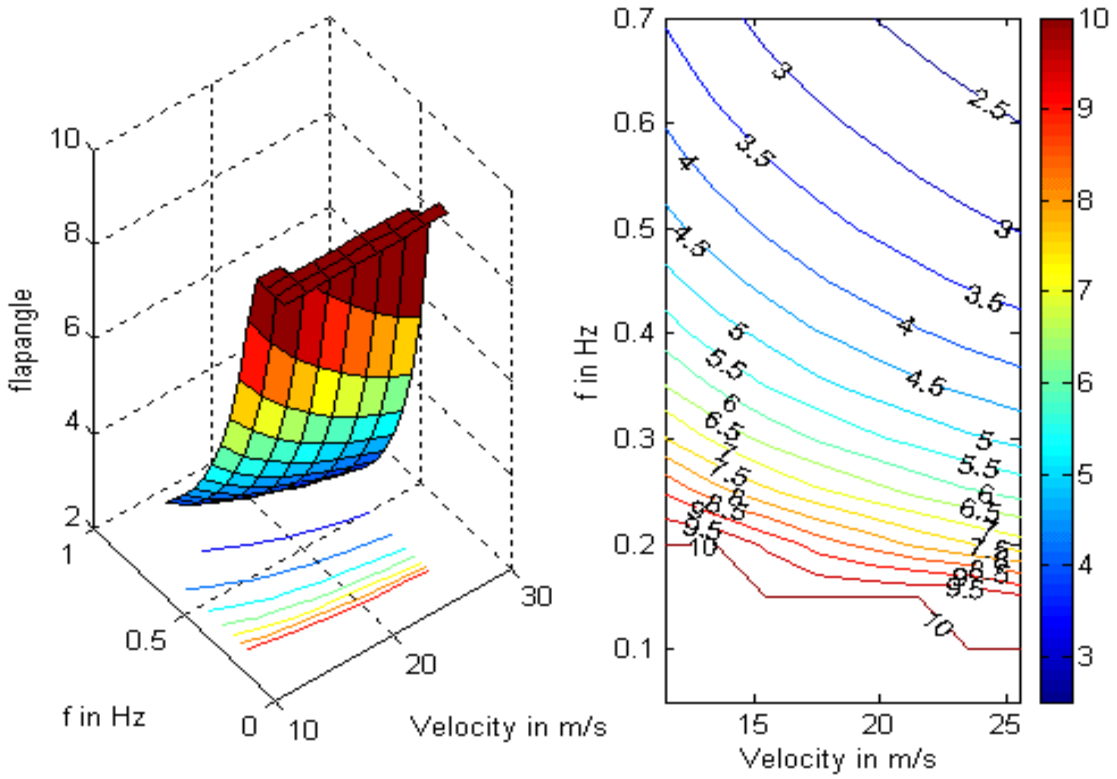

Figure 43. *Light Hawk* Flapping Angle Variation

The way in which the flapping angle is tailored to conform to the 200W power constraint is shown in Figure 43. The wing is free to flap to the 10 degree maximum up to 0.2Hz near the stall speed, and 0.1Hz at the high end of the velocity range. The most useful flapping angles vary from 9.5 degrees to 8 degrees at a flapping frequency of 0.2Hz.

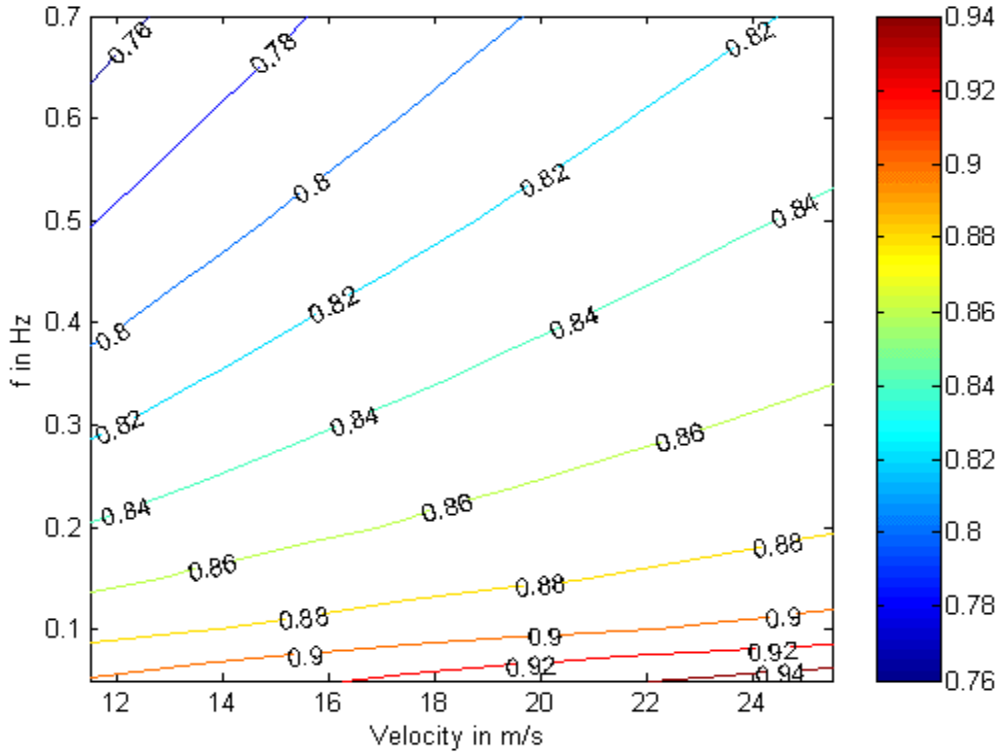

Figure 44. *Light Hawk* Propulsive Efficiency

The variation in propulsive efficiency throughout the velocity and flapping frequency ranges is shown in Figure 44. Propulsive efficiency varies from 85% to 86% depending on flight velocity at minimum sink or L/D_{max}.

3. Sustainer Results

The sustainer system is modeled around the *Light Hawk* aircraft. The code was run using a specified power constraint of 2875W, the amount required to arrest sink-rate and provide for a 0.85m/s rate of climb.

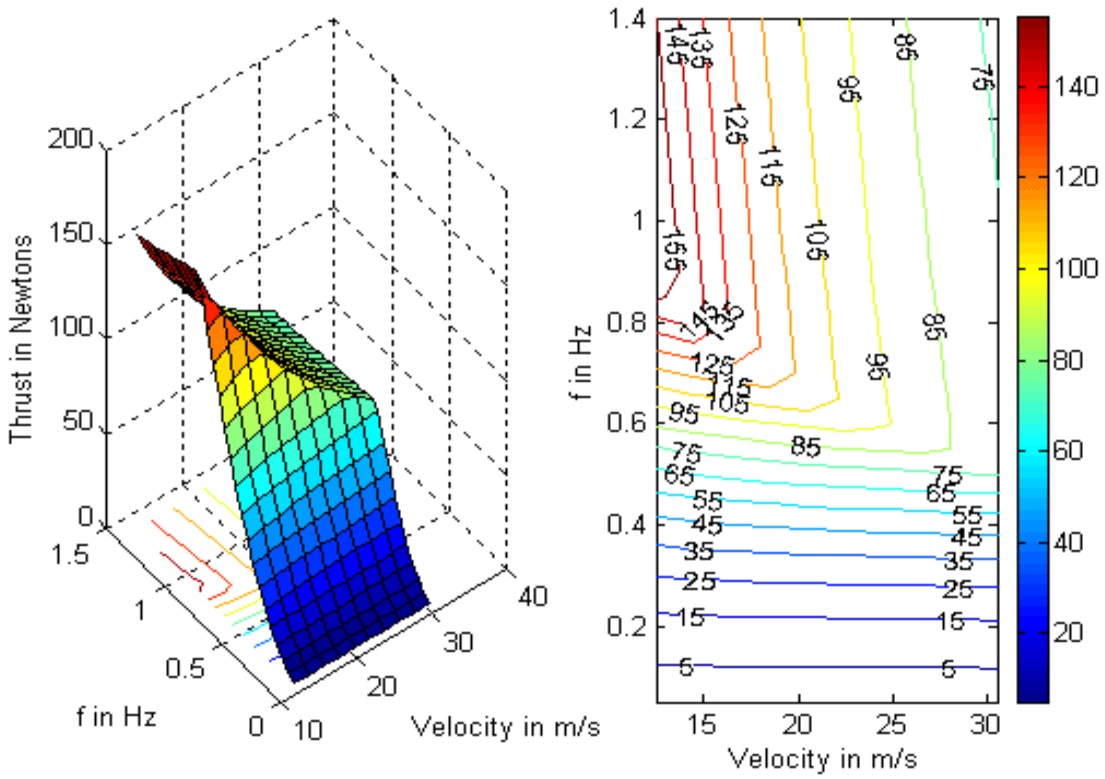

Figure 45. Sustainer Thrust Production

The highest thrust levels are achievable at low flight velocities, as shown in Figure 45. This is similar in behavior to propeller thrust production, where static thrust is the highest value, and increases in airspeed cause a reduction in thrust due to the decrease in induced blade pitch angles.

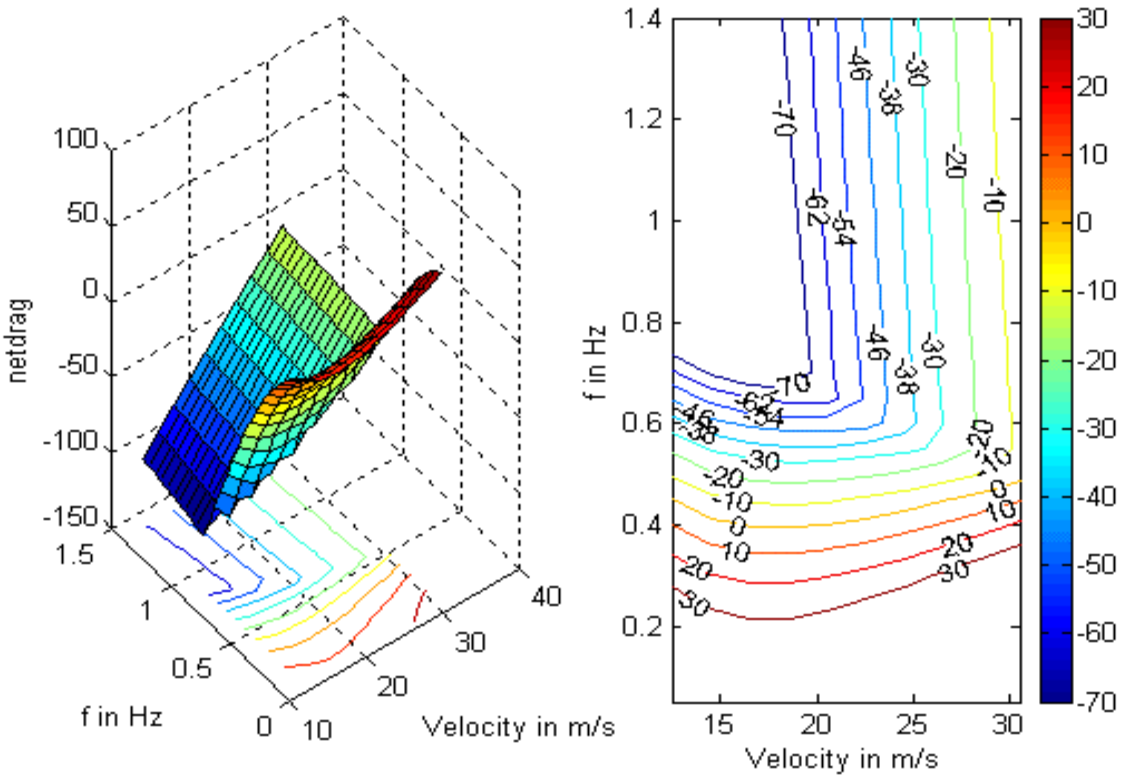

Figure 46. Sustainer Net Drag

Negative contour lines indicate thrust is greater than drag, as shown in Figure 46. The thrust required to arrest sink-rate for a *Light Hawk* is 45N, represented by the net drag contour line of zero. The sustainer produces sufficient thrust throughout the *Light Hawk's* flight speed envelope to arrest sink rate. Flying along the zero contour line essentially provides the *Light Hawk* with an L/D of infinity; of interest for pilots using the system to "buy time" to search for better conditions while minimizing the power drain on the batteries. The power requirement of flying along this contour line varies from 700W at 15m/s up to 1800W at 31m/s.

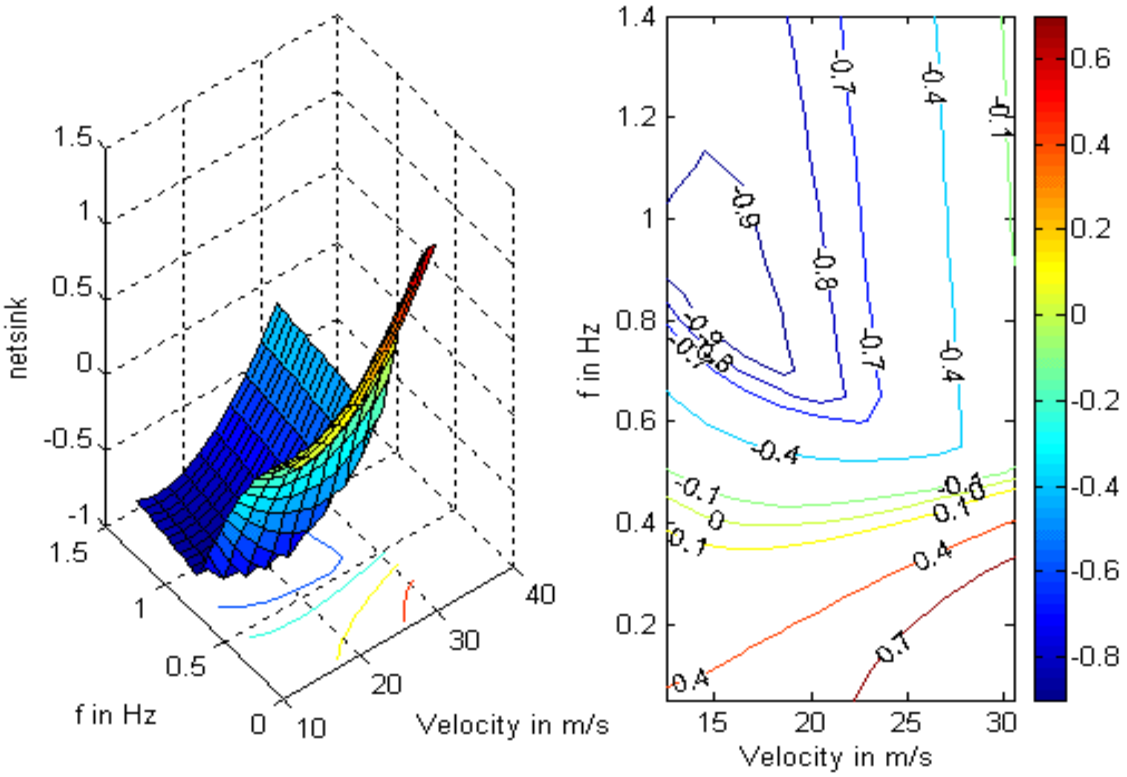

Figure 47. Sustainer Climb and Sink Rates

The performance goal of the sustainer aircraft is a climb rate of 0.85m/s. This is available from a flapping frequency of 0.68Hz at a flight velocity of 19m/s, as shown in Figure 47. The zero sink-rate contour, where sink-rate is arrested, occurs as low as 0.4Hz at a flight speed of 16m/s.

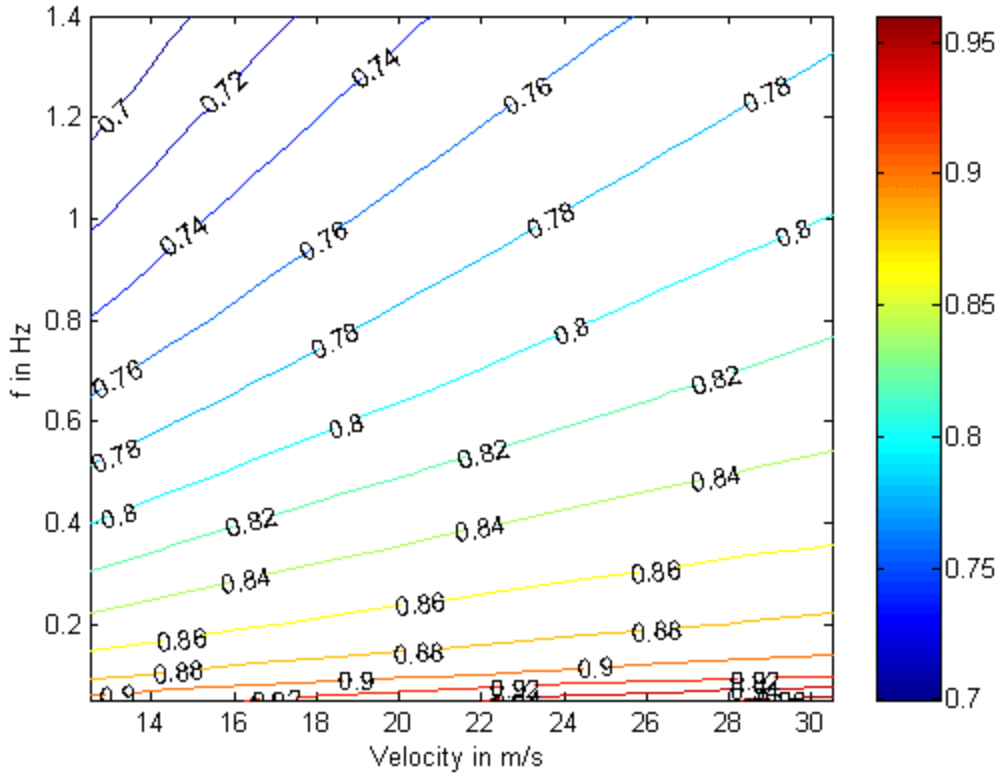

Figure 48. Sustainer Propulsive Efficiency

As expected, propulsive efficiency suffers as the flapping frequency increases and the flight speed decreases, shown here in Figure 48. The highest efficiency occurs where the sustainer system's usefulness is negligible. As the old adage goes: "efficiency doesn't propel, thrust does." If the intent is to use the sustainer to arrest the sink-rate and return to base; the pilot needs to fly at zero sink-rate by setting a 0.4Hz flapping frequency as shown in Figure 47, which yields a propulsive efficiency of 0.80 to 0.85, depending on flight speed. However, if the pilot needs to perform a full power 0.85m/s rate of climb, propulsive efficiency drops to 0.78. Even at this level, this system is vastly superior to existing sustainer systems currently on the market.

Looking at the motorglider/sustainer database available in Appendix D, the system efficiencies for sustainer systems start at 46% for the *Duo Discus T* up to 50% for the *Discus 2T*. The system efficiency is defined here as the combination of propeller efficiency and the losses caused by drag on the exposed propulsion system. These systems, as discussed before, are characterized by their use of small diameter, multi-

bladed propellers. The propulsive systems' motors consist of small two-stroke units that produce best power at 5750-6500 rpm. The propellers are direct-drive, or with small reduction gearing, thus they turn at very high speeds that decrease efficiency. In addition, the multiple blades cause interference losses that further decrease propeller efficiency.

The system efficiency for a *Light Hawk* based sustainer consists of the propulsive efficiency, stated above as varying between 78% and 85% depending on flight speed, and mechanical losses, estimated at 5%. The total system efficiency for the flapping-wing sustainer would vary between 74.1% and 80.8%, dependent on flight speed- a significant increase from the *Discus*' 46% to 50%.

IV. CONCLUSIONS

In this paper, flapping-wing propulsion as a means of drag reduction was investigated numerically. This study was conducted with the hope that the inherent flexibility of high aspect ratio sailplane wings could be harnessed to flap at their natural frequencies.

The numerical method used a strip-theory approach, applying 3-D corrections to 2-D data. Thrust and power coefficients were computed for flapping-wing sections. Spanwise load factors were applied to calculate total wing thrust production and power consumption. The approach was deemed suitable as results from this numerical method compared favorably with established CMARC 3-D results.

New applications of the method were used to determine trends in thrust and power coefficients with changes in velocity, flapping angle, and flapping frequency parameters. With the information acquired from these results, a constraining code was written to determine what combinations of these parameters would provide for the highest thrust given specified power constraints.

The results of these aircraft-tailored constraining codes clearly show that marked improvements in minimum sink and L/D_{max} performance parameters for ultralight sailplanes are possible by means of human-powered flapping-wing propulsion. Theoretical decreases in minimum sink are 16% for the *SparrowHawk*, and 24% for the *Light Hawk* sailplanes. Likewise, L/D_{max} may also be improved 15% from 36.5:1 to 42:1, and 20% from 35:1 to 41.8:1, respectively. These gains in performance would be possible with high propulsive efficiencies in the 85% to 88% range.

The *Light Hawk*-based sustainer system can arrest sink-rate and provide for a 0.85m/s rate of climb using just 2875W (3.9bhp). In addition, zero sink-rate can be maintained throughout the *Light Hawk's* flight envelope from as low as 700W (0.94bhp). These results come with a favorable propulsive efficiency range of 78% to 85%, and total system efficiencies of 74.1% to 80.8%, depending on flight speed.

THIS PAGE INTENTIONALLY LEFT BLANK

V. RECOMMENDATIONS

Using 2-D panel-code data in a strip-theory approach allows for a rather inexpensive means of studying flapping-wing propulsion. There are virtually endless flapping-wing configurations and parameters where this numerical method could be applied. This study concerned itself with limited power applications to offset airframe drag. To further probe in this direction, more time could be spent studying the extreme cases: low frequency with large flapping angle propulsion, and high frequency with small flapping angle propulsion. Perhaps a combination could be applied to drag reduction in large commercial aircraft surfaces.

From a numerical analysis view, more time could be spent refining the method to investigate both plunging and pitching airfoil motions. The task is a daunting one, as it would require interpolating data from 4-D matrices that would include: plunge amplitude, pitch amplitude, phase, and frequency.

From a structural standpoint, ways of tuning the natural frequency of wings to desired levels could be studied. By giving control of this parameter to the pilot, the aircraft flight envelope need not be restricted to avoid flutter. Perhaps it is not necessary. Maybe high aspect ratio, flexible wings with fixed low natural frequencies can be sufficiently controlled at higher flight speeds through active controls (i.e. fly-by-wire).

Obviously, more time could be spent refining the flapping mechanism. A wind-tunnel model would help verify the numerical results experimentally. A flying model of a sustainer system would also be beneficial.

THIS PAGE INTENTIONALLY LEFT BLANK

APPENDIX A. SAILPLANE SPREADSHEET

						1/3 bhp avail	Total Efficiency = 0.8075 (.95mech*.85aero)											
	density = .002377					248.6w				total power output=200.7w								
		kgm			m/s	Newtons			AIAA	&dragradius			L/Dmax	m^2	DN/m^2	m	m	
CLASS	A/C	mtow	mow	L/D	U	Drag	kW	bhp	bhp	HPVPO	newL/D	Cd	CL	S	W/Smax	b	c	A/C
Two Seat	ETA	848.81	685.00	60	30.73	138.74	4.26	5.72	5.72	4.69	62.95	0.013	0.774	18.58	44.796	30.90	0.60	ETA
	ASH25	748.95	604.00	54.3	27.25	135.27	3.69	4.94	4.94	5.43	57.42	0.018	0.990	16.32	45.018	25.00	0.65	ASH25
	DuoDiscus	700.04	565.00	45	23.75	152.56	3.62	4.86	4.86	5.52	47.63	0.027	1.216	16.35	41.983	20.00	0.82	DuoDiscus
	DG505	748.95	604.00	44.5	30.55	165.05	5.04	6.76	6.76	3.97	46.34	0.016	0.702	18.29	40.148	22.00	0.83	DG505
	DG1000	748.95	604.50	46.5	33.33	157.96	5.26	7.06	7.06	3.80	48.34	0.013	0.616	17.53	41.893	20.00	0.88	DG1000
	Nimbus3DT	798.88	644.00	67	24.32	137.45	3.34	4.48	4.48	5.98	60.63	0.022	1.279	16.90	46.356	25.00	0.68	Nimbus3DT
	SB-10	848.81	685.00	46.3	27.01	179.79	4.86	6.51	6.51	4.12	46.29	0.022	0.996	16.70	44.507	23.00	0.81	SB-10
	Janus	699.02	564.00	40.9	27.27	167.61	4.57	6.13	6.13	4.38	42.77	0.021	0.870	17.30	39.625	20.00	0.86	Janus
	G-103 II	599.16	483.50	33	27.27	176.06	4.86	6.51	6.51	4.12	34.42	0.022	0.736	17.52	33.532	18.00	0.97	G-103 II
	ASK-21	599.16	484.00	31.7	27.27	185.36	5.05	6.78	6.78	3.96	33.01	0.023	0.719	17.95	32.734	17.00	1.06	ASK-21
	PW-6B	539.24	435.00	34	26.39	155.54	4.10	5.50	5.50	4.87	35.74	0.024	0.813	15.25	34.674	16.00	0.95	PW-6B
FAI 15m	KA-6	299.58	242.00	30	22.86	97.93	2.24	3.00	3.00	8.93	32.94	0.025	0.740	12.40	23.686	15.00	0.83	KA-6
	Libelle301	349.51	282.00	40.5	22.92	84.63	1.94	2.60	2.60	10.31	45.16	0.026	1.121	9.50	36.061	15.00	0.63	Libelle301
	Std Cirrus	389.45	315.00	37	21.79	109.23	2.25	3.02	3.02	8.89	40.61	0.035	1.307	10.04	38.027	15.00	0.67	Std Cirrus
	Mosquito	449.37	363.00	38.9	25.73	113.29	2.91	3.91	3.91	6.86	41.77	0.029	1.109	9.80	44.958	15.00	0.65	Mosquito
	MiniNimbus	449.37	363.00	37.2	26.24	118.47	3.11	4.17	4.17	6.43	39.76	0.028	1.055	9.90	44.494	15.00	0.66	MiniNimbus
	ASW 20	453.38	366.00	41.7	29.33	106.63	3.13	4.19	4.19	6.40	44.55	0.019	0.804	10.50	42.349	15.00	0.70	ASW 20
	ASW 27	499.16	403.00	45.6	20.97	107.35	2.25	3.02	3.02	8.88	50.05	0.044	2.018	9.00	54.372	15.00	0.60	ASW 27
	LS-3a	471.34	380.00	38.6	26.67	119.75	3.19	4.28	4.28	6.26	41.18	0.026	1.010	10.50	44.026	15.00	0.70	LS-3a
	LS-6	524.26	423.00	42	22.92	122.42	2.61	3.76	3.76	7.13	45.22	0.036	1.516	10.53	46.640	15.00	0.70	LS-6
	Discus2a/b	525.00	424.00	39	26.76	132.02	3.53	4.74	4.74	5.66	41.34	0.030	1.155	10.16	50.652	15.00	0.68	Discus2a/b
	LS-8	524.26	423.00	41.3	24.70	124.49	3.07	4.12	4.12	6.51	44.17	0.032	1.311	10.50	46.970	15.00	0.70	LS-8
	DG-200	449.37	363.00	40.5	32.41	108.81	3.53	4.73	4.73	5.67	42.93	0.017	0.685	10.00	44.081	15.00	0.67	DG-200
	DG-600	524.26	423.00	40.5	24.70	126.95	3.14	4.20	4.20	6.38	43.26	0.031	1.256	10.95	46.935	15.00	0.73	DG-600
	LAK-17a	452.79	365.00	40.6	26.76	109.37	2.93	3.92	3.92	6.83	43.58	0.028	1.118	9.06	49.008	15.00	0.60	LAK-17a
	APIS 15	299.60	241.50	40	25.21	73.45	1.85	2.48	2.48	10.80	44.84	0.015	0.616	12.26	23.956	15.00	0.82	APIS 15
	Genesis 2	525.27	424.00	43.5	30.14	118.42	3.57	4.79	4.79	5.60	46.08	0.019	0.830	11.15	46.194	15.00	0.74	Genesis 2
	SZD55.1	499.71	403.00	44	33.41	111.38	3.72	4.99	4.99	5.38	46.50	0.017	0.749	9.57	51.208	15.00	0.64	SZD55.1
	SZD-Diana	409.42	330.00	47	24.38	85.43	2.08	2.79	2.79	9.60	51.89	0.029	1.351	8.16	49.219	15.00	0.54	SZD-Diana
World	Russia4C	233.42	188.00	34.7	24.70	65.97	1.63	2.18	2.18	12.28	39.56	0.023	0.796	7.70	29.720	12.60	0.61	Russia4C
	APIS 13	244.75	197.00	38	24.70	63.17	1.56	2.09	2.09	12.82	43.59	0.016	0.620	10.36	23.169	13.00	0.80	APIS 13
	APIS UL	229.80	185.00	38	23.67	59.31	1.40	1.88	1.88	14.25	44.31	0.017	0.634	10.36	21.753	13.00	0.80	APIS UL
	PW-5	299.58	241.50	31	27.80	94.77	2.63	3.53	3.53	7.59	33.55	0.020	0.611	10.16	28.904	13.44	0.76	PW-5
	L33 Solo	339.52	274.00	33	25.21	100.90	2.54	3.41	3.41	7.86	35.82	0.024	0.778	11.00	30.268	14.11	0.78	L33 Solo
									AIAA									
SparrowHawk		mtow	mow	L/D	U	Drag	kW	bhp	bhp	HPVPO	newL/D	Cd	CL	S	W/S	b	c	A/C
	minsink	158.64	188.10	30	19.55	51.86	1.01	1.36	2.00	19.73	37.37	0.034	1.022	6.50	23.920			Sparrow
		158.64	128.00	36	27.98	43.22	1.21	1.62	1.62	16.54	43.13	0.014	0.499	6.50	23.920	11.00	0.59	
CarbonDragon		151.84	122.00	26	15.65	57.27	0.90	1.20	1.20	22.32	33.47	0.027	0.699	14.22	10.475	13.41	1.06	Cdragon
		151.84	123.00	24	11.62	62.04	0.72	0.97	0.97	27.73	33.21							
Light Hawk		161.00	129.00	35	16.94	45.11	0.76	1.02	1.02	26.17	47.41	0.022	0.767	11.71	13.487	15.00	0.78	Light
Open	ASW 17	609.12	491.00	49	23.75	121.91	2.89	3.88	3.88	6.91	52.64	0.024	1.166	14.94	40.258	20.00	0.74	ASW 17
	ASW 22BL	748.95	605.00	57	24.17	128.86	3.11	4.18	4.18	6.42	60.91	0.022	1.231	16.67	44.064	26.40	0.63	ASW 22BL
	DG-600/17	524.26	423.00	46	23.15	111.77	2.59	3.47	3.47	7.73	49.85	#####	####	0.00	#DIV/0!	17.00	0.00	DG-600/17
	LAK-17a	452.79	365.00	49	24.70	90.62	2.24	3.00	3.00	8.94	53.61	0.025	1.210	9.62	45.215	16.00	0.55	LAK-17a
powered	ASH26	524.86	424.00	50	26.64	102.95	2.74	3.68	3.68	7.29	53.99	0.020	1.014	11.68	44.069	18.00	0.65	ASH26
	Nimbus3	748.95	604.00	60	22.13	122.42	2.71	3.63	3.63	7.38	64.78	0.024	1.467	16.69	44.015	24.50	0.68	Nimbus3
	A/C	mtow	mow	L/D	U	Drag	kW	bhp	bhp	HPVPO	newL/D	Cd	CL	S	W/Smax	b	c	A/C
		kgm			m/s	Newtons			AIAA	&dragradius			L/Dmax	m^2	DN/m^2	m	m	

			min sink						kW req'd at 175ft/min ROC	as per Discus req'd		Nat freq Hz	k	(2*PI*f*c/Us) =f = k*Us/(2*PI*c) k=0.4	k=0.25	k=0.1	k=.05	
		m/s	m/s			min sink	min sink											
A/C	AR	sink	Us	bhp	kW	CL	Redux	newsink	Sustain	kW	SysEta			f	f	f	f	A/C
ETA	51.39		0.00	0.00	0.00		#DIV/0!	#DIV/0!						0.000	0.000	0.000	0.000	ETA
ASH25	36.31	0.480	22.92	4.54	3.36	1.399	5.930	0.43	9.91	23.5	0.421	1.52	0.272	2.236	1.398	0.559	0.280	ASH25
DuoDiscus	24.47	0.591	23.75	5.45	4.06	1.216	4.938	0.66	10.16	22.0	0.462	2.32	0.502	1.849	1.156	0.462	0.231	DuoDiscus
DG505	26.46	0.710	16.66	7.00	5.22	2.360	3.643	0.66	11.75	23.5	0.499	2.34	0.734	1.276	0.797	0.319	0.159	DG505
DG1000	22.62	0.000	21.67	0.00	0.00	1.457	#DIV/0!	#DIV/0!										DG1000
Nimbus3DT	36.96	0.491	24.32	5.16	3.85	1.279	5.214	0.47	10.81	25.1	0.431			2.291	1.432	0.573	0.286	Nimbus3DT
SB-10	28.29	0.568	25.21	6.23	4.65	1.143	4.318	0.53	12.04	26.7	0.451	4.9	0.993	1.974	1.234	0.493	0.247	SB-10
Janus	23.13	0.732	25.70	6.73	5.02	0.980	3.998	0.70	11.11	22.0	0.506			1.891	1.182	0.473	0.236	Janus
G-103 II	18.49	0.747	22.12	5.89	4.39	1.119	4.589	0.71	9.61	18.8	0.510			1.447	0.904	0.362	0.181	G-103 II
ASK-21	16.10	0.753	21.10	5.94	4.43	1.201	4.532	0.72	9.65	18.8	0.512	2.88	0.906	1.272	0.795	0.318	0.159	ASK-21
PW-6B	16.79	0.750	22.22	5.32	3.97	1.146	5.056	0.71	8.67	16.9	0.511			1.484	0.928	0.371	0.186	PW-6B
KA-6	18.14			0.00	0.00		#DIV/0!	#DIV/0!						0.000	0.000	0.000	0.000	KA-6
Libelle301	23.67	0.591	22.92	2.72	2.03	1.121	9.691	0.53	5.07	10.2	0.498			2.303	1.439	0.576	0.288	Libelle301
Std Cirrus	22.40	0.631	21.79	3.23	2.41	1.307	8.319	0.56	5.81	11.3	0.511			2.072	1.295	0.518	0.259	Std Cirrus
Mesquite	22.95	0.610	23.20	3.61	2.69	1.364	7.462	0.56	6.60	13.1	0.504			2.260	1.412	0.565	0.282	Mesquite
Minilimbus	22.72	0.640	23.15	3.79	2.82	1.355	7.107	0.59	6.74	13.1	0.515			2.232	1.395	0.558	0.279	Minilimbus
ASW 20	21.43	0.619	23.47	3.69	2.75	1.255	7.287	0.57	6.70	13.2	0.507			2.135	1.334	0.534	0.267	ASW 20
ASW 27	24.99	0.561	20.97	3.68	2.75	2.018	7.302	0.52	7.10	14.5	0.488	2.67	0.480	2.224	1.390	0.556	0.278	ASW 27
LS-3a	21.43	0.619	18.01	3.84	2.86	2.215	7.009	0.58	6.97	13.7	0.507			1.638	1.024	0.410	0.205	LS-3a
LS-6	21.37	0.591	22.92	4.08	3.04	1.518	6.594	0.55	7.61	15.3	0.498			2.079	1.300	0.520	0.260	LS-6
Discus2a/b	22.14	0.604	21.61	4.17	3.11	1.771	6.452	0.56	7.68	15.3	0.502	2.85	0.561	2.030	1.269	0.508	0.254	Discus2a/b
LS-8	21.43	0.631	20.68	4.35	3.25	1.887	6.180	0.59	7.81	15.3	0.511			1.872	1.170	0.468	0.234	LS-8
DG-200	22.61	0.619	24.02	3.86	2.73	1.247	7.352	0.57	6.64	13.1	0.507	2.3	0.401	2.294	1.434	0.574	0.287	DG-200
DG-600	20.64	0.591	23.76	4.08	3.04	1.359	6.594	0.55	7.61	15.3	0.498	2.47	0.477	2.070	1.294	0.517	0.259	DG-600
LAK-17a	24.83	0.570	21.61	3.40	2.53	1.713	7.921	0.52	6.48	13.2	0.491			2.278	1.424	0.569	0.285	LAK-17a
APIS 15	18.36	0.585		2.31	1.72		11.659	0.52	4.33	8.7	0.496							
Genesis 2	20.18	0.579	25.83	4.00	2.99	1.130	6.720	0.54	7.56	15.3	0.494			2.212	1.383	0.553	0.277	Genesis 2
SZD55.1	23.61	0.540	21.90	3.55	2.65	1.743	7.583	0.50	7.00	14.6	0.481							SZD55.1
SZD-Diana	27.68	0.591	27.78	3.19	2.38	1.041	8.444	0.54	6.94	11.9	0.498			3.252	2.032	0.813	0.406	SZD-Diana
Russia4C	20.62	0.640	22.13	1.97	1.47	0.991								2.305	1.440	0.576	0.288	Russia-4C
APIS 13	16.31	0.570	19.51	1.84	1.37	0.994												APIS 13
APIS UL	16.31	0.570	18.90	1.72	1.29	0.994												APIS UL
PW-5	17.77	0.951	27.80	3.75	2.80	0.611	7.175	0.88	5.41	8.7	0.619			2.340	1.462	0.585	0.292	PW-5
L33 Solo	18.11	0.953	19.04	0.06	0.05	1.364	423.283	-2.76						1.555	0.972	0.389	0.194	L33 Solo
A/C	AR	sink	Us	bhp	kW	CL			Sustain	kW	Eta			f	f	f	f	
Sparrow																		SPARROWHAWK
	18.62	0.533	19.55	1.11	0.83	1.022	24.158	0.40	2.21	4.6	0.479			2.106	1.316	0.526	0.263	
Cirragon	12.66	0.509	11.62	1.02	0.76	1.266	26.449	0.37	2.08	4.4	0.470							CARBON DRAGON
Light	19.22	0.412	12.50	0.87	0.65	1.409	30.875	0.28	2.05	4.7	0.438							Light Hawk
ASW 17	26.96	0.549	23.75	4.40	3.28	1.166	6.117	0.52	8.59	19.1	0.449			2.038	1.274	0.509	0.255	ASW 17
ASW 22BL	41.80	0.427	23.15	4.21	3.14	1.342	6.396	0.40	9.66	23.5	0.411			2.334	1.459	0.584	0.292	ASW 22BL
DG-600/17	#####	0.492	21.61	3.32	2.48	#DIV/0!	8.097	0.44	7.05	16.5	0.428	2.13	0.000	######	#DIV/0!	######	######	DG-600
LAK-17a	32.99	0.488	22.64	2.91	2.17	1.440	9.257	0.44	6.11	14.2	0.430			2.642	1.651	0.660	0.330	LAK-17a
ASH26	27.75	0.479	21.61	3.31	2.47	1.541	8.139	0.44	7.04	16.5	0.427			2.120	1.325	0.530	0.265	ASH26
Nimbus3	35.97	0.357	21.61	3.52	2.62	1.539	7.654	0.33	9.15	23.5	0.389	1.4	0.277	2.020	1.263	0.505	0.253	Nimbus3
A/C	AR	sink	Us	bhp		CL			Sustain	kW	SysEta			f	f	f	f	A/C
		m/s	m/s			min sink						Hz		k = 0.4	k = 0.25	k = 0.1	k = 0.05	

APPENDIX B. SCHEMPP-HIRTH SUSTAINERS

Duo Discus T

Motorsegler
mit "Turbo" Hilfsantrieb

- **Sehr einfache Triebwerks-Bedienung**
- **Geringes Mehrgewicht**
- **ca. 200 km Reichweite (nach Sägezahnmethode)**
- **Gute Steigleistung und leise**

Powered sailplane
with "Turbo" power system

- **Very simple engine control**
- **Low additional weight**
- **Range approx. 110 nm - based on sawtooth (climb/glide) method**
- **Good climb rate - low noise**

Schempp-Hirth Flugzeuge mit dem einmaligen "Turbo"-Antriebssystem (nach Prof. Oehler) sind die technologisch brillante Verwirklichung einer Konzeption, welche als Alternative zu selbststartenden Motorseglern schon von Wolf Hirth anerkannt worden war und sich längst in Hunderten anderer Modelle weltweit bewährt hat.

Die Vorteile dieses Antriebs liegen dabei im wesentlichen in seiner Betriebssicherheit, der einfachen Bedienung und Wartung, im unkomplizierten Aufbau und nicht zuletzt im geringen Gewicht, so daß im Vergleich zu reinen Segelflugzeugen (deren Einsatzspektrum durch den "Turbo" natürlich weit übertroffen wird) Leistungseinbußen praktisch nicht zu verzeichnen sind.

Das "Turbo"-Antriebssystem ist in erster Linie als "Flautenschieber" und Rückkehrhilfe gedacht. Außenlandungen können jetzt also mit höchstmöglicher Sicherheit vermieden werden. Es kann aber nach einem Auto-, Winden- oder Flugzeugschlepp auch zum Wandersegelflug oder z.B. zum Einstieg in eine Welle eingesetzt werden.

Schempp-Hirth aircraft with their unique "Turbo" system are the technologically brilliant realization of a concept which Wolf Hirth in his day acknowledged as an alternative to self-launching powered sailplanes and is long since being proven worldwide in hundreds of our models.

The most substantial advantages of this power system are its operational reliability, simple engine control and maintenance, an uncomplicated structure and last but not least its low weight. This means that compared with pure sailplanes (the utilisation spectrum of which is, of course, widely surpassed) performance penalties are practically non-existent.

The "Turbo" propulsion system is primarily intended to overcome dead air conditions and to avoid tedious retrieves - off-field landings may now be safely avoided. Secondly the "Turbo" also makes possible soaring safaris or, for instance, wave exploratory flights from places where launching facilities by auto, winch or aerotow exist.

Foto: Peter F. Selinger

Der "Duo Discus T" wird durch einen 22 kW SOLO Zweizylinder-Zweitakt-Motor angetrieben und durch eine elektrische Spindel mit Gasfederunterstützung aus- und eingefahren. Anlasser, Choke oder Gashebel sind nicht erforderlich - der Motor springt schon bei ca. 95 km/h durch den Windmühleneffekt der untersetzten und lärmoptimierten Vielblatt-Faltluftschraube von selbst an und läuft stets mit der eingestellten vollen Leistung.

Das Abstellen erfolgt durch Ausschalten der Zündung und Zurücknehmen der Fahrt. Eingefahren wird nach Triebwerksstillstand ohne Rücksicht auf die Propellerstellung - die Blätter falten sich automatisch ein. Eine Stromversorgung (12 V) ist nur für den Spindelantrieb, die Kraftstoff-Zusatzpumpe und die ILEC Multifunktions-Triebwerkssteuerung erforderlich. Letztere ist auf Wunsch auch für den hinteren Sitz erhältlich.

The "Duo Discus T" is powered by a 22 kW SOLO two-cylinder, two-stroke engine which extends/retracts by means of an electrical spindle drive, assisted by a gas strut. Starter, choke or throttle are not required - the engine is started by the windmilling effect of the geared- and noise-optimized multi-blade folding propeller at a speed of about 51 knots and is preset to operate always at full power.

The engine is stopped by switching "off" the ignition and reducing the speed. Once the windmilling prop has stopped, the power plant is retracted regardless of the position of the prop blades as they fold up automatically.
Electrical power (12 V) is only required for spindle drive, booster pump and ILEC multi-function engine control unit. On request the latter is also available for the rear seat.

Selbstverständlich kann der "Duo Discus T" auch jederzeit in ein reguläres Segelflugzeug zurückverwandelt werden, da Motor, Propeller und Spindel (und damit etwa 35 kg Gewicht) in kurzer Zeit entfernt werden können - die im Flugzeug verbleibenden Komponenten werden durch den serienmäßigen Kohlefaserrumpf des "Duo Discus T" leicht ausgeglichen.

Of course the "Duo Discus T" may also be converted any time into a pure sailplane, as the engine with prop and spindle drive are quickly removable (thus saving a mass of approx. 77 lb) - the remaining power plant components are easily compensated by the standard carbon fiber fuselage.

Leistungsdaten

Spannweite	20.0	m
Flügelfläche	16.4	m^2
Flächenbelastung	31.7 - 42.7	kg/m^2
Gleitzahl	45	
Leergewicht ca.	450	kg
Höchstgewicht	700	kg
Tankinhalt ca.	16.0	ltr

Performance data

Wing span	65.62	ft
Wing area	176.53	sqft
Wing loading	6.5 - 8.7	lb/sqft
Best L/D	45	
Emty mass approx.	992	lb
Max. all-up mass	1543	lb
Tank capacity approx.	4.2	U.S. gal

Änderungen vorbehalten

SCHEMPP-HIRTH FLUGZEUGBAU KIRCHHEIM/TECK
Krebenstraße 25 • D-73230 Kirchheim/Teck • Telefon (07021) 72 98 0 • Telefax (07021) 72 98 199

Diamant-2T

Standardklasse
Hochleistungs-Motorsegler
(nicht eigenstartfähig)

- **Sehr einfache Triebwerksbedienung**
- **Geringes Gewicht des Antriebssystems**
- **"Sägezahn"-Reichweite über 300 km**
- **Gute Steigleistung**

Standard Class
High Performance Powered Sailplane
(not capable of self-launching)

- **Very simple engine control**
- **Low weight of power plant**
- **"Sawtooth"-range approx. 160 nm**
- **Good climb rate**

Eine Idee setzt sich durch ..... und ist heute eine weltweit im Einsatz befindliche und bewährte Alternative zu selbststartenden Motorseglern und reinen Segelflugzeugen:

Das "Turbo"-Antriebssystem für Schempp-Hirth-Flugzeuge (nach Prof. Oehler).

Die Vorteile gegenüber Selbststartern liegen dabei im wesentlichen im unkomplizierten Aufbau dieses Hilfsantriebes, in der einfachen Bedienung und Wartung, in der damit verbundenen Betriebssicherheit und vor allem im erheblich geringeren Gewicht.
Selbst der Vergleich mit normalen Segelflugzeugen geht zu Gunsten des "Turbo"-Systems aus, da Einbußen in den Leistungen und Eigenschaften praktisch nicht zu verzeichnen sind, deren Einsatzspektrum aber um ein Vielfaches übertroffen wird:
Schließlich können Dank des Hilfsantriebes nicht nur Flau- n überbrückt und Außenlandungen mit höchstmöglichster Sicherheit vermieden werden, auch im Wandersegelflug oder z.B. bei der Suche nach Wellenaufwinden hat sich das "Turbo"-System längst bewährt (wobei das anerkannt gute Flügelprofil die um etwa 4 kg/m² höhere Flächenbelastung mühelos verkraftet !)

An idea is spreading ..... and today there is a world-wide operated and proven alternative to self-launching motor-gliders and pure sailplanes:

The "Turbo" propulsion system for Schempp-Hirth aircraft (by Prof. Oehler).

Compared with self-launching sailplanes, the greatest advantages are the uncomplicated structure of the power system, the simple control and maintenance, the associated operational reliability and in particular, the considerably lighter weight.
Even a comparison with pure sailplanes comes out in favour of the "Turbo" propulsion system, since the penalties in performance and handling are virtually non-existent.
Their utilization spectrum, however, is widely surpassed:
Not only may dead-air conditions be overcome and off-field landings safely avoided, the "Turbo" sustainer engine is also well suited for "soaring safaris" or for instance, exploratory wave flights (thanks to its acknowledged fine airfoil section the approx. 0.8 lb/ft² higher wing loading is taken with ease).

Aus- und eingefahren wird das Zweizylinder-Zweitakt-Triebwerk (SOLO, Type 2350, 15.3 kW) mittels eines elektrischen Spindelantriebes, der über ein speziell für den "Turbo"-Antrieb entwickeltes Multifunktions-Bedienteil angesteuert wird, welches mit Leuchtdioden auch Drehzahlbereiche, Triebwerksendstellungen, Batteriespannung usw. anzeigt.

Zu bedienen sind nur Zündschalter, Brandhahn und Dekompressionsgriff. Anlasser, Choke oder Gashebel gibt es nicht.

Der Motor springt durch den Windmühleneffekt der Vielblatt-Luftschraube bei ca. 130 km/h von selbst an und läuft dann stets mit der eingestellten vollen Leistung.
Das Abstellen des Triebwerks erfolgt durch "Zündung aus" und Zurücknehmen der Fahrt auf ca. 90 bis 100 km/h. Eingefahren wird nach Stillstand des Motors ohne Rücksicht auf die Propellerstellung, da sich die Blätter automatisch falten.

Für Standardklasse-Wettbewerbe kann der DISCUS-2T natürlich jederzeit in ein reines Segelflugzeug zurückverwandelt werden, da sich das Triebwerk mit Luftschraube und Akku in kürzester Zeit entfernen läßt (und damit fast 30 kg Gewicht eingespart werden).

The SOLO two-cylinder, two-stroke engine (type 2350, 15.3 kW) is extended and retracted by means of an electrical spindle drive, which is operated by an ILEC multifunction control unit, purposely developed for the "Turbo" system. Its LED signals provide information on RPMs, battery voltage, extreme positions of the power plant etc.

The only engine controls are ignition switch, fuel shut-off valve and decompression handle. Starter, choke or throttle are not needed.

The engine is started by the windmilling effect of the multi-blade folding propeller at about 70 knots and is preset to operate at full power.
It is stooped by switching the igniton to "OFF" and reducing the speed to about 49 to 54 knots. Once the windmilling propeller has stopped, the power plant is retracted regardless of the position of the propeller blades - they fold up automatically.

For sanctioned contests, the DISCUS-2T can be quickly restored to a sailplane complying with the Standard Class rules, as the engine, propeller and battery are quickly removable (thus giving a weight saving of almost 66 lb).

TECHNISCHE DATEN

Spannweite	15.00	m
Flügelfläche	10.16	m^2
Flügelstreckung	22.2	
Leergewicht ca.	290	kg
Maximales Fluggewicht	525	kg
Flächenbelastung	35.5 - 51.7	kg/m^2
"Sägezahn"-Reichweite bei festem 12.5 l Rumpftank ca.	300	km

TECHNICAL DATA

Wing span	49.21	ft
Wing area	109.36	ft^2
Aspect ratio	22.2	
Emty mass approx.	639	lb
Max. all-up mass	1157	lb
Wing loading	7.3 - 10.6	lb/ft^2
Range in "saw tooth" - mode with fixed 3.3 Gal fuselage tank approx.	160	nm

Änderungen vorbehalten

SCHEMPP-HIRTH FLUGZEUGBAU KIRCHHEIM/TECK
Krebenstraße 25 • D-73230 Kirchheim/Teck • Telefon (07021) 72 98 0 • Telefax (07021) 72 98 199

APPENDIX C. FAR PART 103 REGULATION

FAR PART 103

ULTRALIGHT VEHICLES

Subpart A- General

103.1 Applicability

This part prescribes the rules governing the operation of ultralight vehicles in the United States. For the purposes of this part, an ultralight vehicle is a vehicle that:

a. Is used or intended to be used for manned operation in the air by a single occupant;

b. Is used or is intended to be used for recreation or sport purposes only;

c. Does not have any U.S. or foreign airworthiness certificate; and

d. If unpowered, weighs less then 155 pounds; or

e. If powered:

1. Weighs less than 254 pounds empty weight, excluding floats and safety devices which are intended for deployment in a potentially catastrophic situation;

2. Has a fuel capacity not exceeding 5 U.S. gallons;

3. Is not capable of more than 55 knots calibrated airspeed at full power in level flight; and

4. Has a power-off stall speed which does not exceed 24 knots calibrated airspeed.

THIS PAGE INTENTIONALLY LEFT BLANK

APPENDIX D. MOTORGLIDER AND SUSTAINER SPREADSHEET

	density = .002377								assume hpo=200w		
			kgm			m/s	Newtons		%dragredux		
CLASS	A/C	kW	mtow	ROC	L/D	U	Drag	kW	bhp	HPVPO	newL/D	A/C
motorglider	Stemme	69	849	2.5	48	27.1	173.46	4.70	6.30	4.25	50.13	Stemme
	ASH26	37	525	3.9	49	26.7	105.08	2.81	3.76	7.13	52.76	ASH26
	Silent	20.9	290	2.5	31	27.2	91.74	2.50	3.35	8.01	33.70	Silent
	Silent AE1	13	300	2	31	27.2	94.91	2.58	3.46	7.75	33.60	Silent AE1
	RussiaAC5m	18.6	233.4	2.79	34.5	24.7	66.35	1.64	2.20	12.20	39.30	RussiaAC5m
	Nimbus4DM	44	820	3	59	30.73	136.30	4.19	5.62	4.77	61.96	Nimbus4DM
	Nimbus4M	47	800	3.1	60	25.00	130.76	3.27	4.38	6.12	63.91	Nimbus4M
	Ventus 2cM	37	525	3.2	39	25.5	132.02	3.37	4.51	5.94	41.46	Ventus 2cM
	Apis15self	29.5	300	4	40	25.6	73.55	1.88	2.53	10.62	44.75	Apis15self
sustainer	Nimbus4DT	19.6	800	0.85	59	24.32	132.98	3.23	4.34	6.18	62.89	Nimbus4DT
	Nimbus4T	19.6	800	0.85	60	25	130.76	3.27	4.38	6.12	63.91	Nimbus4T
	Ventus 2cT	15.3	525	0.89	39	25.5	132.02	3.37	4.51	5.94	41.46	Ventus 2cT
	Discus2T	15.3	525	0.89	39	26.76	132.02	3.53	4.74	5.66	41.34	Discus2T
	DuoDiscusT	22	700	0.9	45	23.75	152.55	3.62	4.86	5.52	47.63	DuoDiscusT
	SparrowHawk	3.15	200	0.85	36	24.18	54.48	1.32	1.77	15.18	42.44	SparrowHawk
										#DIV/0!		
	LightHawk	2.87	200	0.85	35	16.94	56.04	0.95	1.27	21.07	44.34	LightHawk

										min sink			
		L/Dmax	m^2	DN/m^2	m	m			m/s	m/s			
A/C	Cd	CL	S	W/Smax	b	c	AR	p diam	sink	Us	POWER	SysEta	A/C
Stemme	0.02	0.99	18.7	44.52	23	0.81	28.29		0.6	25.2	25.811	0.374	Stemme
ASH26	0.02	1.01	11.68	44.08	18	0.65	27.74		0.48	22	22.551	0.609	ASH26
Silent	0.02	0.61	10.3	27.61	12	0.86	13.98	1.09	0.7	20.83	9.101	0.436	Silent
Silent AE1	0.02	0.63	10.3	28.56	12	0.86	13.98	1.92	0.78	20.83	8.179	0.629	Silent AE1
RussiaAC5m	0.02	0.80	7.7	29.73	12.6	0.61	20.62	1.09	0.78	25	8.172	0.439	RussiaAC5m
Nimbus4DM	0.01	0.77	17.96	44.78	26.50	0.68	39.10		0.36	21.61	26.996	0.614	Nimbus4DM
Nimbus4M	0.02	1.15	17.86	43.93	26.40	0.68	39.02		0.38	24.32	27.303	0.581	Nimbus4M
Ventus 2cM	0.03	1.18	11	46.81	18	0.61	29.45		0.55	23	19.308	0.522	Ventus 2cM
Apis15self	0.01	0.60	12.26	24.00	15	0.82	18.35						Apis15self
Nimbus4DT	0.02	1.21	17.96	43.68	26.5	0.68	39.10	1.00	0.36	21.61	9.470	0.483	Nimbus4DT
Nimbus4T	0.02	1.14	17.96	43.68	26.4	0.68	38.81	1.00	0.38	22	9.650	0.492	Nimbus4T
Ventus 2cT	0.03	1.34	9.67	53.24	15	0.64	23.27	0.83	0.55	24	7.409	0.484	Ventus 2cT
Discus2T	0.03	1.16	10.16	50.68	15	0.68	22.15	0.83	0.6	21.61	7.666	0.501	Discus2T
DuoDiscusT	0.03	1.22	16.35	41.99	20	0.82	24.46	0.95	0.59	23.75	10.229	0.465	DuoDiscusT
SparrowHawk	0.02	0.84	6.5	30.18	11	0.59	18.62		0.533	19.67	2.713	0.861	SparrowHawk
LightHawk	0.02	0.78	14.22	13.79	15	0.95	15.82		0.412	12.5	2.475	0.862	LightHawk

THIS PAGE INTENTIONALLY LEFT BLANK

APPENDIX E. NUMERICAL ANALYSIS VALIDATION CODE

```
%This program loads NACA 0012 airfoil section UPOT data to compare output with CMARC
%EULER SOLUTIONS FOR FINITE-SPAN FLAPPING-WING
%CMARC data: k = 0.2 / Phi = 10 degrees
clear;
clc;
tic
%CMARC data 3-D interpolator
data = load('h:\thesis\CMARC2.m');
index = 1;
for ARi = (1 : 4);
   for ki = (2 : 5);
      for YBi = (1 : 20);
         K3(ARi, ki, YBi) = data(index, 1);
         AR3(ARi, ki, YBi) = data(index, 2);
         YB3(ARi, ki, YBi) = data(index, 3);
         CP3(ARi, ki, YBi) = data(index, 4);
         CT3(ARi, ki, YBi) = data(index, 5);
         index = index + 1;
      end
   end
end
ki = 1;
for ARi = (1 : 4);
   for YBi = (1 : 20);
      K3(ARi, ki, YBi) = 0.0;
      AR3(ARi, ki, YBi) = AR3(ARi,2,YBi);
      YB3(ARi, ki, YBi) = YB3(ARi,2,YBi);
      CP3(ARi, ki, YBi) = CP3(ARi, 2, YBi);
      CT3(ARi, ki, YBi) = CT3(ARi, 2, YBi);
   end
end
AA=load('h:\Thesis\naca.m');                  % Entire data ~ Row 1 --> H values & Col 1 --> K values
[RAA CAA]=size(AA);                           % Size of A
A=AA(2:RAA,2:CAA);                            % Data set stripped of H and K values
[r c]=size(A);                          % Determines size of 'Data Matrix'
```

```
loop=floor(r/3);                    % Determines number of rows for each Matrix (CT, CW, Eta)
for jj=1:loop                       % Loop to Separate CT from CW from Eta as function of H & K
   count1=(3*jj-2);                 % Row 1,4,7,...
   count2=(3*jj-1);                 % Row 2,5,8,...
   count3=(3*jj);                   % Row 3,6,9,...
   CTMAT(jj,:)=[A(count1,:)];           % CT Data only
   CWMAT(jj,:)=[A(count2,:)];           % CW Data only
   ETAMAT(jj,:)=[A(count3,:)];          % Eta Data only
end
[rCT cCT]=size(CTMAT);              % Determines Size of CT Matrix
[rCW cCW]=size(CWMAT);              % Determines Size of CW Matrix
[rETA cETA]=size(ETAMAT);           % Determines Size of Eta Matrix
HData=AA(1,2:CAA);                  % List of possible H values
HLow=min(HData);                    % Lower Range Value for H
HHigh=max(HData);                   % Higher Range Value for H
KData=AA(2:3:RAA,1);                % List of possible K values
KLow=min(KData);                    % Lower Range Value for K
KHigh=max(KData);                   % Higher Range Value for K
AR = 20;
halfspan = 10;
flapspan = 10;
Cr = 1;
maxx = input('Enter the number of stations to divide flapspan into: ');% User Input for Desired number of stations to divide flap span into
flapangle = 10; %flapangle value in degrees
xstart = halfspan - flapspan;
incr = flapspan/maxx;
i = 1
n = 0;
for (U = 1)
   m = 0;
   n = n + 1;
   for (f = 0.03183) %provides a k of 0.2
      m = m + 1;
      v(n,m) = U;
      w(n,m) = f;
      xstart = halfspan - flapspan;
      incr = flapspan/maxx;
      sumthrust = 0;
```

```
    i = 1;
      for (span = incr/2 : incr : flapspan)% spanwise length of flapping section
        if i == 1,
          x(i) = incr;
          chord(i) = Cr;%-((Cr-Ctip)/flapspan)*x(i) + Cr;% chord variation along span
          chordmean(i) = Cr;%(Cr + chord(i))/2;
        else
          x(i) = x(i-1) + incr;
          chord(i) = Cr;%-((Cr-Ctip)/flapspan)*x(i) + Cr;% chord variation along span
          chordmean(i) = Cr;%(chord(i-1) + chord(i))/2;
        end
        flaparea(i) = incr.*chordmean(i);              % calculates the given station's area
        k = (2*pi*f.*chordmean(i))/U;                  % reduced frequency
        h(i) = sin(pi*flapangle/180)*span./chordmean(i);    % half amplitude
        YB(i) = (xstart + span)/halfspan;
        Cpweight = interp3(K3, AR3, YB3, CP3, k, AR, YB(i), 'cubic');
        Cp(i) = interp2(HData, KData, CWMAT,  h(i), k,'spline') * Cpweight;
        Ctweight = interp3(K3, AR3, YB3, CT3, k, AR, YB(i), 'cubic');
        Ct(i) = interp2(HData, KData, CTMAT,  h(i), k,'spline') * Ctweight;
        i = i + 1;
      end
  Cttotal = sum(Ct)/maxx
  Cptotal = sum(Cp)/maxx
  eta = Cttotal/Cptotal
  end
end
%Comparison with 3-D full-span flapping CMARC data: k = 0.2 / Phi = 10 degrees
y_b = [0.01960 0.07830 .15615 .23305 .30855 .38210 .45325 .52165 .58685 .64845 .70605 .75925 .80775 .85130
.88960 .92245 .94960 .97085 .98615 .99540 .99925];
C_p = [0.0007376 0.0041704 0.0115127 0.0223720 0.0366277 0.0538903 0.0736208 0.0951396 0.1175756 0.1399260
0.1610122 0.1794388 0.1936275 0.2018591 0.2022146 0.1929398 0.1737156 0.1467240 0.1211826 0.1261563
0.0676601];
C_t = [0.0033870 0.0070250 0.0135320 0.0229270 0.0350160 0.0493550 0.0654280 0.0824910 0.0996940 0.1160150
0.1303410 0.1414530 0.1480750 0.1490030 0.1432130 0.1307500 0.1108120 0.0822070 0.0427050  -0.0802290 -
0.1121230];
figure(1)
hold on
plot(YB, Cp, 'kx')
plot(y_b, C_p, 'k--')
TITLE('k = 0.2, Phi = 10 degrees')
```

```
xlabel('Y/B'); ylabel('Cp')
legend('MATLAB Code','CMARC Data')
figure(2)
hold on
plot(YB, Ct, 'k:')
plot(y_b, C_t, 'k--')
TITLE('k = 0.2, Phi = 10 degrees')
xlabel('Y/B'); ylabel('Ct')
legend('MATLAB Code','CMARC Data')
toc
```

APPENDIX F. EXAMPLE OF TREND FINDING CODE (1ST OF 3): FLAPPING ANGLE AND VELOCITY VARIATION FOR USER-DEFINED FLAPPING FREQUENCY

```
%This program varies flapangle and velocity
clear;
clc;
tic
%CMARC data 3-D interpolator
data = load('h:\thesis\CMARC2.m');
index = 1;
for ARi = (1 : 4);
   for ki = (2 : 5);
      for YBi = (1 : 20);
         K3(ARi, ki, YBi) = data(index, 1);
         AR3(ARi, ki, YBi) = data(index, 2);
         YB3(ARi, ki, YBi) = data(index, 3);
         CP3(ARi, ki, YBi) = data(index, 4);
         CT3(ARi, ki, YBi) = data(index, 5);
         index = index + 1;
      end
   end
end
ki = 1;
for ARi = (1 : 4);
   for YBi = (1 : 20);
      K3(ARi, ki, YBi) = 0.0;
      AR3(ARi, ki, YBi) = AR3(ARi,2,YBi);
      YB3(ARi, ki, YBi) = YB3(ARi,2,YBi);
      CP3(ARi, ki, YBi) = CP3(ARi, 2, YBi);
      CT3(ARi, ki, YBi) = CT3(ARi, 2, YBi);
   end
end
AA=load('h:\thesis\nlf041440.m');              % Entire data ~ Row 1 --> H values & Col 1 --> K values
[RAA CAA]=size(AA);                            % Size of A
A=AA(2:RAA,2:CAA);                             % Data set stripped of H and K values
[r c]=size(A);                                 % Determines size of 'Data Matrix'
loop=floor(r/3);                               % Determines number of rows for each Matrix (CT, CW, Eta)
```

```
  for jj=1:loop                    % Loop to Separate CT from CW from Eta as function of H & K
    count1=(3*jj-2);               % Row 1,4,7,...
    count2=(3*jj-1);               % Row 2,5,8,...
    count3=(3*jj);                 % Row 3,6,9,...
    CTMAT(jj,:)=[A(count1,:)];     % CT Data only
    CWMAT(jj,:)=[A(count2,:)];     % CW Data only
    ETAMAT(jj,:)=[A(count3,:)];    % Eta Data only
  end
[rCT cCT]=size(CTMAT);             % Determines Size of CT Matrix
[rCW cCW]=size(CWMAT);             % Determines Size of CW Matrix
[rETA cETA]=size(ETAMAT);          % Determines Size of Eta Matrix
HData=AA(1,2:CAA);                 % List of possible H values
HLow=min(HData);                   % Lower Range Value for H
HHigh=max(HData);                  % Higher Range Value for H
KData=AA(2:3:RAA,1);               % List of possible K values
KLow=min(KData);                   % Lower Range Value for K
KHigh=max(KData);                  % Higher Range Value for K
rho = 1.22511;  %standard s.l. density kg/m^3
flapangle = 0;
U = 0;
%the input section asks for several individual inputs and ranges for the other parameters
halfspan=input('Enter halfspan of aircraft in meters:  ');  % User Input for half span of aircraft
percentflap=input('Enter fraction of span that will flap  '); %User input
        flap_span=input('Enter 0 to apply this percentage or 1 for a full span flap:  ');% User Input for Desired Flap span
  if flap_span == 0,
    flapspan=percentflap*halfspan,%calculates flapspan
    else flap_span == 1,
    flapspan=halfspan,    %the entire span flaps
  end
Cr=input('Enter Cr value of flapspan in meters:  ');% User Input for Desired Root Chord
Ctip=0.4*Cr;                       %ties Ctip to Cr via 0.4 taper ratio
AR = input('Enter the Aspect Ratio of the aircraft:  '); %User input for AR
        maxx=input('Enter the number of stations to divide flapspan into:  ');% User Input  for Desired number of stations to divide flap span into
f=input('Enter flapping frequency in Hz:  ');% User Input for flapping frequency
%Lighthawk Data
        Udata = [11 11.5 12 12.5 13 13.5 14 14.5 15 15.5 16 16.5 17 17.5 18 18.5 19 19.5 20 20.5 21 21.5 22 22.5 23 23.5 24 24.5 25 25.5 26 26.5 27 27.5 28 28.5 29 29.5 30 30.5 31 31.5 32];
%LightHawk Data
```

```
Dragdata = [59.6497 56.6736 54.1285 51.9726 50.1565 48.6422 47.4010 46.3981 45.6205 45.0350 44.6277
44.3893 44.2897 44.3267 44.4894 44.7669 45.1509 45.6337 46.1945 46.8524 47.5867 48.3888 49.2491
50.1884 51.1642 52.2132 53.3061 54.4456 55.6352 56.8778 58.1343 59.4476 60.7981 62.1870 63.5895
65.0299 66.5091 67.9986 69.5256 71.0588 72.6277 74.2326 75.8370];
n = 0;
for (flapangle = .8: 0.75: 15)%5 degrees to 10 degrees in 0.5 degree increments (17)
    n = n + 1;
    m = 0;
    for (U = 12: 0.5: 18.0)
        m = m + 1;
        drag = interp1(Udata, Dragdata, U,'spline');
        v(n,m) = flapangle;
        w(n,m) = U;
        xstart = halfspan - flapspan;
        incr = flapspan/maxx;
        sumthrust = 0;
        sumpower = 0;
        i = 1;
        for (span = incr/2 : incr : flapspan)% spanwise length of flapping section
          if i == 1,
            x(i) = incr;
            chord(i) =-((Cr-Ctip)/flapspan)*x(i) + Cr;% chord variation along span
            chordmean(i) = (Cr + chord(i))/2;
          else
             x(i) = x(i-1) + incr;
             chord(i) =-((Cr-Ctip)/flapspan)*x(i) + Cr;% chord variation alongspan
             chordmean(i) = (chord(i-1) + chord(i))/2;
          end
        YB = (xstart + span)/halfspan;
        flaparea = incr*chordmean(i);                % calculates the given station's area
        k = (2*pi*f*chordmean(i))/U;                 % reduced frequency
        h = sin(pi*flapangle/180)*span/chordmean(n);    % half amplitude
        Cpweight = interp3(K3, AR3, YB3, CP3, k, AR, YB, 'linear');
        Cw(i) = interp2(HData, KData, CWMAT, h, k,'spline') * Cpweight;
        sumpower = sumpower + Cw(i)*.5*flaparea*rho*U^3;
        Ctweight = interp3(K3, AR3, YB3, CT3, k, AR, YB, 'linear');
        Ct(i) = interp2(HData, KData, CTMAT, h, k,'spline') * Ctweight;
        sumthrust = sumthrust + Ct(i)*.5*flaparea*rho*U^2;
        i = i + 1;
        end
```

```
    power(n,m) = 2*sumpower;
    thrust(n,m) = 2*sumthrust;
    eta(n,m) = (thrust(n,m)*U)/power(n,m);
    netdrag(n,m) = drag - thrust(n,m); %net drag after flap thrust is subtracted
    neweta(n,m) = netdrag(n,m)*U/power(n,m);
    netsink(n,m) = U * netdrag(n,m)/1556.930; %net sink-rate as a function of U and drag
    end
end
figure(1)
subplot(1,2,1)
surfc (v, w, thrust), xlabel('Flapangle in degrees'), ylabel('Velocity in m/s'), zlabel('Thrust in Newtons')
vec=[4,6,8,10,12,14,16,18,20,24,28,32,40,50,60,70];
subplot(1,2,2)
[ccc,hhh] = contour(v, w, thrust, vec);
xlabel('Flapangle in degrees'), ylabel('Velocity in m/s')
clabel(ccc,hhh); colorbar
figure(2)
subplot(1,2,1)
surfc (v, w, power), xlabel('Flapangle in degrees'), ylabel('Velocity in m/s'), zlabel('Power in Watts')
vec=[25,50,75,100,150,200,250,300,400,500,750,1000,1250,1500,2000,2500];
subplot(1,2,2)
[ccc,hhh] = contour(v, w, power, vec);
xlabel('Flapangle in degrees'), ylabel('Velocity in m/s')
clabel(ccc,hhh); colorbar
figure(3)
subplot(1,2,1)
surfc (v, w, eta), xlabel('Flapangle in degrees'), ylabel('Velocity in m/s'), zlabel('Efficiency')
subplot(1,2,2)
[ccc,hhh] = contour(v, w, eta);
xlabel('Flapangle in degrees'), ylabel('Velocity in m/s')
clabel(ccc,hhh); colorbar
vec=[1,2,3,4,5,10,15,20,25,30,35,40,50,75,100,150,200,250];
figure(4)
[ccc,hhh] = contour(v, w, neweta);
xlabel('Flapangle in degrees'), ylabel('Velocity in m/s')
clabel(ccc,hhh); colorbar
vec=[-0.8,-0.6,-0.4,-0.2,0,0.2,0.4,0.6];
figure(5)
[ccc,hhh] = contour(v, w, netsink, vec);
```

```
xlabel('Flapangle in degrees'), ylabel('Velocity in m/s')
clabel(ccc,hhh); colorbar
toc
end
```

THIS PAGE INTENTIONALLY LEFT BLANK

APPENDIX G. CONSTRAINING CODE 1: HUMAN-POWERED SPARROWHAWK

```
%This program varies velocity and frequency with a user defined maximum input power restriction
%this program calls up thrust1b.m and power1b.m functions
clear;
clc;
tic
%CMARC data 3-D interpolator
data = load('h:\thesis\CMARC2.m');
index = 1;
for ARi = (1 : 4);
   for ki = (2 : 5);
      for YBi = (1 : 20);
         K3(ARi, ki, YBi) = data(index, 1);
         AR3(ARi, ki, YBi) = data(index, 2);
         YB3(ARi, ki, YBi) = data(index, 3);
         CP3(ARi, ki, YBi) = data(index, 4);
         CT3(ARi, ki, YBi) = data(index, 5);
         index = index + 1;
      end
   end
end
ki = 1;
for ARi = (1 : 4);
   for YBi = (1 : 20);
      K3(ARi, ki, YBi) = 0.0;
      AR3(ARi, ki, YBi) = AR3(ARi,2,YBi);
      YB3(ARi, ki, YBi) = YB3(ARi,2,YBi);
      CP3(ARi, ki, YBi) = CP3(ARi, 2, YBi);
      CT3(ARi, ki, YBi) = CT3(ARi, 2, YBi);
   end
end
%downloads UPOT generated data and sorts coefficients
AA=load('h:\thesis\nlf041440.m');          % Entire data ~ Row 1 --> H values & Col 1 --> K values
[RAA CAA]=size(AA);                        % Size of A
A=AA(2:RAA,2:CAA);                         % Data set stripped of H and K values
```

```
[r c]=size(A);                    % Determines size of 'Data Matrix'
loop=floor(r/3);                  % Determines number of rows for each Matrix (CT, CW, Eta)
   for jj=1:loop                  % Loop to Separate CT from CW from Eta as function of H & K
      count1=(3*jj-2);            % Row 1,4,7,...
      count2=(3*jj-1);            % Row 2,5,8,...
      count3=(3*jj);              % Row 3,6,9,...
      CTMAT(jj,:)=[A(count1,:)];  % CT Data only
      CWMAT(jj,:)=[A(count2,:)];  % CW Data only
      ETAMAT(jj,:)=[A(count3,:)]; % Eta Data only
   end
[rCT cCT]=size(CTMAT);            % Determines Size of CT Matrix
[rCW cCW]=size(CWMAT);            % Determines Size of CW Matrix
[rETA cETA]=size(ETAMAT);         % Determines Size of Eta Matrix
for n=1:rCT
   for m=1:cCT
      if ( CTMAT(n,m) > 99 ),
         CTMAT(n,m) = 0.0;
      end
      if ( CWMAT(n,m) > 99 ),
         CWMAT(n,m) = 0.0;
      end
   end
end
HData=AA(1,2:CAA);                % List of possible H values
HLow=min(HData);                  % Lower Range Value for H
HHigh=max(HData);                 % Higher Range Value for H
KData=AA(2:3:RAA,1);              % List of possible K values
KLow=min(KData);                  % Lower Range Value for K
KHigh=max(KData);                 % Higher Range Value for K
rho = 1.22511;                    % standard s.l. density kg/m^3
delta = 0.001;
er = +0.005;
pi = acos(-1);
%input section asks for several individual inputs and ranges for the other parameters
AR = input('Enter the Aspect Ratio of the aircraft:  '); %User input for AR
halfspan=input('Enter halfspan of aircraft in meters:  ');% User Input for half span of aircraft
percentflap=input('Enter fraction of span that will flap:  '); %User input span fraction
        flap_span=input('Enter 0 to apply this percentage or 1 for a full span flap:  ');% User Input for Desired Flap
        span
```

```
   if flap_span == 0,
      flapspan=percentflap*halfspan,      %calculates flapspan
      else flap_span == 1,
      flapspan=halfspan,                  %the entire span flaps
   end
Cr=input('Enter Cr value of flapspan in meters:  ');% User Input for Desired Root Chord
Ctip=0.4*Cr;                              %ties Ctip to Cr via 0.4 taper ratio


        maxx=input('Enter the number of stations to divide flapspan into:  ');%Desired number of stations to divide
        flapspan into
powermax=input('Enter the maximum power that is available for propulsion:  ');
flapangle0=input('Enter flapangle value in degrees:  ');% User Input for maximum flap angle
%SparrowHawk Data
        Udata = [17.554 18.178 18.872 19.651 20.535 21.549 22.730 24.128 25.820 27.927 30.651 34.367 39.876
        44.897 49.312 69.565];
%SparrowHawk Data
        Dragdata = [73.874 65.914 60.094 54.778 50.070 47.678 44.806 43.100 42.817 42.617 45.232 50.346 61.130
        76.650 95.302 183.925];
n = 0;
for (U = 18: 2: 34.0) %Sparrowhawk velocity range
   m = 0;
   n = n + 1;
   flapangle = flapangle0;
   drag = interp1(Udata, Dragdata, U,'spline');
   for (f = 0.05: 0.05: 1.0)  %Sparrowhawk frequency range
     m = m + 1;
     v(n,m) = U;
     w(n,m) = f;
     dP = 10;
%calls up function power1b
          [Cw, sumpower] = power1b(flapspan, halfspan, Cr, Ctip, maxx, f, U, flapangle, HData, KData, CWMAT,
          rho, K3, AR3, YB3, CP3, AR);
     power(n,m) = 2*sumpower;
     iter = 0;
     %Iterative method for finding max thrust given limited power
       if power(n,m) >= powermax,
        flapangle2 = flapangle;
       powern2 = power(n,m);
        flapangle1 = flapangle2 - er;
         while abs(dP) >= delta
```

```
            [Cw, sumpower] = power1b(flapspan, halfspan, Cr, Ctip, maxx, f, U, flapangle1, HData, KData, CWMAT, rho, K3, AR3, YB3, CP3, AR);
        powern1 = 2*sumpower;
            flapanglen = abs(flapangle2 - (powern2 - powermax) * (flapangle2 - flapangle1)/(powern2 - powern1));
        dP = powern1 - powermax;
        powern2 = powern1;
        flapangle2 = flapangle1;
        flapangle1 = flapanglen;
        iter = iter + 1;
        if iter >= 50
            powern1 = 0;
            flapangle1 = 0;
            dP = 0
        end
      end
      power(n,m) = powern1;
      flapangle = flapangle1;
    end
    %calls up function thrust1b
            [Ct, sumthrust] = thrust1b(flapspan, halfspan, Cr, Ctip, maxx, f, U, flapangle, HData, KData, CTMAT, rho, K3, AR3, YB3, CT3, AR);
    thrust(n,m) = 2*sumthrust;
    netdrag(n,m) = drag - thrust(n,m); %net drag after flap thrust is subtracted
    netsink(n,m) = U * netdrag(n,m)/1556.930; %net sink-rate as a function of U and drag
    flaparray(n,m) = flapangle;
    eta(n,m) = (thrust(n,m)*U)/power(n,m);
  end
end
%plotting section
figure(1)
subplot(1,2,1)
surfc (v, w, netsink), xlabel('Velocity in m/s'), ylabel('f in Hz'), zlabel('netsink')
subplot(1,2,2)
vec=[.55,.555,.56,.57,.59,.61,.65,.7,.8,.9];
[ccc,hhh] = contour(v, w, netsink, vec);
xlabel('Velocity in m/s'), ylabel('f in Hz')
clabel(ccc,hhh); colorbar
figure(2)
subplot(1,2,1)
```

```
surfc (v, w, netdrag), xlabel('Velocity in m/s'), ylabel('f in Hz'), zlabel('netdrag')
subplot(1,2,2)
vec=[35.5,35.75,36.25,37,38.5,40,43,47,51,55,58];
[ccc,hhh] = contour(v, w, netdrag, vec);
xlabel('Velocity in m/s'), ylabel('f in Hz')
clabel(ccc,hhh); colorbar
figure(3)
subplot(1,2,1)
surfc (v, w, thrust), xlabel('Velocity in m/s'), ylabel('f in Hz'), zlabel('Thrust in Newtons')
subplot(1,2,2)
vec=[2:1:50];
[ccc,hhh] = contour(v, w, thrust, vec);
xlabel('Velocity in m/s'), ylabel('f in Hz')
clabel(ccc,hhh); colorbar
figure(4)
subplot(1,2,1)
surfc (v, w, power), xlabel('Velocity in m/s'), ylabel('f in Hz'), zlabel('Power in Watts')
subplot(1,2,2)
vec=[10,25,50,75,100,130,160,190,199.99];
[ccc,hhh] = contour(v, w, power, vec);
xlabel('Velocity in m/s'), ylabel('f in Hz')
clabel(ccc,hhh); colorbar
figure(5)
subplot(1,2,1)
surfc (v, w, flaparray), xlabel('Velocity in m/s'), ylabel('f in Hz'), zlabel('flap angle')
subplot(1,2,2)
vec=[3:1:15];
[ccc,hhh] = contour(v, w, flaparray, vec);
xlabel('Velocity in m/s'), ylabel('f in Hz')
clabel(ccc,hhh); colorbar
figure(6)
vec=[0.76:.02:.96];
[ccc,hhh] = contour(v, w, eta, vec);
xlabel('Velocity in m/s'), ylabel('f in Hz')
clabel(ccc,hhh); colorbar
toc
```

THIS PAGE INTENTIONALLY LEFT BLANK

APPENDIX H. CONSTRAINING CODE 2: HUMAN-POWERED LIGHT HAWK/ LIGHT HAWK-BASED SUSTAINER

```
%This program varies velocity and frequency with a user defined maximum input power restriction
%this program calls up thrust1b.m and power1b.m functions
clear;
clc;
tic
%CMARC data 3-D interpolator
data = load('h:\thesis\CMARC2.m');
index = 1;
for ARi = (1 : 4);
   for ki = (2 : 5);
      for YBi = (1 : 20);
         K3(ARi, ki, YBi) = data(index, 1);
         AR3(ARi, ki, YBi) = data(index, 2);
         YB3(ARi, ki, YBi) = data(index, 3);
         CP3(ARi, ki, YBi) = data(index, 4);
         CT3(ARi, ki, YBi) = data(index, 5);
         index = index + 1;
      end
   end
end
ki = 1;
for ARi = (1 : 4);
   for YBi = (1 : 20);
      K3(ARi, ki, YBi) = 0.0;
      AR3(ARi, ki, YBi) = AR3(ARi,2,YBi);
      YB3(ARi, ki, YBi) = YB3(ARi,2,YBi);
      CP3(ARi, ki, YBi) = CP3(ARi, 2, YBi);
      CT3(ARi, ki, YBi) = CT3(ARi, 2, YBi);
   end
end
%downloads UPOT generated data and sorts coefficients
AA=load('h:\thesis\nlf041440.m');          % Entire data ~ Row 1 --> H values & Col 1 --> K values
[RAA CAA]=size(AA);                        % Size of A
A=AA(2:RAA,2:CAA);                         % Data set stripped of H and K values
```

```
[r c]=size(A);                    % Determines size of 'Data Matrix'
loop=floor(r/3);                  % Determines number of rows for each Matrix (CT, CW, Eta)
   for jj=1:loop                  % Loop to Separate CT from CW from Eta as function of H & K
      count1=(3*jj-2);            % Row 1,4,7,...
      count2=(3*jj-1);            % Row 2,5,8,...
      count3=(3*jj);              % Row 3,6,9,...
      CTMAT(jj,:)=[A(count1,:)];  % CT Data only
      CWMAT(jj,:)=[A(count2,:)];  % CW Data only
      ETAMAT(jj,:)=[A(count3,:)]; % Eta Data only
   end
[rCT cCT]=size(CTMAT);            % Determines Size of CT Matrix
[rCW cCW]=size(CWMAT);            % Determines Size of CW Matrix
[rETA cETA]=size(ETAMAT);         % Determines Size of Eta Matrix
for n=1:rCT
   for m=1:cCT
      if ( CTMAT(n,m) > 99 ),
         CTMAT(n,m) = 0.0;
      end
      if ( CWMAT(n,m) > 99 ),
         CWMAT(n,m) = 0.0;
      end
   end
end
HData=AA(1,2:CAA);                % List of possible H values
HLow=min(HData);                  % Lower Range Value for H
HHigh=max(HData);                 % Higher Range Value for H
KData=AA(2:3:RAA,1);              % List of possible K values
KLow=min(KData);                  % Lower Range Value for K
KHigh=max(KData);                 % Higher Range Value for K
rho = 1.22511;                    % standard s.l. density kg/m^3
delta = 0.001;
er = +0.005;
pi = acos(-1);
%input section asks for several individual inputs and ranges for the other parameters
AR = input('Enter the Aspect Ratio of the aircraft:  '); %User input for AR
halfspan=input('Enter halfspan of aircraft in meters:  ');% User Input for half span of aircraft
percentflap=input('Enter fraction of span that will flap:  '); %User input span fraction
        flap_span=input('Enter 0 to apply this percentage or 1 for a full span flap:  ');% User Input for Desired Flap
        span
```

```
   if flap_span == 0,
      flapspan=percentflap*halfspan,      %calculates flapspan
      else flap_span == 1,
      flapspan=halfspan,                  %the entire span flaps
   end
Cr=input('Enter Cr value of flapspan in meters:  ');% User Input for Desired Root Chord
Ctip=0.4*Cr;                              %ties Ctip to Cr via 0.4 taper ratio


        maxx=input('Enter the number of stations to divide flapspan into:  ');%Desired number of stations to divide
        flapspan into
powermax=input('Enter the maximum power that is available for propulsion:  ');
flapangle0=input('Enter flapangle value in degrees:  ');% User Input for maximum flap angle
%LightHawk Data
        Udata = [11 11.5 12 12.5 13 13.5 14 14.5 15 15.5 16 16.5 17 17.5 18 18.5 19 19.5 20 20.5 21 21.5 22 22.5 23
        23.5 24 24.5 25 25.5 26 26.5 27 27.5 28 28.5 29 29.5 30 30.5 31 31.5 32];
%LightHawk Data
        Dragdata = [59.6497 56.6736 54.1285 51.9726 50.1565 48.6422 47.4010 46.3981 45.6205 45.0350 44.6277
        44.3893 44.2897 44.3267 44.4894 44.7669 45.1509 45.6337 46.1945 46.8524 47.5867 48.3888 49.2491
        50.1884 51.1642 52.2132 53.3061 54.4456 55.6352 56.8778 58.1343 59.4476 60.7981 62.1870 63.5895
        65.0299 66.5091 67.9986 69.5256 71.0588 72.6277 74.2326 75.8370];
n = 0;
for (U = 11.5: 2: 26.0) %Lighthawk velocity range
   m = 0;
   n = n + 1;
   flapangle = flapangle0;
   drag = interp1(Udata, Dragdata, U,'spline');
   for (f = 0.05: 0.05: 0.7)  %Lighthawk frequency range
     m = m + 1;
     v(n,m) = U;
     w(n,m) = f;
     dP = 10;
%calls up function power1b
          [Cw, sumpower] = power1b(flapspan, halfspan, Cr, Ctip, maxx, f, U, flapangle, HData, KData, CWMAT,
          rho, K3, AR3, YB3, CP3, AR);
     power(n,m) = 2*sumpower;
     iter = 0;
     %Iterative method for finding max thrust given limited power
       if power(n,m) >= powermax,
         flapangle2 = flapangle;
        powern2 = power(n,m);
         flapangle1 = flapangle2 - er;
```

```
        while abs(dP) >= delta
                [Cw, sumpower] = power1b(flapspan, halfspan, Cr, Ctip, maxx, f, U, flapangle1, HData, KData, CWMAT, rho, K3, AR3, YB3, CP3, AR);
         powern1 = 2*sumpower;
                 flapanglen = abs(flapangle2 - (powern2 - powermax) * (flapangle2 - flapangle1)/(powern2 - powern1));
         dP = powern1 - powermax;
         powern2 = powern1;
         flapangle2 = flapangle1;
         flapangle1 = flapanglen;
         iter = iter + 1;
         if iter >= 50
            powern1 = 0;
            flapangle1 = 0;
            dP = 0;
         end
        end
        power(n,m) = powern1;
        flapangle = flapangle1;
      end
      %calls up function thrust1b
                [Ct, sumthrust] = thrust1b(flapspan, halfspan, Cr, Ctip, maxx, f, U, flapangle, HData, KData, CTMAT, rho, K3, AR3, YB3, CT3, AR);
      thrust(n,m) = 2*sumthrust;
      netdrag(n,m) = drag - thrust(n,m); %net drag after flap thrust is subtracted
      netsink(n,m) = U * netdrag(n,m)/1556.930; %net sink-rate as a function of U and drag
      flaparray(n,m) = flapangle;
      eta(n,m) = (thrust(n,m)*U)/power(n,m);
   end
end
 %plotting section
figure(1)
subplot(1,2,1)
surfc (v, w, netsink), xlabel('Velocity in m/s'), ylabel('f in Hz'), zlabel('netsink')
subplot(1,2,2)
vec=[.31,.32,.34,.36,.40,.44,.48,.52,.58,.64,.70,.78,.84];
[ccc,hhh] = contour(v, w, netsink, vec);
xlabel('Velocity in m/s'), ylabel('f in Hz')
clabel(ccc,hhh); colorbar
figure(2)
```

```
subplot(1,2,1)
surfc (v, w, netdrag), xlabel('Velocity in m/s'), ylabel('f in Hz'), zlabel('netdrag')
subplot(1,2,2)
vec=[34:34.25:34.50,35.5,36.5,38,40,42,44,46,48,50];
[ccc,hhh] = contour(v, w, netdrag, vec);
xlabel('Velocity in m/s'), ylabel('f in Hz')
clabel(ccc,hhh); colorbar
figure(3)
subplot(1,2,1)
surfc (v, w, thrust), xlabel('Velocity in m/s'), ylabel('f in Hz'), zlabel('Thrust in Newtons')
subplot(1,2,2)
vec=[2:1:50];
[ccc,hhh] = contour(v, w, thrust, vec);
xlabel('Velocity in m/s'), ylabel('f in Hz')
clabel(ccc,hhh); colorbar
figure(4)
subplot(1,2,1)
surfc (v, w, power), xlabel('Velocity in m/s'), ylabel('f in Hz'), zlabel('Power in Watts')
subplot(1,2,2)
vec=[10,25,50,75,100,130,160,190,199.99];
[ccc,hhh] = contour(v, w, power, vec);
xlabel('Velocity in m/s'), ylabel('f in Hz')
clabel(ccc,hhh); colorbar
figure(5)
subplot(1,2,1)
surfc (v, w, flaparray), xlabel('Velocity in m/s'), ylabel('f in Hz'), zlabel('flapangle')
subplot(1,2,2)
vec=[2.5:.5:10];
[ccc,hhh] = contour(v, w, flaparray, vec);
xlabel('Velocity in m/s'), ylabel('f in Hz')
clabel(ccc,hhh); colorbar
figure(6)
vec=[0.74:.02:.96];
[ccc,hhh] = contour(v, w, eta, vec);
xlabel('Velocity in m/s'), ylabel('f in Hz')
clabel(ccc,hhh); colorbar
figure(7)
subplot(1,2,1)
surfc (v, w, flaparray), xlabel('Velocity in m/s'), ylabel('f in Hz'), zlabel('flapangle')
```

```
subplot(1,2,2)
surfc (v, w, power), xlabel('Velocity in m/s'), ylabel('f in Hz'), zlabel('Power in Watts')
toc
```

APPENDIX I. POWER FUNCTION CALLED BY CONSTRAINING CODES

```
%this function is a requirement for the restrictimizeB.m program
        function [Cw, sumpower] = power1b(flapspan, halfspan, Cr, Ctip, maxx, f, U, flapangle, HData,
        KData, CWMAT, rho, K3, AR3, YB3, CP3, AR);
   xstart = halfspan - flapspan;
   incr = flapspan/maxx;
   sumpower = 0;
      n = 1;
        for (span = incr/2 : incr : flapspan)% spanwise length of flapping section
           if n == 1,
              x(n) = incr;
             chord(n) =-((Cr-Ctip)/flapspan)*x(n) + Cr;% chord variation along span
             chordmean(n) = (Cr + chord(n))/2;
           else
              x(n) = x(n-1) + incr;
             chord(n) =-((Cr-Ctip)/flapspan)*x(n) + Cr;% chord variation along span
             chordmean(n) = (chord(n-1) + chord(n))/2;
           end
        YB = (xstart + span)/halfspan;
        flaparea = incr*chordmean(n);              % calculates the given station's area
        k = (2*pi*f*chordmean(n))/U;               % reduced frequency
        h = sin(pi*flapangle/180)*span/chordmean(n);    % half amplitude
        Cpweight = interp3(K3, AR3, YB3, CP3, k, AR, YB, 'linear');
        Cw(n) = interp2(HData, KData, CWMAT,  h, k,'spline') * Cpweight;
       sumpower = sumpower + Cw(n)*.5*flaparea*rho*U^3;
       n = n + 1;
       end
```

THIS PAGE INTENTIONALLY LEFT BLANK

APPENDIX J. THRUST FUNCTION CALLED BY CONSTRAINING CODES

```
%this function is a requirement for the restrictimizeB.m program
        function [Ct, sumthrust] = thrust1b(flapspan, halfspan, Cr, Ctip, maxx, f, U, flapangle, HData,
        KData, CTMAT, rho, K3, AR3, YB3, CT3, AR);
   xstart = halfspan - flapspan;
   incr = flapspan/maxx;
   sumthrust = 0;
      n = 1;
       for (span = incr/2 : incr : flapspan)% spanwise length of flapping section
          if n == 1,
             x(n) = incr;
            chord(n) =-((Cr-Ctip)/flapspan)*x(n) + Cr;% chord variation along span
            chordmean(n) = (Cr + chord(n))/2;
          else
             x(n) = x(n-1) + incr;
            chord(n) =-((Cr-Ctip)/flapspan)*x(n) + Cr;% chord variation along span
            chordmean(n) = (chord(n-1) + chord(n))/2;
          end
          YB = (xstart + span)/halfspan;
          flaparea = incr*chordmean(n);              % calculates the given station's area
          k = (2*pi*f*chordmean(n))/U;               % reduced frequency
         h = sin(pi*flapangle/180)*span/chordmean(n);    % half amplitude
          Ctweight = interp3(K3, AR3, YB3, CT3, k, AR, YB, 'linear');
          Ct(n) = interp2(HData, KData, CTMAT,  h, k,'spline') * Ctweight;
         sumthrust = sumthrust + Ct(n)*.5*flaparea*rho*U^2;
          n = n + 1;
       end
```

THIS PAGE INTENTIONALLY LEFT BLANK

LIST OF REFERENCES

1. Teng, N. H., "The Development of a Computer Code for the Numerical Solution of Unsteady, Inviscid and Incompressible Flow over an Airfoil," Master's Thesis, Naval Postgraduate School, Monterey, California, June 1987.

2. Knoller, R., "Die Gesetz des Luftwiderstandes," Flug- und Motortechnik (Wien), Vol. 3, No. 21, 1909, pp. 1-7.

3. Betz, A., "Ein Beitrag zur Erklarung des Segelfluges," Zeitschrift fur Flugtechnik und Motorluftschiffahrt, Vol. 3, Jan. 1912, pp. 269-272.

4. Jones, K.D., Lund, T.C., Platzer, M.F., "Experimental and Computational Investigation of Flapping-Wing Propulsion for Micro-Air Vehicles," Chapter 16, AIAA Fixed and Flapping-wing Aerodynamics for Micro Air Vehicle Applications, Ed. T. Mueller, AIAA, Reston, VA, 2001, pp. 307-339.

5. Pendaries, C., Boiffier, J.L., Jeanneau, M., "Flexible Aircraft in Conceptual Design HALEs on the Way to Ornithopter," AIAA Paper no. 98-0505, Reno, Nevada, January 1998.

6. Schultz, S., *Princeton Weekly Bulletin*, Vol. 89, No. 8, November 8, 1999.

7. McMasters, J., "The Optimization of Man-Powered Aircraft," AIAA Paper No. 71-798, School of Aeronautics, Astronautics and Engineering Sciences Purdue University, 1971.

8. Correspondence with G. Cole, of Windward Performance LLC, www.windward-performance.com, February-September 2002.

9. Correspondence with D. Howell, of Gliderspport, www.gliderspport.net, February-September 2002.

10. Spicer, J.B., associate professor Johns Hopkins University, Johns Hopkins Magazine, November 1999.)

11. Alexander, R.M., "Springs for Wings," *Science*, Vol. 268, Pressssssssss, 07 April 1995, pp. 50-51.

12. Jones, K.D., Castro, B.M., Mahmoud, O., Pollard, S.J. and Platzer, M. F., "A Collaborative Numerical and Experimental Investigation of Flapping-Wing Propulsion," AIAA Paper No. 2002-0706, Reno, Nevada, January 2002.

13. Hess, J.L. and Smith, A.M.O., "Calculation of Potential Flow About Arbitrary Bodies," *Progress in Aeronautical Sciences*, Vol. 8, Pergamon Press, Oxford, 1966, pp. 1-138.

14. Basu, B. C. and Hancock, G. J., "The Unsteady Motion of a Two-Dimensional Aerofoil in Incompressible Inviscid Flow," *Journal of Fluid Mechanics*, Vol. 87, 1978, pp. 159-168.

15. Jones, K.D., Center, K.B., "Numerical Wake Visualization for Airfoils Undergoing Forced and Aeroelastic Motions," AIAA Paper No. 96-0055, Reno, Nevada, January 1996.

16. Jones, K.D. and Platzer, M. F., "An Experimental and Numerical Investigation of Flapping-Wing Propulsion," AIAA Paper No. 99-0995, Reno, Nevada, January 1999.

17. Jones, K.D., Castro, B.M., Mahmoud, O. and Platzer, M. F., "A Numerical and Experimental Investigation of Flapping-Wing Propulsion in Ground Effect," AIAA Paper No. 2002-0866, Reno, Nevada, January 2002.

18. Jones, K.D. and Platzer, M. F., "Numerical Computation of Flapping-Wing Propulsion and Power Extraction," AIAA Paper No. 97-0826, Reno, Nevada, January 1997.

19. Jones, K.D., Dohring, C.M., and Platzer, M. F., "Experimental and Computational Investigation of the Knoller-Betz Effect," AIAA Journal 36, 1998 pp.1240-1246

20. Radaspiel, R.; Rossow, C. and Swanson, R.C.: Efficient Cell Vertex Multigrid Scheme for the Three-Dimensional Navier-Stokes Equations. **AIAA Journal 28**, 1990, pp. 1464-1472.

21. Kroll, N.; Radaspiel, R. and Rossow, C.: Accurate and Efficient Flow Solvers for 3-D Applications on Structural Meshes. In: VKI Lecture Series 1994-04, "Computational Fluid Dynamics," Brussels, 1994.

22. Rossow, C.; Kroll, N.; Radaspiel, R. and Scherr, S.: Investigation of the Accuracy of Finite Volume Methods for 2- and 3-Dimensional Flow. In: Validation of Computational Fluid Dynamics, AGARD CP-437, Vol. II, 1988, pp. P14-1 to P14-11.

23. Correspondence with S. Pollard, Naval Postgraduate School, July-August 2002.

INITIAL DISTRIBUTION LIST

1. Defense Technical Information Center
   Ft. Belvoir, VA

2. Dudley Knox Library
   Naval Postgraduate School
   Monterey, CA

3. Prof. Max Platzer
   Department of Aeronautics and Astronautics
   Naval Postgraduate School
   Monterey, CA

4. Dr. Kevin D. Jones, Code AA/Jo
   Department of Aeronautics and Astronautics
   Naval Postgraduate School
   Monterey, CA

5. Steve Pollard
   Naval Postgraduate School
   Monterey, CA

6. Albion H. Bowers
   Dryden Flight Research Center
   Mail Stop D2027
   P.O. Box 273
   Edwards, CA

THIS PAGE INTENTIONALLY LEFT BLANK